Shale Resource Development in the U.S.: Part IV. Pore Structure and Hydrocarbon Production

(Max) Qinhong Hu (胡钦红)

maxhu@uta.edu

Department of Earth and Environmental Sciences

University of Texas, Arlington

UT ARLINGTON™

Outline

- **Porosity and permeability**
- **Multiple pore structure characterization approaches**
- **Methane sorption/desorption**
- **Production decline analyses**
- **Summary**

Average First Year Decline

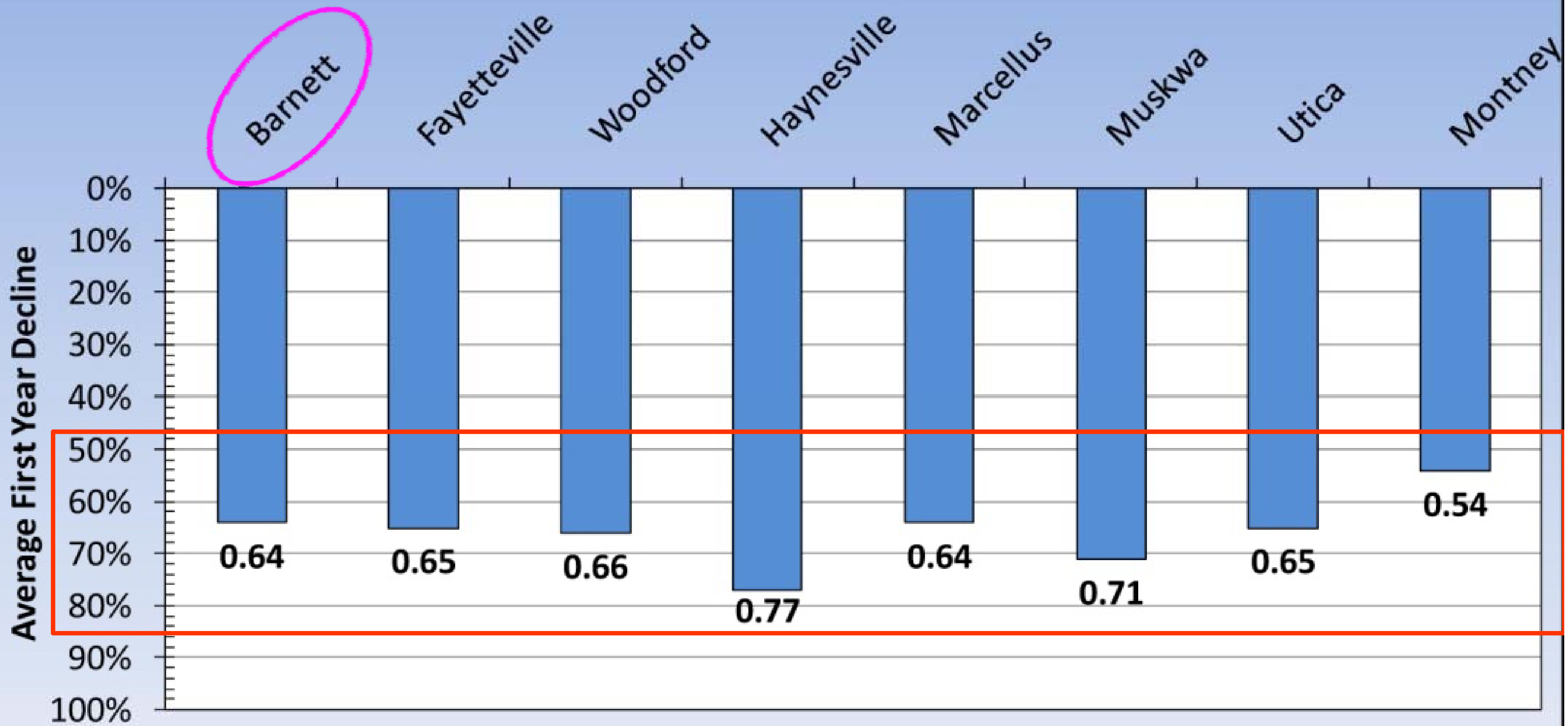

Low gas recovery factor 12–30% for Barnett Shale (King, 2012)

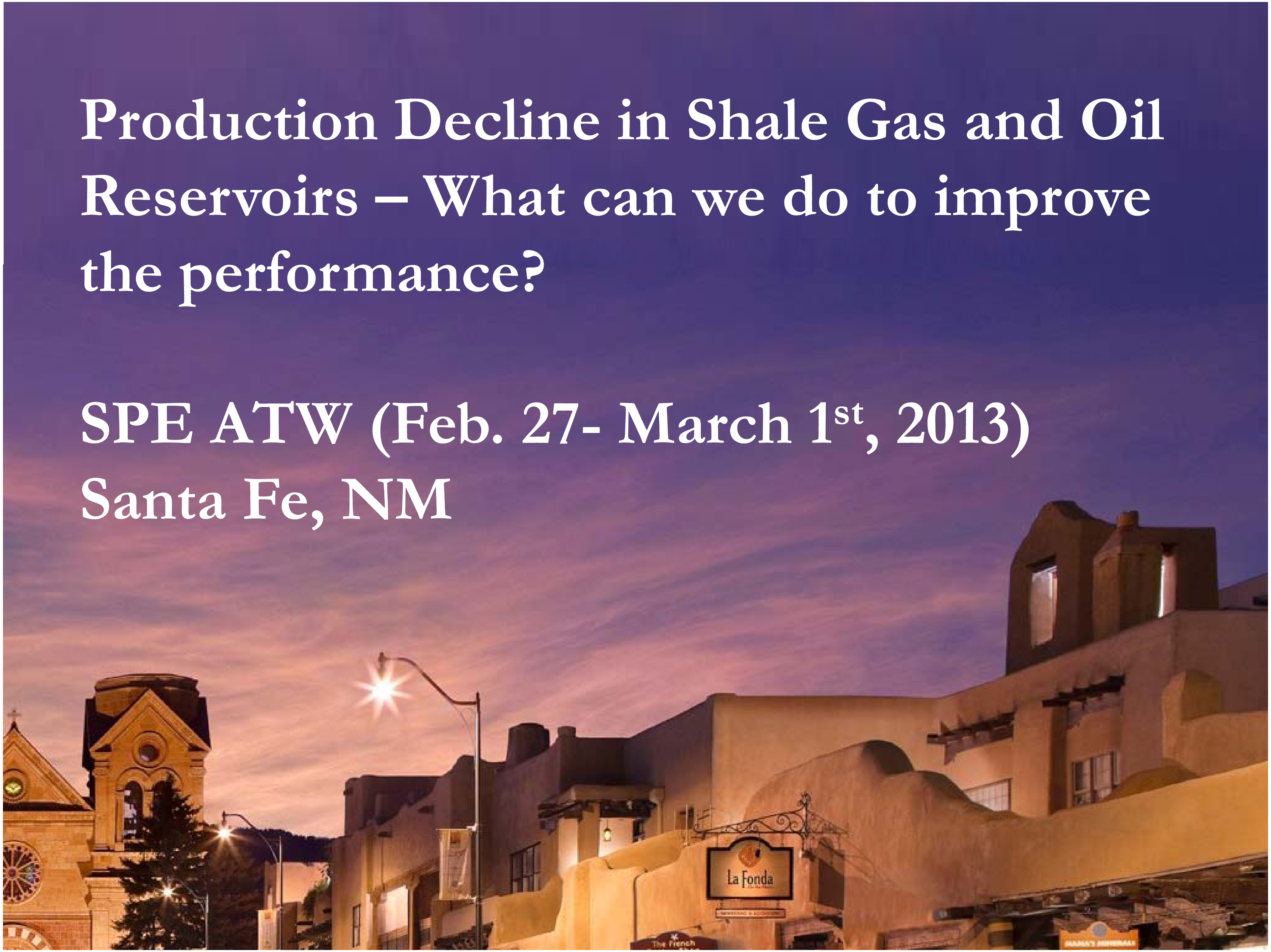
Production Decline in Shale Gas and Oil Reservoirs – What can we do to improve the performance?
SPE ATW (Feb. 27- March 1st, 2013)
Santa Fe, NM
La Fonda

Source: Nature Feb. 2013

"Reality Check"

- Analyzed 65,000 wells from 30 shale–gas and 21 tight–oil fields in US
- Steep declines (80–95% after 3 yrs) for gas well and field productivities
- For Eagle Ford and Bakken tight–oil fields, steep annual decline (~60% 1st yr, 40% 2nd yr, and 30% 3rd yr)
- 7,200 new wells to be drilled, at a cost of $42B annually to offset production decline
- Therefore, production will peak by 2017 and then fall by 40% a year

nature International weekly journal

Home | News & Comment | Research | Careers & Job

Archive > Volume 494 > Issue 7437 > Comment >

⏩ Take the Nature Publishing Group survey for the ch

ARTICLE PRI

view full access

NATURE | COMMENT

Energy: A reality check on t

J. David Hughes

Nature **494**, 307–308 (21 February 2013) | doi:10.
Published online 20 February 2013

Citation | Reprints | Rights & permissions

The production of shale gas and oil in the United Stat
underestimated, says J. David Hughes.

http://www.nature.com/nature/journal/v494/n7437/full/494307a.html

Corresponding author

Correspondence to: J. David Hughes

Comments

2013-05-10 11:39 AM

Robert Ewing said: Comment by Qinhong Hu (U. Texas Arlington) and Robert Ewing (Iowa State U.)

Since 2000, improved technology for horizontal drilling and hydraulic fracturing in the United States has greatly increased hydrocarbon (gas and oil) production from shale formations. Using data from 65,000 shale wells in 30 shale-gas and 21 tight-oil fields in the US, Hughes argued that the shale revolution will be hard to sustain because wells decline rapidly within a few years^1,2^. For example, the top five US plays typically produced 80?95% less gas after three years, and the productivity of new wells in two leading tight-oil plays (Bakken and Eagle Ford) drops by about 60% within the first year. Total gas recovery from the Barnett, the longest producing shale play, was reported to be only 8-15%^3^ for gas in place in 2002, and 12-30%^4^ in 2012, even with hydraulic re-stimulation. While Hughes? article^1^ mentions this steep decline and low overall recovery, investigations into their root cause(s) are surprisingly scarce.

Our work indicates that the key underlying physical cause is the low connectivity of nm-sized shale matrix pores, and the consequent low accessible porosity and slow diffusion to the producing wellbore^5,6^. Microscopic pore characteristics of porous media (e.g., wettability, pore-size distribution, and pore connectivity) control macrosopic fluid flow and chemical transport, such as hydrocarbon recovery. Shale?s low porosity and permeability make it likely that hydrocarbon recovery is limited by pore topology (e.g., density of connections) rather than geometry (e.g., radius). Chemical diffusion in sparsely-connected pore spaces is not well described by classical Fickian behavior; rather, anomalous diffusion is suggested by percolation theory. Micro-scale mapping using laser ablation-inductively coupled plasma-mass spectrometry (LA-ICP-MS) indicates that diffusional tortuosity in the Barnett shale is greater than 10,000: hydrocarbon molecules must migrate 10,000 times farther than the straight line distance to the wellbore. Investigations ignoring low connectivity will miss the causes of steep production decline.

References:

1. Hughes, J.D. 2013. Nature, Vol. 494, pp. 307-308, Feb. 21, 2013.
2. Hughes, J.D. 2013. Drill, Baby, Drill: Can Unconventional Fuels Usher in a New Era of Energy Abundance? Post Carbon Institute, 178 pp.
3. Curtis, J.B., AAPG Bull., 2002, 86(11), 1921-1938.
4. King, G.E. 2012. Hydraulic fracturing 101. SPE 152596.
5. Hu, Q.H. 2012. Pore structure and gas recovery in fractured Barnett shale. Presentation at the Bureau of Economic Geology, University of Texas at Austin, Austin, TX. http://www.beg.utexas.edu/abs/abstract.php?d=2012-09-14.
6. Vaidyanathan, G. ?Geology is behind in steep decline in dry gas wells, researchers say?, November 6, 2012, EnergyWire, Environment and Energy Publishing, LLC.

Science 17 May 2013:
Vol. 340 no. 6134 pp. 1235009-0
DOI:10.1126/science.1235009

REVIEW

Impact of Shale Ga

R. D. Vidic, S. L. Brantley, J.

Qinhong (Max) Hu

Qinhong Hu is faculty at China University of Geosciences (Wuhan) and The University of Texas at Arlington.

Several recent publications give balanced assessments of issues surrounding hydraulic fracturing, including regional water quality, seismicity, and methane emissions (1-3). Contrasting with many discussions regarding water resources, environmental, and health risks of shale resources development, the issue of economic sustainability gets little attention.

Analysis of 65,000 US shale wells shows that hydrocarbon pro¬duction typically drops by 60% within the first year and is 80–95% less after three years, such that that US production will peak in 2017 (4). Total gas recovery from the Barnett, the longest producing (since 1981) US shale play, is only 12–30% of gas in place. The main barrier to sustainable development of US shale, the low connectivity of the nanopores storing and transporting hydrocarbon, is being quietly ignored.

With estimated shale gas reserves greater than the US's and Canada's combined, China has an ambitious shale development program. China has several types of shale (by area, 26% are marine, 56% marine-terrestrial transitional, and 18% terrestrial), whereas nearly all US producing shales are marine. Sinopec recently reported that its 1st marine shale well (Jiao-Ye #1HF, drilled Feb. 14, 2012 and completed Nov. 24) initially produced 2.0×105m3gas/day, and maintained stable daily production of 6.6×104m3 over the next7 months. This production behavior, though of limited duration, is consistent with the 60% 1st year decline observed in US wells Shale geology could be a bottleneck to its sustainable development.

References: 1. R.D. Vidic, S.L. Brantley, J.M. Vandenbossche, D. Yoxtheimer, and J.D. Abad, Impact of shale gas development on regional water quality. Science, Vol. 340, 17 May 2013: 1235009 [DOI:10.1126/science.1235009]. 2. W.L. Ellsworth, Injection-induced earthquakes. Science, Vol. 341, 12 July 2013: 1225942 [DOI: 10.1126/science.1225942]. 3. J. Tollefson, Methane leaks erode green credentials of natural gas. Nature 493, 12, 03 January 2013 [DOI:10.1038/493012a]. 4. J.D. Hughes, Energy: A reality check on the shale revolution. Nature, 21 February 2013, Vol. 494, pp. 307-308. DOI:10.1038/494307a.

Submitted on Mon, 07/29/2013 - 10:30

http://comments.sciencemag.org/content/10.1126/science.1235009#comments

Pore Structure and Low Hydrocarbon Production

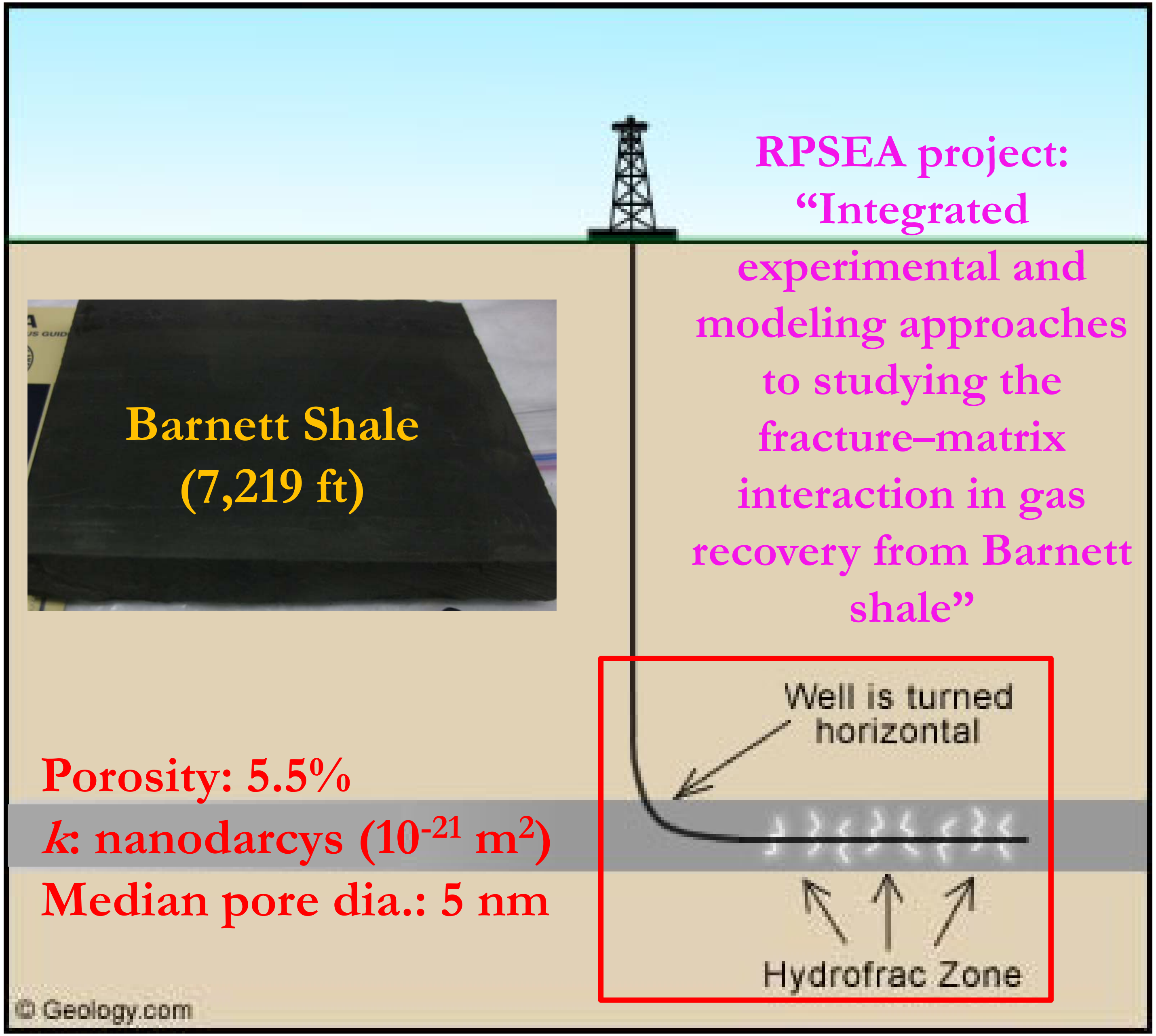

RPSEA project: "Integrated experimental and modeling approaches to studying the fracture–matrix interaction in gas recovery from Barnett shale"

Porosity: 5.5%
k: nanodarcys (10^{-21} m^2)
Median pore dia.: 5 nm

Pore structure

- Amount of gas in place
- Free vs. adsorbed gas
- Tortuous transport pathways
- Gas deliverability from nanopores to well bore

Fracture–Matrix Interaction

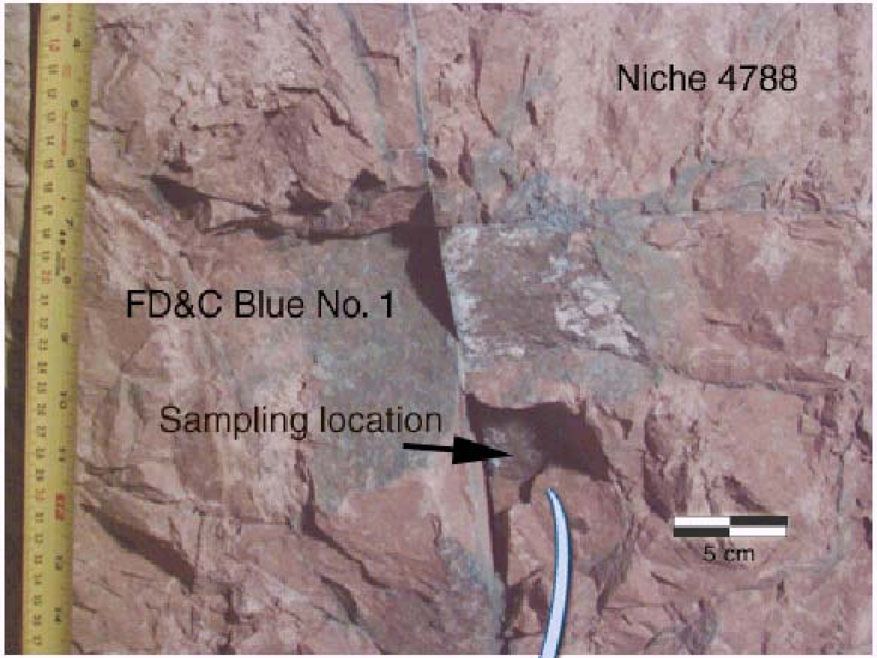

Rock milling in 1998

Field observation (preferential flow in a fracture network) of dye distribution in unsaturated fractured tuff at Yucca Mt.

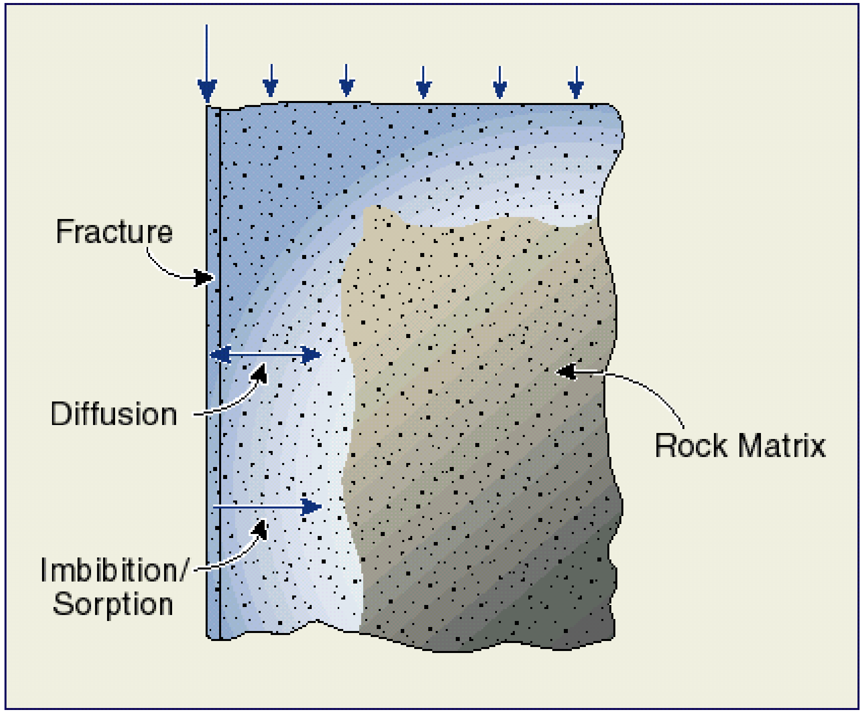

My work on fracture transport starts with this rock

Porosity in Geological Media

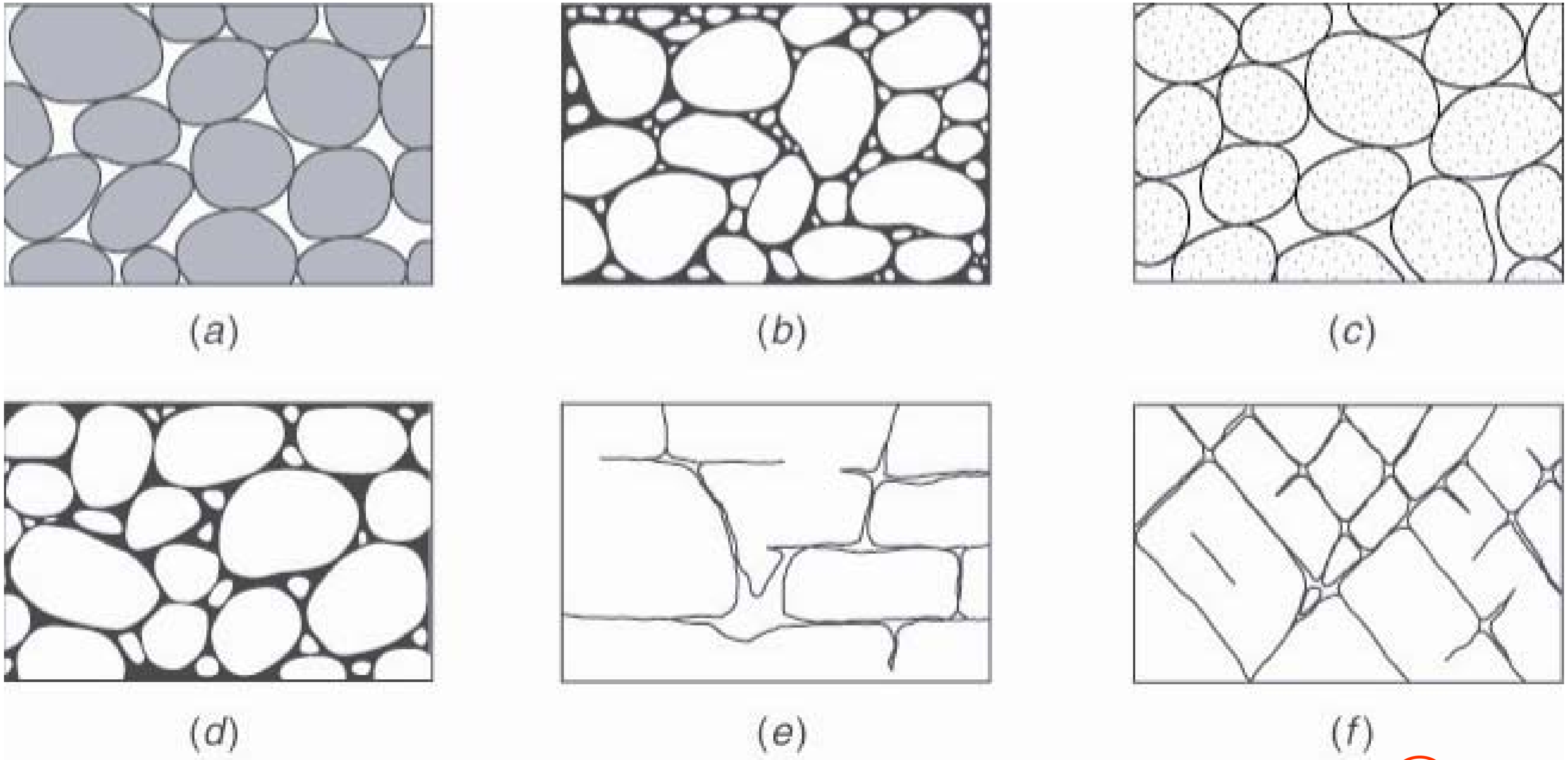

Figure 2.2.1. Examples of rock interstices and the relation of rock texture to porosity. (*a*) Well-sorted sedimentary deposit having high porosity. (*b*) Poorly sorted sedimentary deposit having low porosity. (*c*) Well-sorted sedimentary deposit consisting of pebbles that are themselves porous, so that the deposit as a whole has a very high porosity. (*d*) Well-sorted sedimentary deposit whose porosity has been diminished by the deposition of mineral matter in the interstices. (*e*) Rock rendered porous by solution. (*f*) Rock rendered porous by fracturing.[42]

Meinzer (1923)

Pore Geometry and Topology

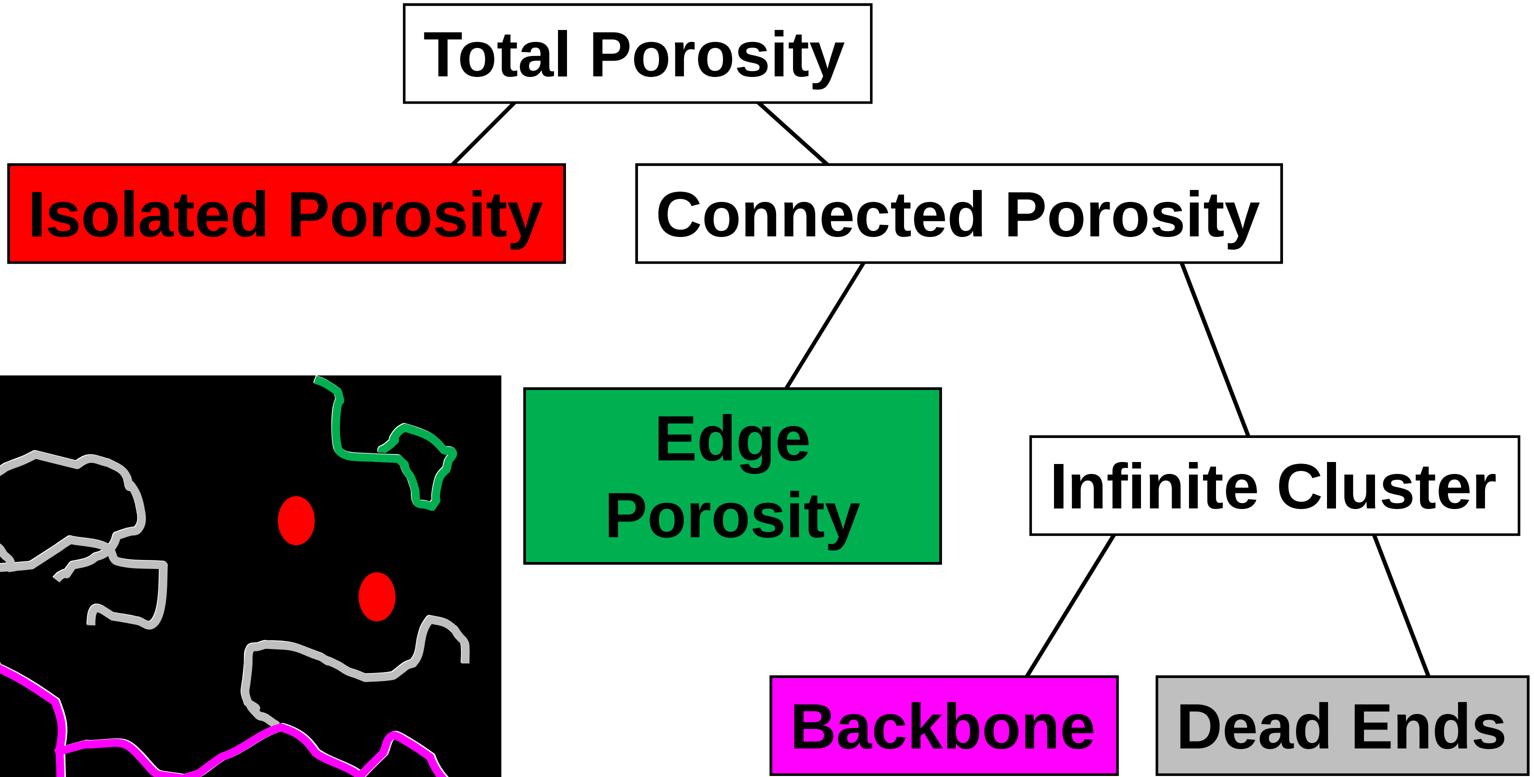

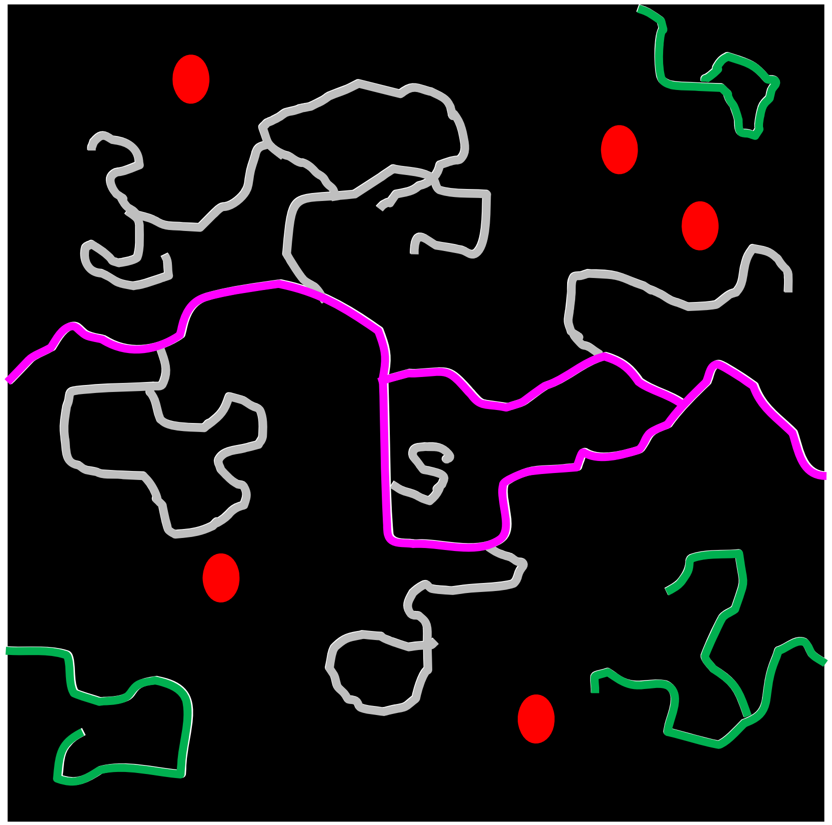

Pore structure:
shape, volume, size, size–distribution, connectivity, and surface area

Recommended Practices for Core Analysis

American Petroleum Institute

API (American Petroleum Institute)

American Petroleum Institute Recommended Practice (API RP) 40. 1998. *Recommended Practice for Core Analysis* (2nd Ed.). Am. Petrol. Inst., Washington, DC.

RECOMMENDED PRACTICE 40
SECOND EDITION, FEBRUARY 1998

API RP40 (1998)

CONTENTS

American Petroleum Institute Recommended Practice (API RP) 40. 1998. *Recommended Practice for Core Analysis* (2nd Ed.). Am. Petrol. Inst., Washington, DC.

Vacuum Saturation Apparatus

1 bar = 14.5 psi = 100,000 Pa = 750 torr ≡ 750 mm Hg

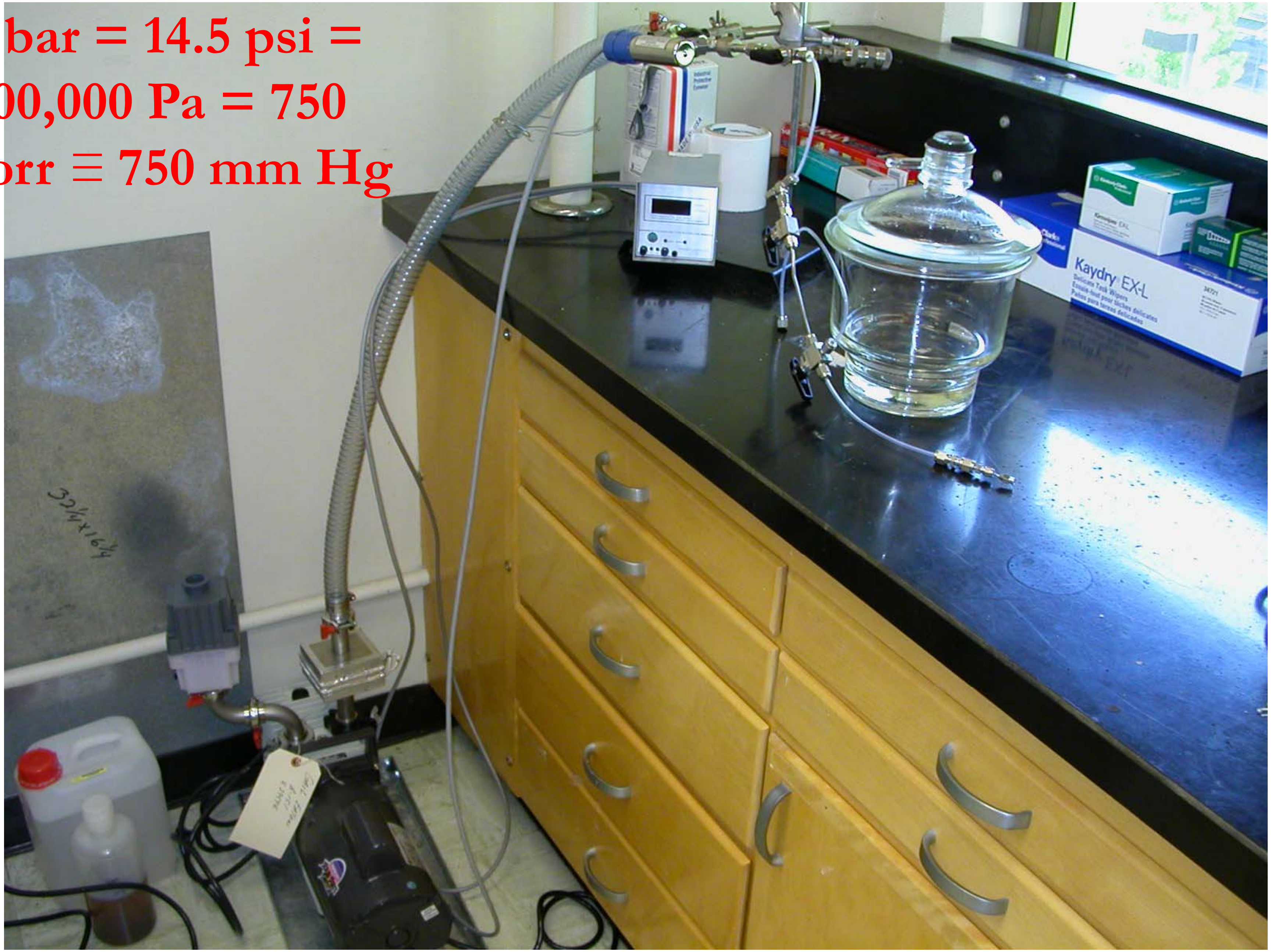

Pulling vacuum of rock samples

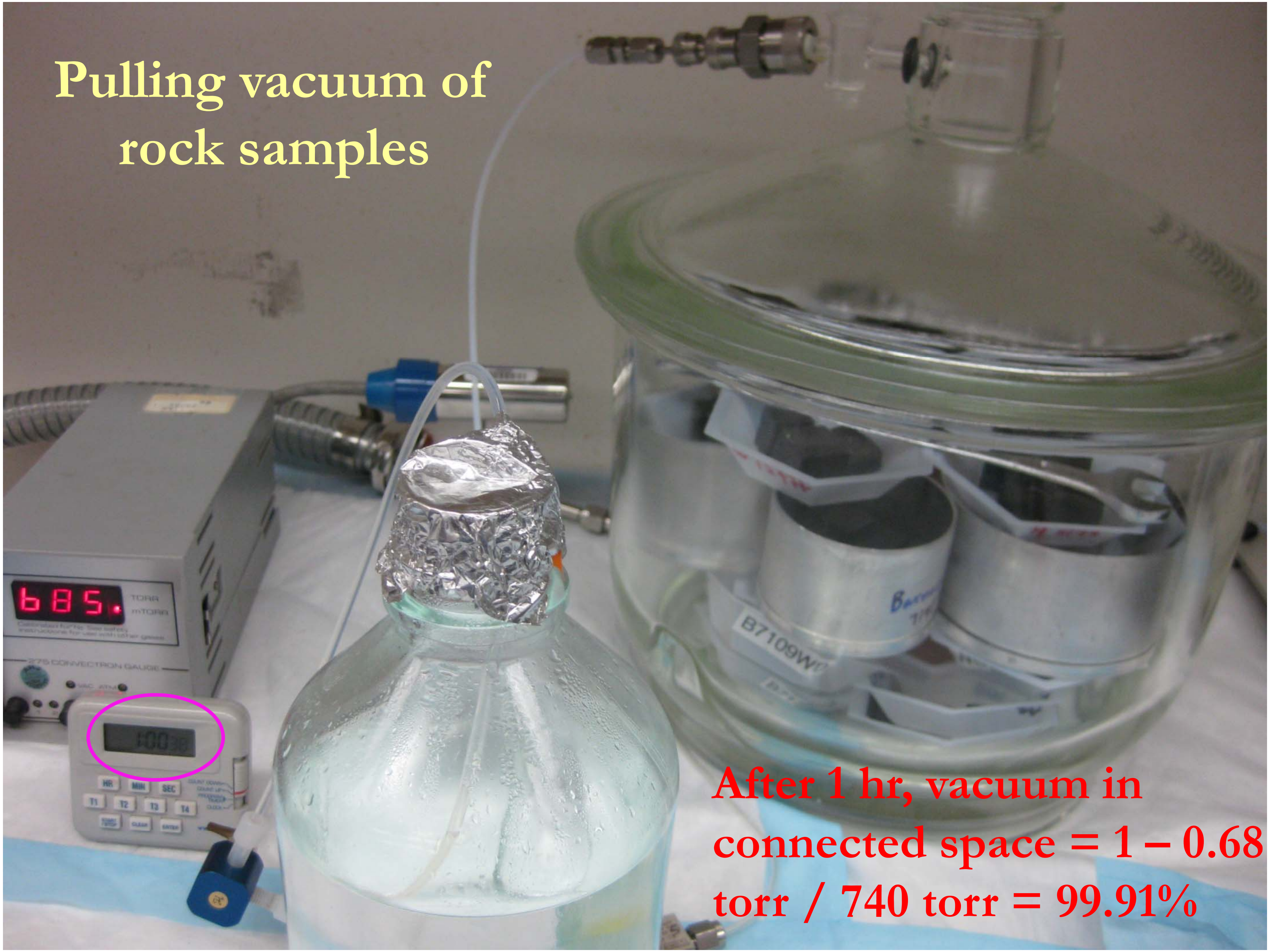

After 1 hr, vacuum in connected space = 1 – 0.68 torr / 740 torr = 99.91%

API RP40 (1998)

CONTENTS

American Petroleum Institute Recommended Practice (API RP) 40. 1998. *Recommended Practice for Core Analysis* (2nd Ed.). Am. Petrol. Inst., Washington, DC.

Table 6-2—Quick Selection and Reference Guide for Permeability Measurements Using Gases*

Reference Section Numbers	Type of Measurement	Approx. Perm. Range, md	Apparatus or Application	Major Advantages	Major Limitations
6.3.1.1 6.3.1.1.1.1	Axial flow, steady state in core plugs	0.1-10,000	Low pressure apparatus with manometers, orifice flow meters	Low capital cost; simple manual system; workhorse for decades; large data base for comparison	Labor intensive; high operating cost; low-stress perms; no slip correction; must check for inertial resistance
6.3.1.1 6.3.1.1.1.2	Axial flow, steady state in core plugs	0.1-10,000	Apparatus with electronic sensors, high pressure. core holder	Can be automated; reservoir stresses can be approximated; better precision and accuracy than with manual system	Must make multiple measurements for gas slippage correction; must check to ensure negligible inertial resistance
6.4.1.1 B.6.8.2	Axial flow, pressure falloff in core plugs	0.001-30,000	Wide range; med. to high stress measurements with corrections for b and β	Well adapted for automation; no flow meters required; can yield reservoir-condition perms (k_{∞}), and k_g	Higher capital cost for automated system with high accuracy pressure transducers and data acquisition system
6.4.1.3 D.6.8.4	Axial flow, pulse-decay in core plugs	.00001-0.1	High stress apparatus for very low perms.	Only method for ultra-low perms; well adapted for automation; porosity can be determined in same apparatus	Requires high pressure, leak-tight system with high quality transducers and data acquisition system—higher capital cost
6.3.1.2	Probe perm., s.s., on whole core	1-10,000	Zero stress, high density, localized measurements for heterogeneous cores	No plug preparation required (core slabbing recommended); relatively fast; can be automated or made portable	Zero stress, non slip corrected perms are high at low end of range; prone to high inertial resistance at high end
6.4.1.2 C.6.8.3	Probe perm., pressure falloff on whole core	0.001-30,000	Zero stress, high density, localized measurements for heterogeneous cores	No plug preparation required (core slabbing recommended); very fast; automated; corrected for b, β	Zero stress perms are high, especially at low end of range; higher capital cost for automated system
6.3.1.3	Transverse, s.s. perm. in whole core	0.02-500	Directional perm. in whole core (or plug) for k_{max} and k_{90^*}	Can measure "horizontal" perm in various directions; averaging obtained using whole-core sample.	Cleaning and preparation of whole core sample more expensive; only k_g obtained without multiple measurements
6.3.1.4	Radial, s. s. perm. in whole core	0.01-250	Average permeability in all radial directions in whole core samples	Measures average "horizontal" permeability in large sample	Difficult to prepare samples; no radial stress; perm. critically dependent on condition of central "wellbore"

*Major advantages of using gas rather than liquid:

a. Easy to use—does not require special saturation techniques.
b. Non-reactive with rock; non-corrosive to equipment.
c. No post-measurement cleanup required.
d. Less prone than liquid to mobilizing fines in rock sample.
e. Does not support microbial growth, nor require special filtration.

Major disadvantages:

a. Requires correction for gas slippage—especially with lower perms.
b. Prone to significant high-velocity inertial resistance in high perm. rock.
c. Necessary leak-tightness harder to achieve than with liquids.
d. In some cases, may be less representative of permeability in reservoir.

API RP40 (1998)

AP–608 Automated Porosimeter–Permeameter

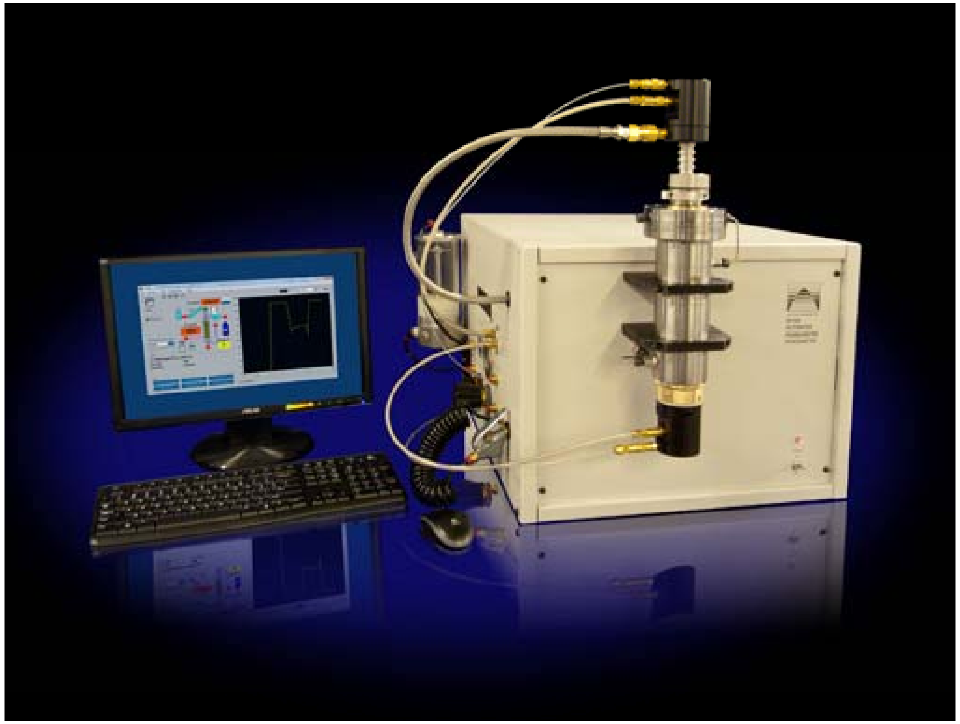

The only truly integrated porosimeter–permeameter in one compact unit in the market

Coretest Systems, Inc.

http://www.coretest.com/product_detail.php?p_id=98

- **A cost–effective ($65K) system for performing automated permeability and porosity (0.01 to >40%) tests at confining pressures up to 10,000 psi, over a wide permeability range (0.001 mD to >10 D, depending on sample size)**
- **The AP–608 uses a pressure decay technique to determine Klinkenberg–corrected permeabilities, slip and turbulence correction factors**

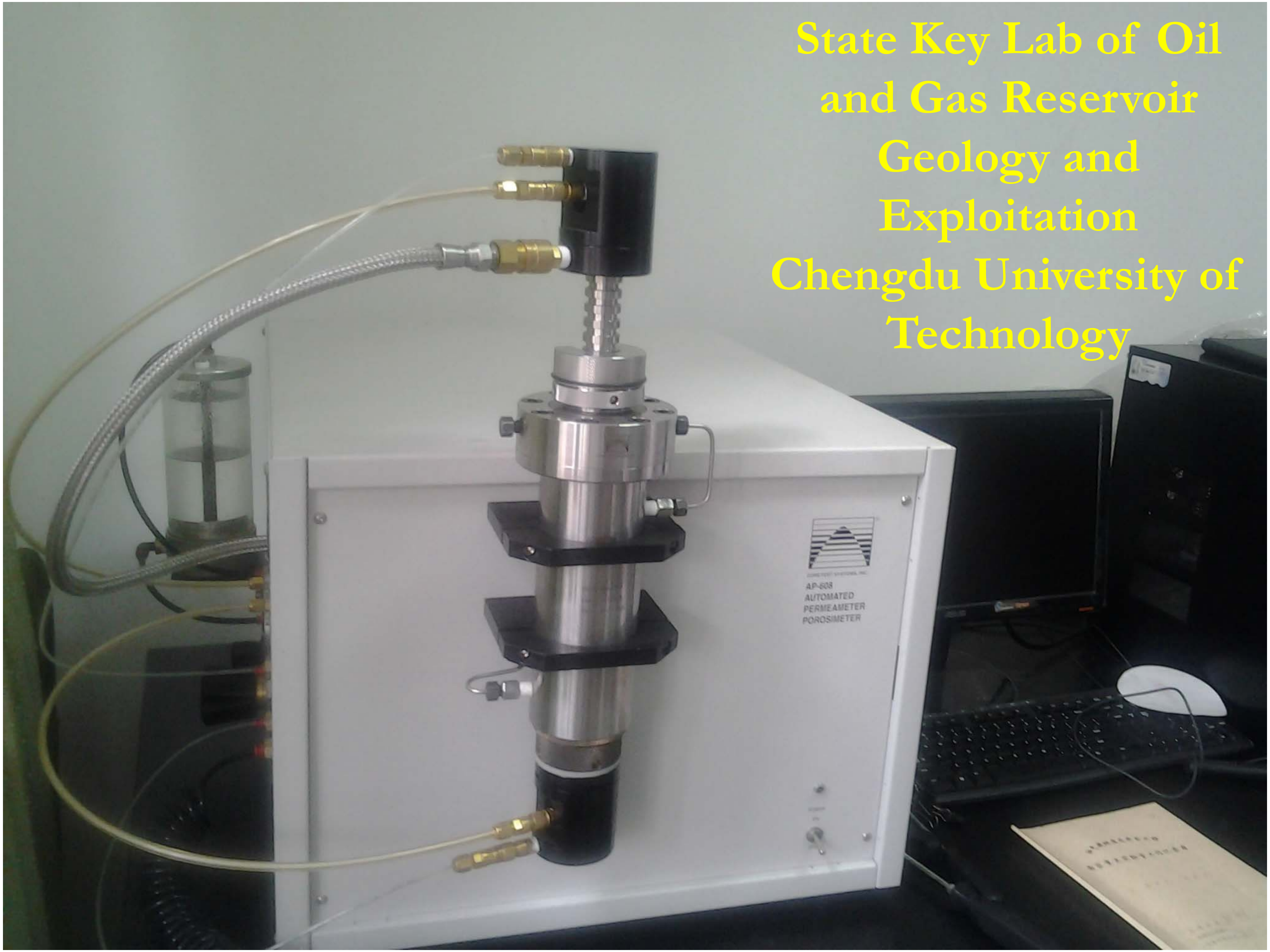
State Key Lab of Oil
and Gas Reservoir
Geology and
Exploitation
Chengdu University of
Technology
AP-608
AUTOMATED
PERMEAMETER
POROSIMETER

NDP–605 NanoDarcy Permeameter (Shale Oil/Gas)

Coretest Systems, Inc.

http://www.coretest.com/product_detail.php?p_id=155

- A fully integrated and computer-controlled system to measure low to very low permeability (10 nD to 0.5 mD, depending on core length and diameter)
- Uses a pulse decay procedure
- Operates at pore pressure up to 2,500 psi and confining pressures up to 9,500 psi
- Core diameter: 1.0”, 1.5”, or 30 mm
- Core length: 0.125” to 3.0”
- Temperature control: forced-air flow to ±0.5°C
- Cost: $200K

http://www.youtube.com/watch?v=e6Sk3KywIEA

July 2012


4-inch
core
samples

4-inch core after being extruded

Conventional Core Analysis

	Unit Price
Plug Acquisition and Plug Handling	
Plug acquisition, drilling with nitrogen gas, per sample	**$50**
Consolidated Plug Type - Standard Analysis	
Includes porosity and grain density by the Boyle's Law technique, horizontal permeability to air by the steady-state or unsteady-state technique, lithology and fluorescence description.	
Standard Analysis @ 1 pressure, per sample	**$92**
Permeability @ first additional pressure, Klinkenberg corrected, per sample	**$45**
Pulse Decay Permeability Measurements	
Specific perm to brine, ambient temp, pulse decay	**$550**
Absolute Pulse Decay Permeability, "cleaned & dried", down to 0.000005 md K_{inf}	**$450**
Shale and Organic-Rich Core Analysis (GRI -95/0496, 1996)	
Fresh Sample	
Bulk density, matrix permeability, gas-filled porosity, gas saturation	
Cleaned and Dry Sample	
Grain density, porosity of interconnected pore space, oil and water saturations	
Samples 1-10, per sample	**$935**
Samples 11-19, per sample	**$825**
Samples 20+, per sample	**$710**

Price sheet in July 2012

Shale Gas Reservoir Core Analysis (GRI Method Used By Core Lab)

Development of Laboratory and Petrophysical Techniques for Evaluating Shale Reservoir

Final Report (GRI-95/0496)
Gas Research Institute, April 1996

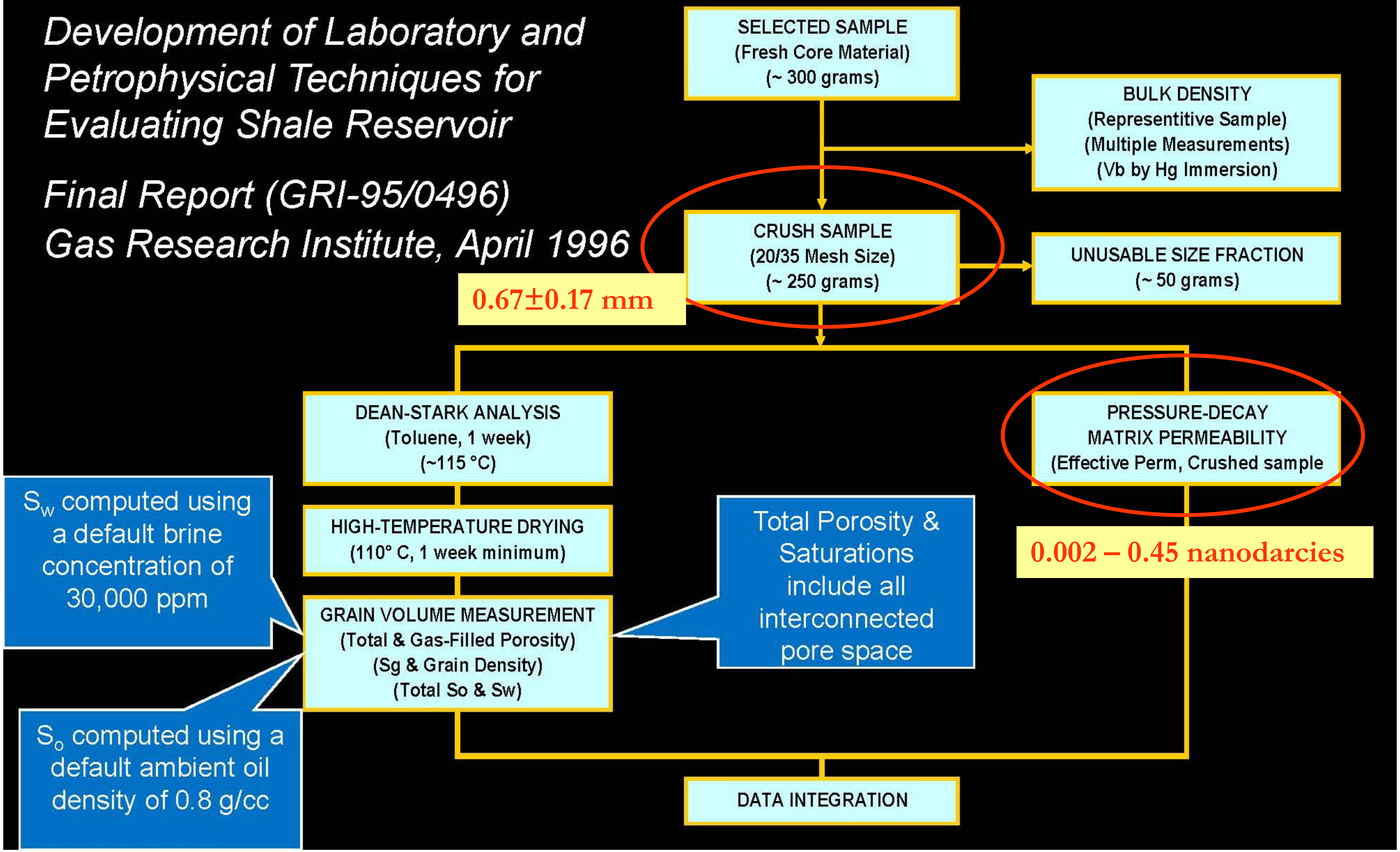

Summary of Rock Properties

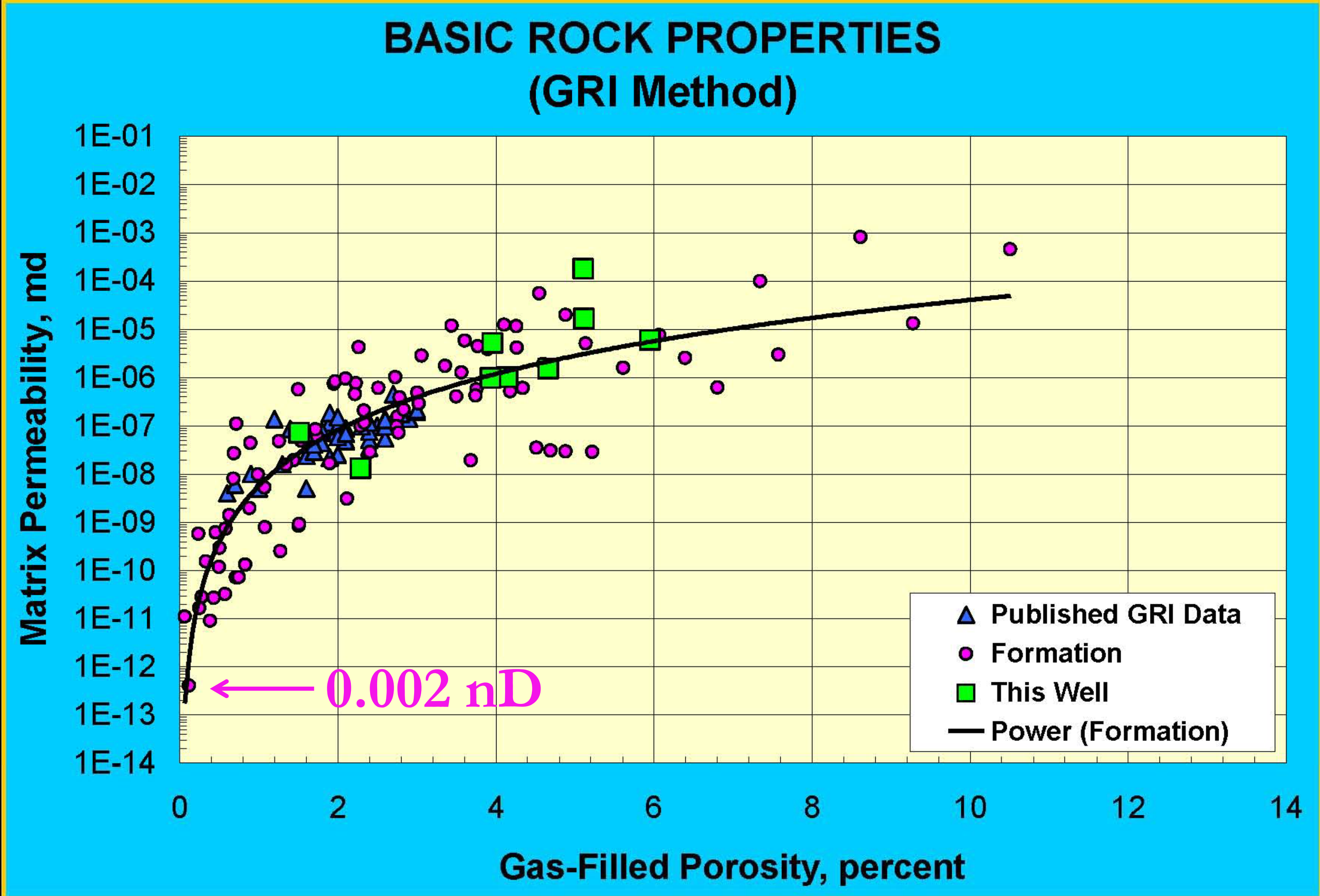

GRI Method Results

Company
Well

CL File No.: HOU-060XXX
Date: October 11, 2006
Analyst(s): MS-JH

Gas Shale Core Analysis

		As received				Dry & Dean Stark Extracted Conditions (2)			
Sample	Depth (ft)	Bulk Density (g/cc)	Matrix Permeability (1) (mD)	Gas-filled Porosity (%)	Gas Saturation (%)	Grain Density (g/cc)	Porosity (%)	Oil Saturation (3) (%)	Water Saturation (4) (%)
8	12839.00	2.596	2.13E-08	1.39	31.2	2.685	4.46	0.0	68.8
9	12851.20	2.588	4.36E-12	0.10	4.9	2.621	2.02	12.7	82.4
10	12863.30	2.643	4.06E-13	0.11	4.7	2.685	2.42	6.8	88.5
11	12875.30	2.618	1.27E-12	0.09	3.5	2.661	2.55	0.0	96.5
12	12887.30	2.604	8.58E-11	0.10	6.6	2.630	1.56	0.0	93.4

Footnotes:

(1) Matrix Permeability is an effective Kg determined from pressure decay results on the fresh, crushed, 20/35 mesh size sample.
(2) Dean Stark extracted sample (20/35 mesh size) dried at 110 °C. Porosity and saturations are relative to total interconnected pore space.
(3) Oil volume computed assuming an oil density of 0.8 g/cc
(4) Water volume corrected assuming a brine concentration of 30,000 ppm NaCl with an ambient density of 1.018 g/cc

Reference: "Development of Laboratory and Petrophysical Techniques for Evaluating Shale Reservoirs", GRI-95/0496, Gas Research Institute, April 1996

Shortcomings of GRI (crushed–rock) Technique

- Absence of overburden stress
- No Klinkenberg correction: under low pore pressures, gas flow through tight shales may be in the free–molecular–flow regime or transition regime
- Darcy's law (continuum assumption) may not be valid

Sinha et al. (2012); SPE152257

- Inconsistency and lack of standard analytical expression: the GRI report does not give a detailed methodology for interpreting the raw data, and each lab develops its own proprietary technique for interpreting the data

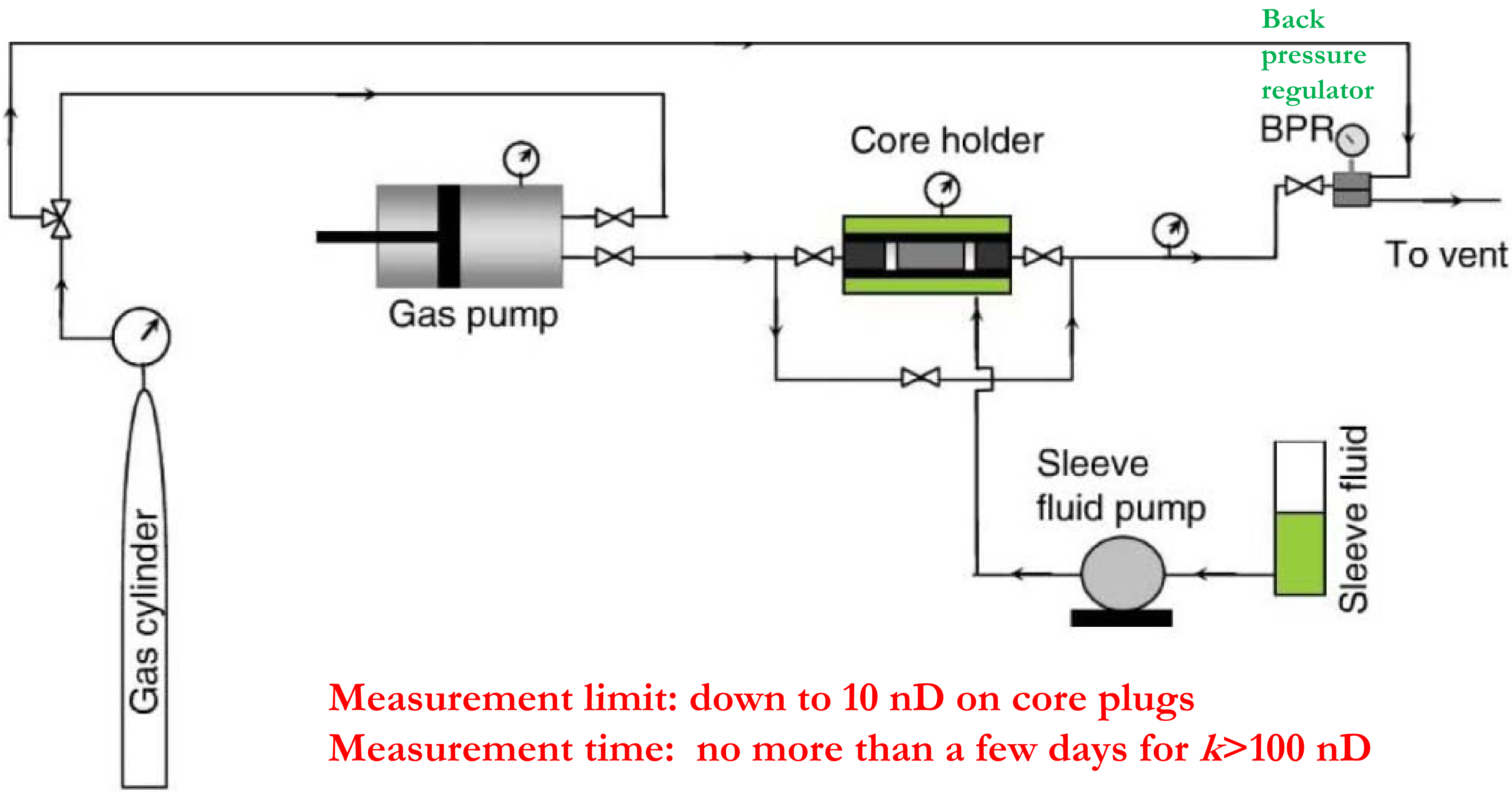

Measurement limit: down to 10 nD on core plugs

Measurement time: no more than a few days for *k*>100 nD

Fig. 1—Schematic of steady-state apparatus for measuring permeability on very-tight-rock samples.

Sinha, S., E.M. Braun, Q.R. Passey, S.A. Leonardi, A.C. Wood, T. Zirkle, J.A. Boros, and R.A. Kudva. 2012. Advances in measuring standards and flow properties measurements for tight rocks such as shales. SPE152257.

Sinha et al. (2012); SPE152257

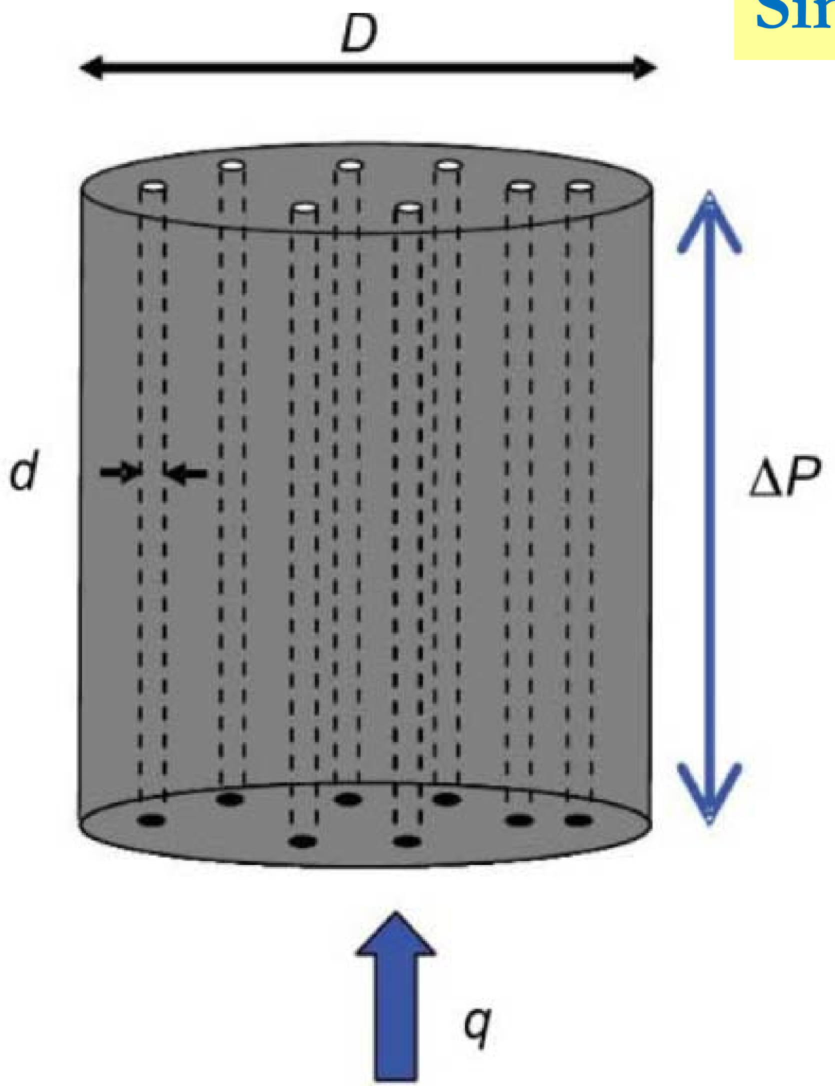

Fig. 2—Sketch of capillary-based permeability standard.

Fig. 3—Capillary-based permeability standard (47-μm-diameter channel).

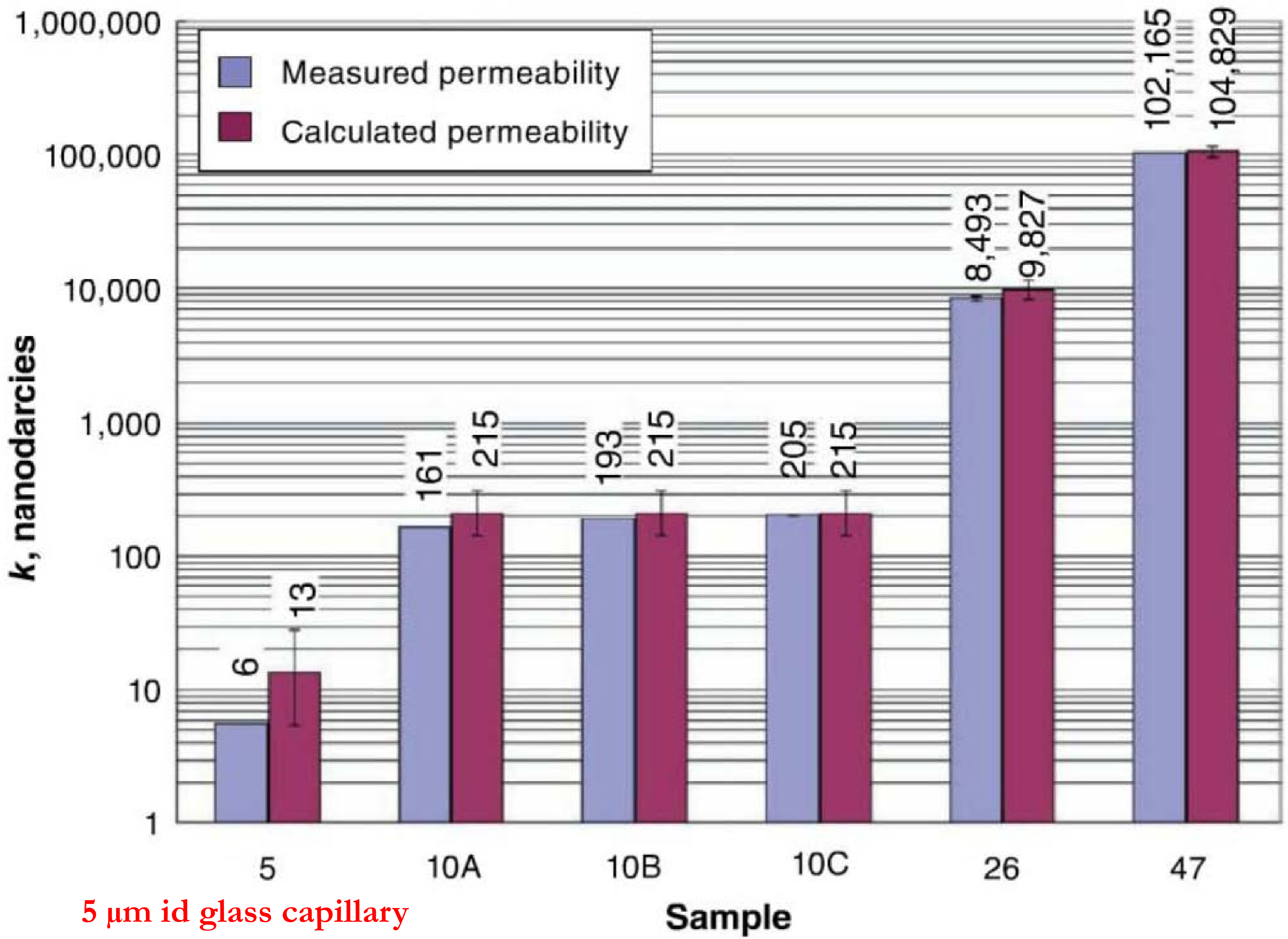

5 µm id glass capillary

Fig. 4—Measured and calculated permeability of six different permeability-calibration standards.

Sinha et al. (2012); SPE152257

Intraparticle organic nanopores

Ar ion–beam milling and field emission gun SEM: **resolve pores as small as 5 nm**

Loucks et al. (2009)

Where is the porosity?

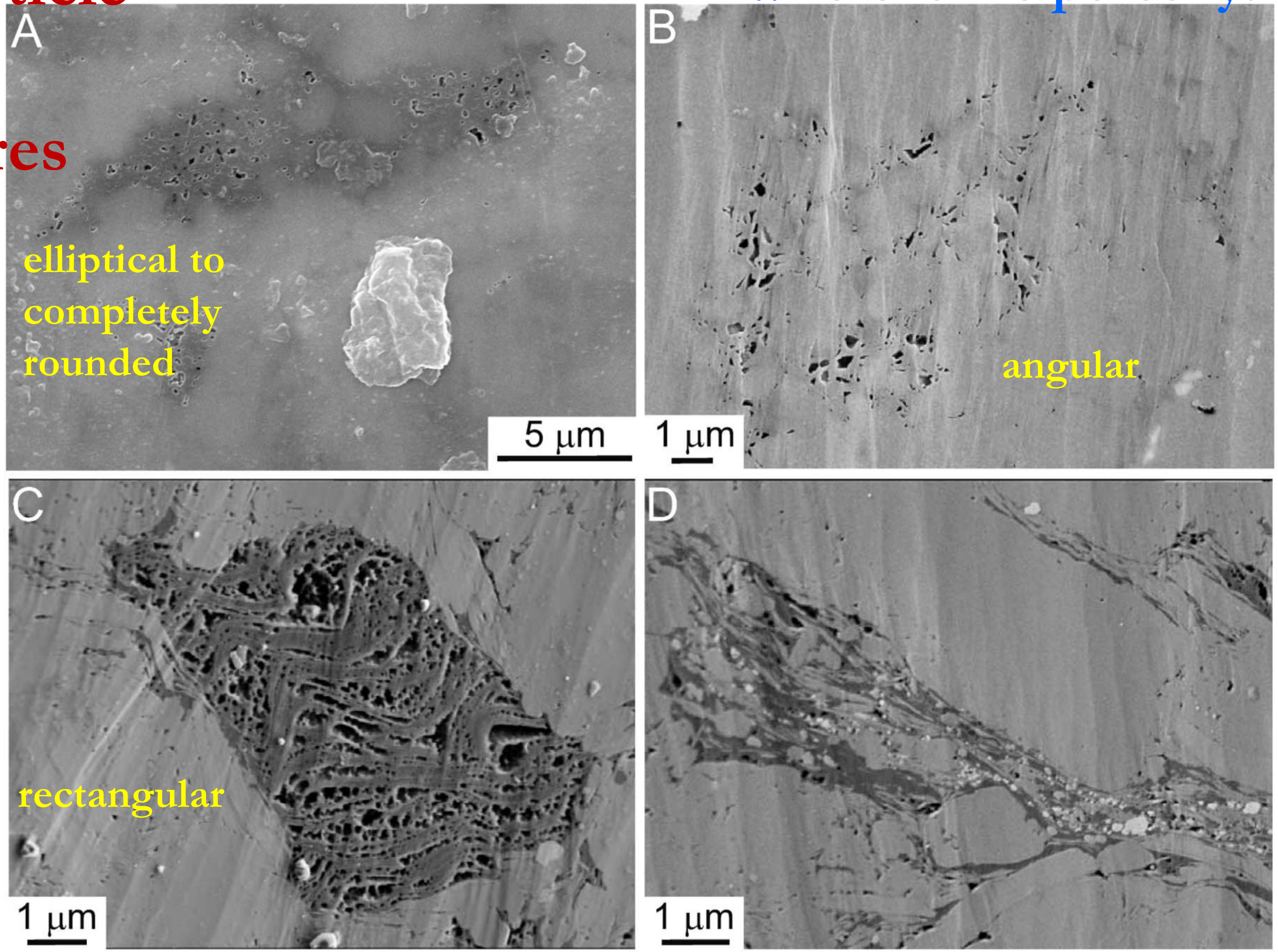

FIG. 5.—Nanopores associated with organic matter in the Barnett Shale. **A)** Elliptical to complexly rounded nanopores in an organic grain. Darker materials are organics. BSE image. Blakely #1, 2,167.4 m. **B)** Angular nanopores in a grain of organic matter. SE image. Blakely #1, 2,167.4 m. Accelerating voltage = 10 kV; working distance = 6 mm. **C)** Rectangular nanopores occurring in aligned convoluted structures. SE image. T.P. Sims #2, ~ 2,324 m. Accelerating voltage = 2 kV; working distance = 3 mm. **D)** Nanopores associated with disseminated organic matter. Carbon-rich grains are dark gray; nanopores are black. SE image. T.P. Sims #2, ~ 2,324 m. Accelerating voltage = 2 kV; working distance = 2 mm.

Nelson (2009)

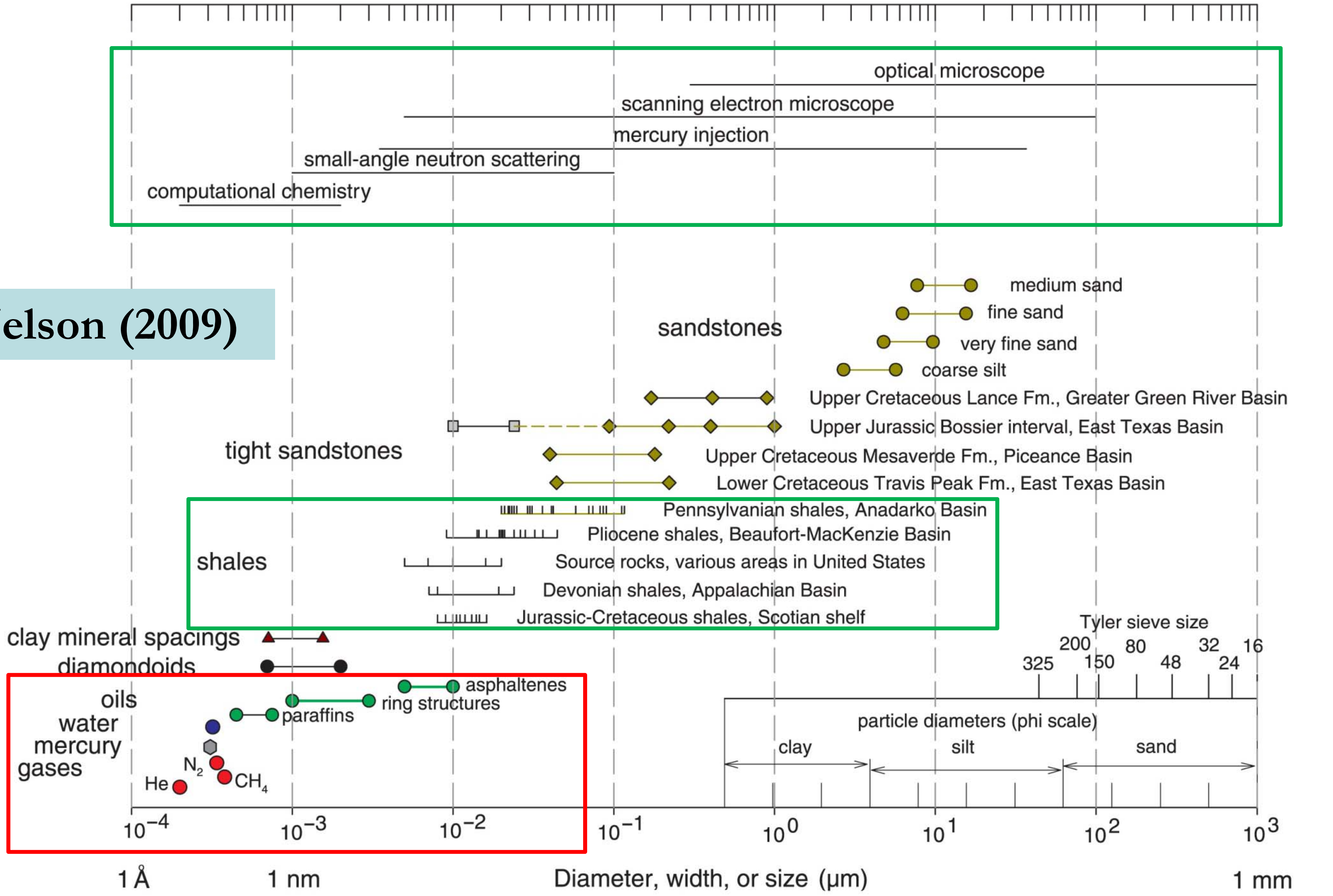

Figure 2. Sizes of molecules and pore throats in siliciclastic rocks on a logarithmic scale covering seven orders of magnitude. Measurement methods are shown at the top of the graph, and scales used for solid particles are shown at the lower right. The symbols show pore-throat sizes for four sandstones, four tight sandstones, and five shales. Ranges of clay mineral spacings, diamondoids, and three oils, and molecular diameters of water, mercury, and three gases are also shown. The sources of data and measurement methods for each sample set are discussed in the text.

Gas Transport Mechanisms

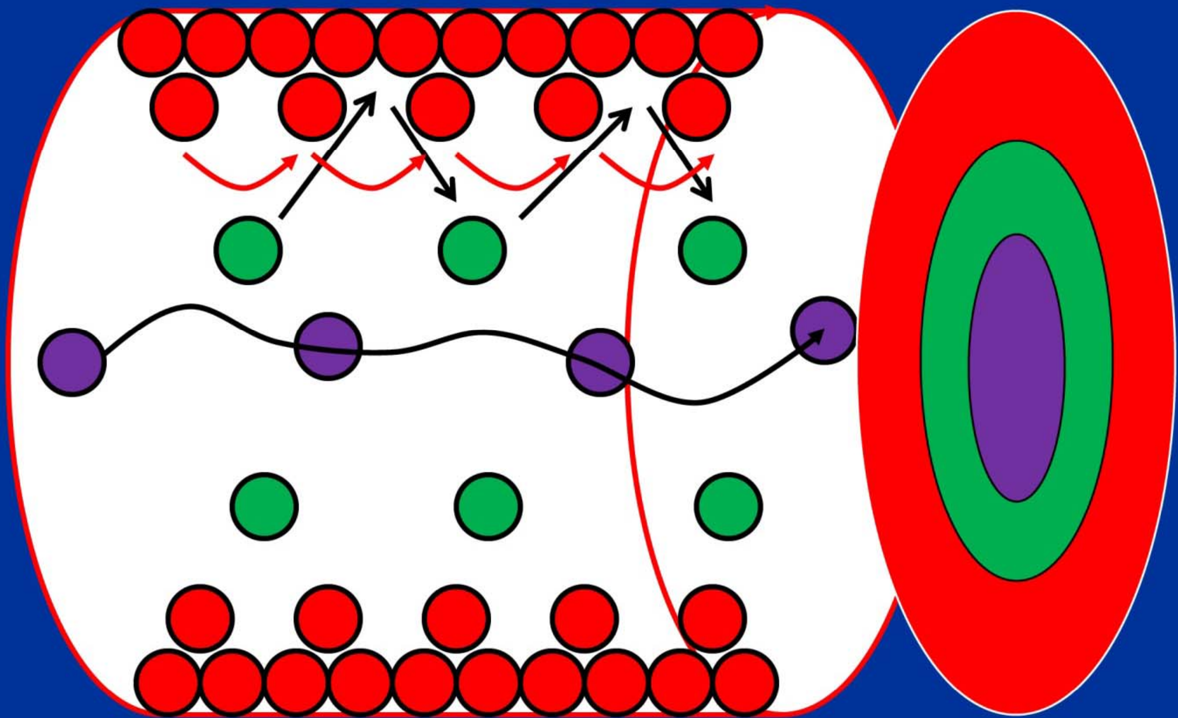

Adsorbed phase diffusion

Knudsen diffusion

Gaseous viscous flow

As the tube size gets smaller, flow regime changes to the point that viscous (Darcy) flow vanishes.

Modified after (Bae and Do, 2005)

Outline

- Porosity and permeability
- **Multiple pore structure characterization approaches**
- Methane sorption/desorption
- Production decline analyses
- Summary

Shale Gas Flow: Matrix "diffusion" vs. "Darcy" flow

drive your car out of neighbor hood blind-folded

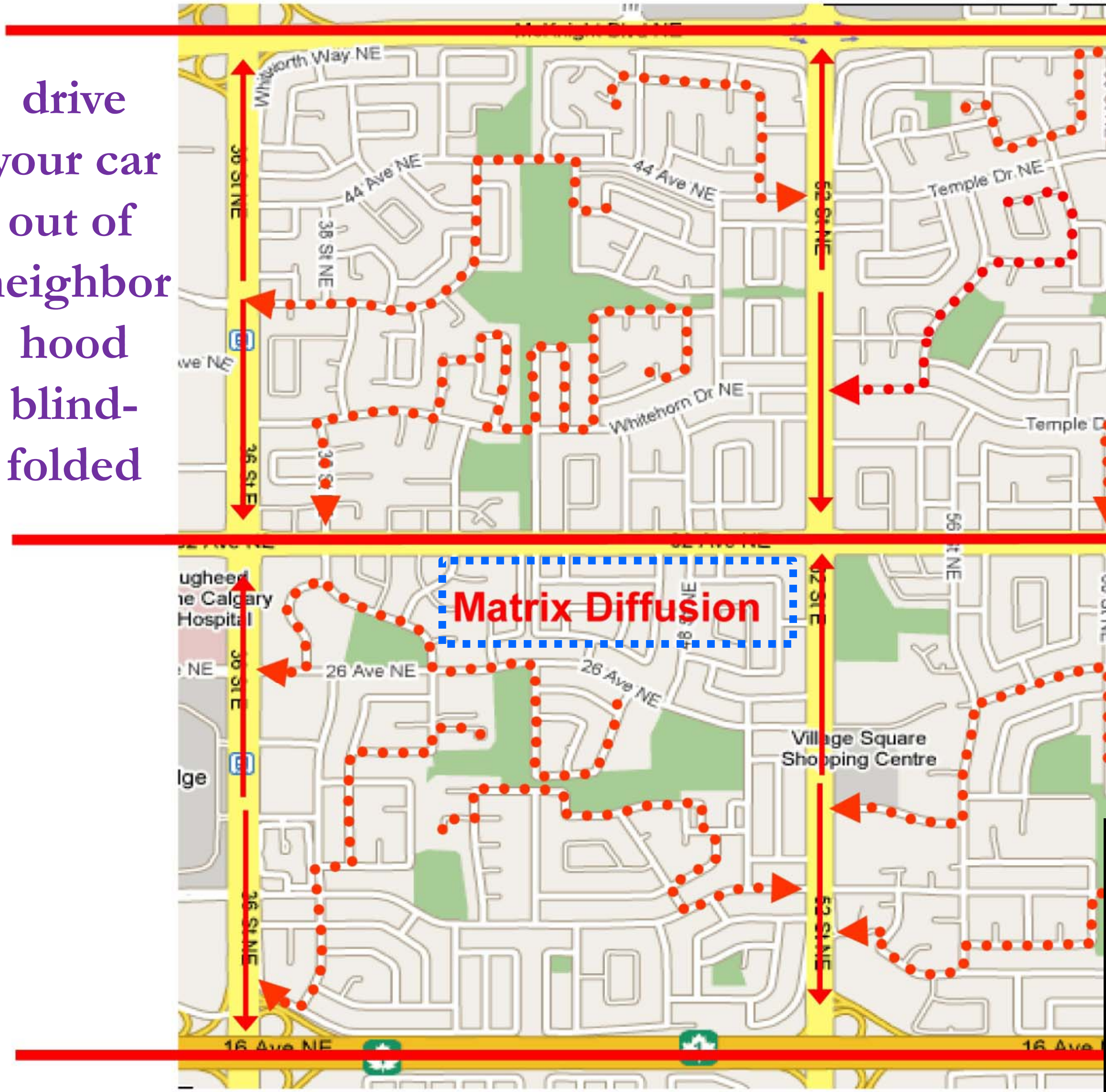

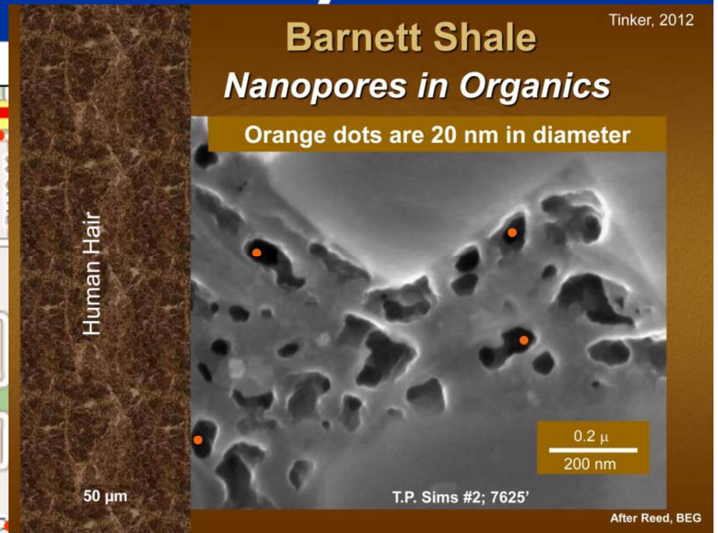

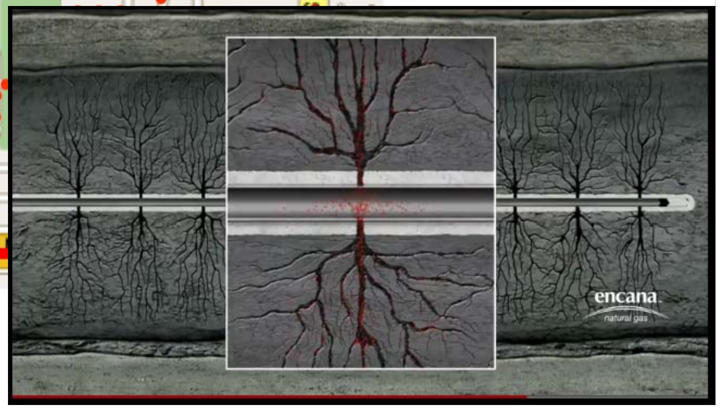

http://www.transcanada.com/customerexpress/docs/presentations_general/2009_North_American_Shale_Gas_Overview_NECA.pdf

Three Data Points ← anecdotal

- Gas molecule movement in shale on the order of 10 feet in the lifetime of a well - Dr. Mohan Kelcar, University of Tulsa.
- Gas molecule movement of about a meter/year modeled by Nexen's Unconventional Team, presented at Global Gas Shales Summit, Warsaw, Poland.
- Gas molecule movement of a few feet/year modeled by Dr. Chunlou Li, Shale Gas Technology Group.

→ ~1 m/yr movement (advection vs. diffusion ?)

LaFollette, R. 2010. Key Considerations for Hydraulic Fracturing of Gas Shales. Manager, Shale Gas Technology, BJ Services Company, September 9, 2010. www.pttc.org/aapg/lafollette.pdf

Pore Connectivity and Diffusion

- Same mathematics for diffusion and imbibition:

$$\frac{\partial c}{\partial t} = \frac{\partial}{\partial x}\left[D_s(\theta) \frac{\partial c}{\partial x} \right]$$

$$\frac{\partial \theta}{\partial t} = \frac{\partial}{\partial x}\left[D(\theta) \frac{\partial \theta}{\partial x} \right]$$

- Affected the same way by pore connectivity:

Pore connectivity:	**High**	**Low**
	Classical	**Anomalous**
Time–dependence:		
Distance to front	$t^{0.5}$	$t^{0.263}$
Diffusion coefficient	constant	$t^{-0.48}$
Distance–dependence:		
Diffusion coefficient	constant	$t^{-1.83}$

Ewing and Horton (2002)

Percolation Theory

The mathematics of how macroscopic properties result from local (microscopic) connections

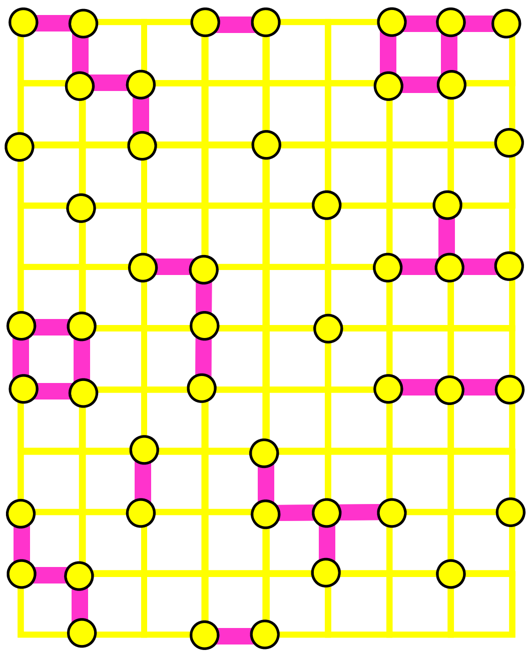

***p* is the local connection probability**

percolation threshold

$0.5 < p_c < 0.66$

(for 2D square lattice)

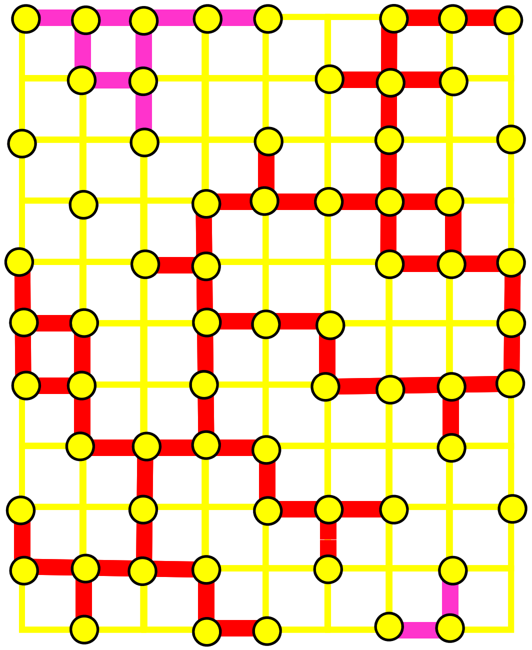

***p* = 0.5**

***p* = 0.66**

"Ant in a labyrinth"

↕

Solute in a pore system

Multiple Approaches to Studying Pore Structure

- Imbibition with samples of different shapes (UTA)
- Edge–accessible porosity (UTA)
- Liquid and gas diffusion (UTA)
- Mercury injection porosimetry (UTA)
- N_2 adsorption isotherm (Saitama Univ.; Quantachrome)
- Water vapor adsorption isotherm (UTA)
- Nuclear Magnetic Resonance Cryoporometry (Lab-Tools, Ltd., UK)
- SEM imaging after Wood's metal impregnation (Univ. Hannover; Swiss EPMA)
- Microtomography (high–resolution, synchrotron) (PNNL–EMSL; Swiss Light Source; Univ. Hannover; Saitama Univ.)
- Focused Ion Beam/SEM imaging (PNNL–EMSL)
- *Small–Angle Neutron Scattering (SANS) (LANL, NIST)*
- Pore–scale network modeling (ISU)

http://www.beg.utexas.edu/abs/abstract.php?d=2012-09-14


Core Research Center of
the Bureau of Economic
Geology (BEG) in Texas

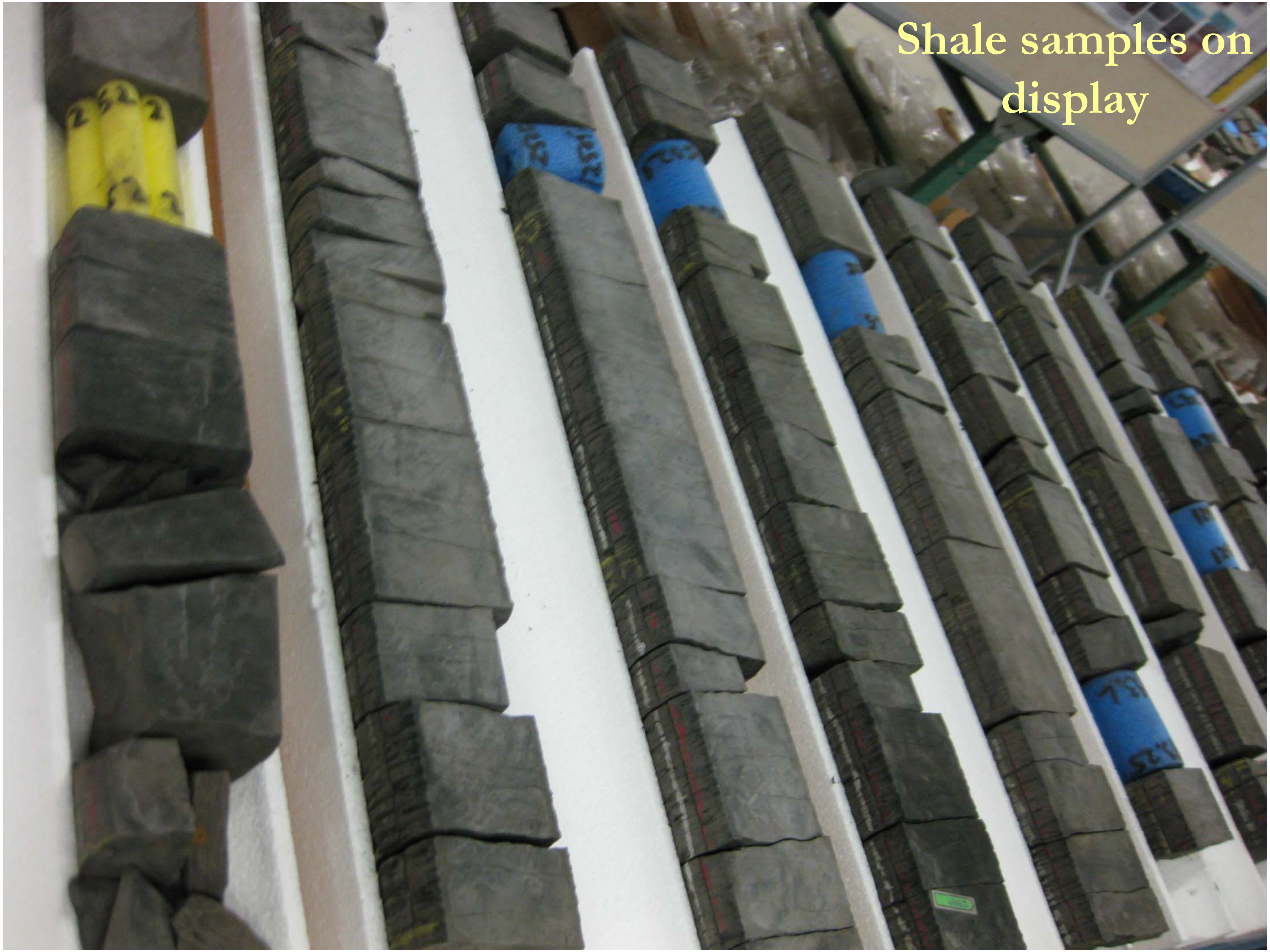
Shale samples on display

(Spontaneous) Imbibition Test

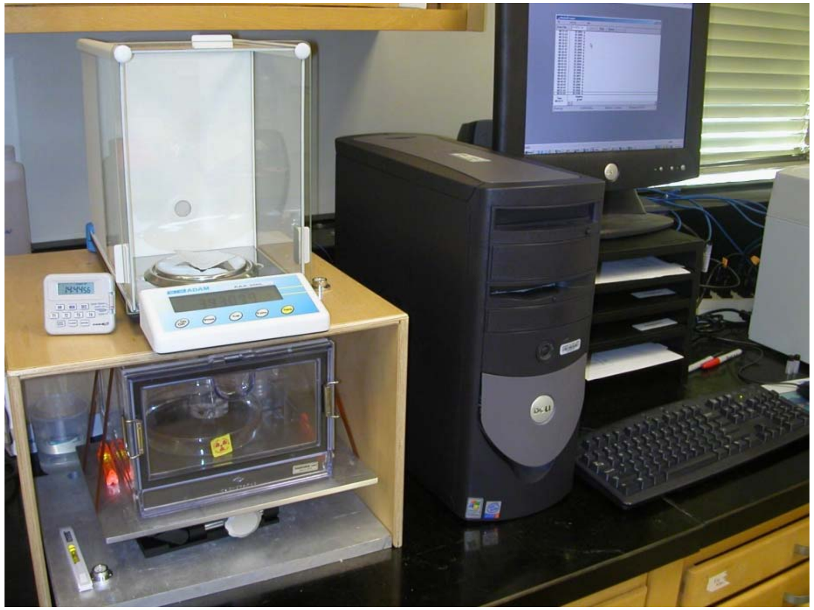

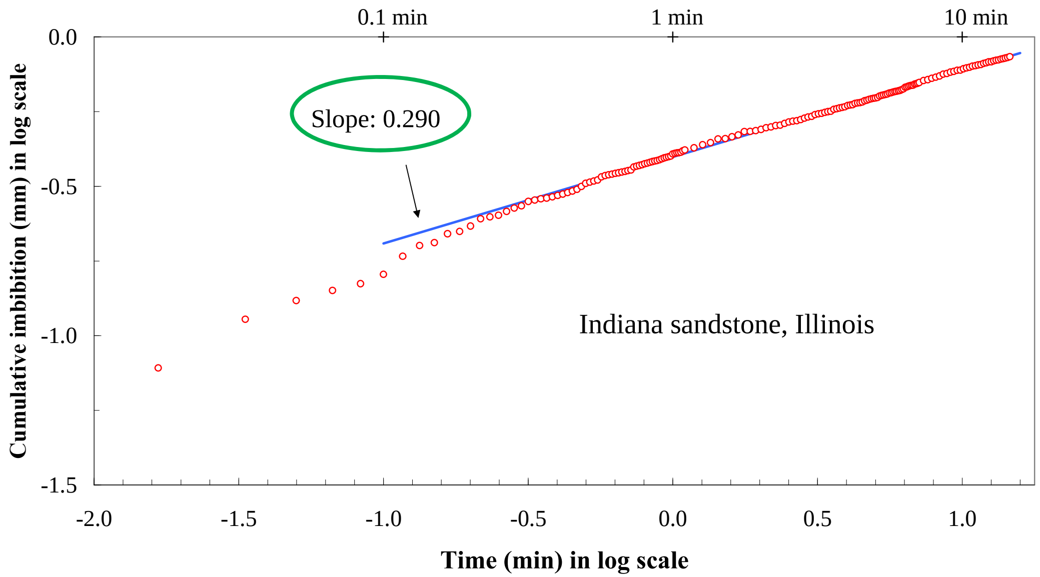

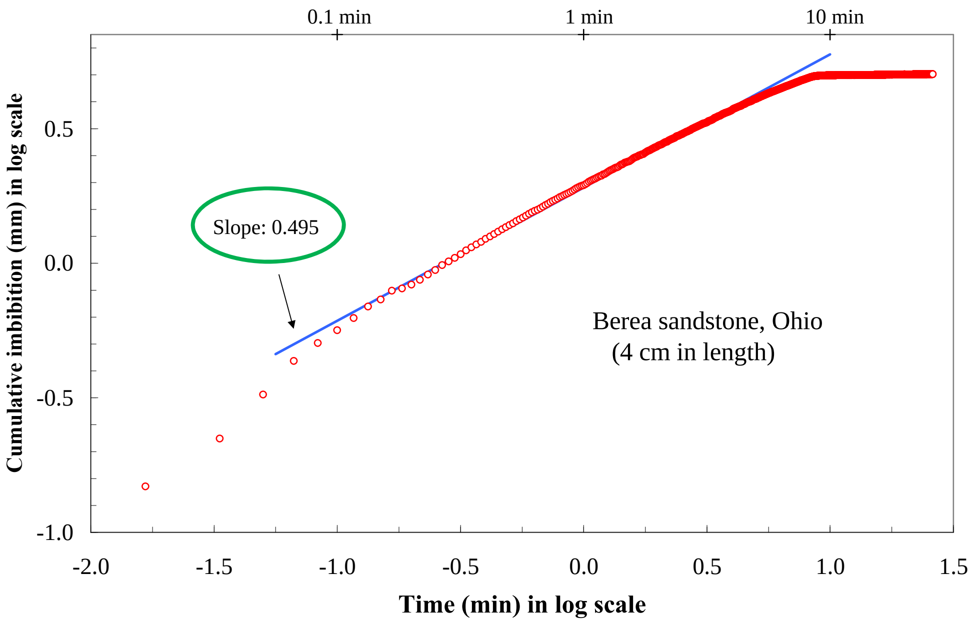

- Rock sample epoxy–coated along length → 1D flow
- Imbibition rate monitored continuously over time

Imbibition Results for Barnett Shale Samples

Depth	Sample dimension	Height/width	Imbibition slope
7,109 ft (2,167 m)	1.33 cm L×1.76 cm W ×1.43 cm H (Vertical)	0.93	0.214 ±0.059 (N=3)
	1.76 cm L×1.72 cm W ×1.32 cm H (Horizontal)	0.76	0.291 ±0.027 (N=3)
7,136 ft (2,175 m)	1.38 cm L×1.71 cm W ×1.72 cm H (Vertical)	1.12	0.269 ±0.0045 (N=3)
	1.73 cm L×1.73 cm W ×1.21 cm H (Horizontal)	0.70	0.216 ±0.040 (N=3)
7,169 ft (2,185 m)	1.35 cm L×1.79 cm W ×1.81 cm H (Vertical)	1.16	0.273 ±0.050 (N=3)
	1.24 cm L×1.78 cm W ×1.32 cm H (Horizontal)	0.87	0.357 ±0.006 (N=3)
7,199 ft (2,194 m)	1.24 cm L×1.74 cm W ×1.67 cm H (Vertical)	1.12	0.284 ±0.062 (N=3)
	1.74 cm L×1.72 cm W × 1.26 cm H (Horizontal)	0.67	0.282 ±0.047 (N=3)
7,219 ft (2,200 m)	1.37 cm L×1.74 cm W × 1.95 cm H (Vertical)	1.25	0.306 ±0.019 (N=3)
	1.69 cm L×1.71 cm W ×1.36 cm H (Horizontal)	0.80	0.264 ±0.046 (N=3)

Imbibition Results: Shape Effect

Rock	Core height/width	Imbibition slope
Berea Sandstone	1.18	0.649 ± 0.022
	2.35	0.488 ± 0.006
	4.71	0.494 ± 0.008
Welded tuff	0.40	0.513 ± 0.014
	1.00	0.371 ± 0.024
Dolomite	0.40	0.487 ± 0.035
	1.00	0.344 ± 0.004 → 0.556 ± 0.048
	1.16	0.300 ± 0.036
Indiana Sandstone	0.40	0.272 ± 0.047
	1.16	0.253 ± 0.006
	2.33	0.291 ± 0.008

Pore-Scale Network: Imbibition Simulation

- p is pore connectivity probability;

  p_c is the percolation threshold

- **Slope = 0.5 at high p**
- **Slope = 0.26 at p=p_c**
- **At intermediate p values, at some time or distance to the wetting front, the slope transitions from 0.26 to 0.50**

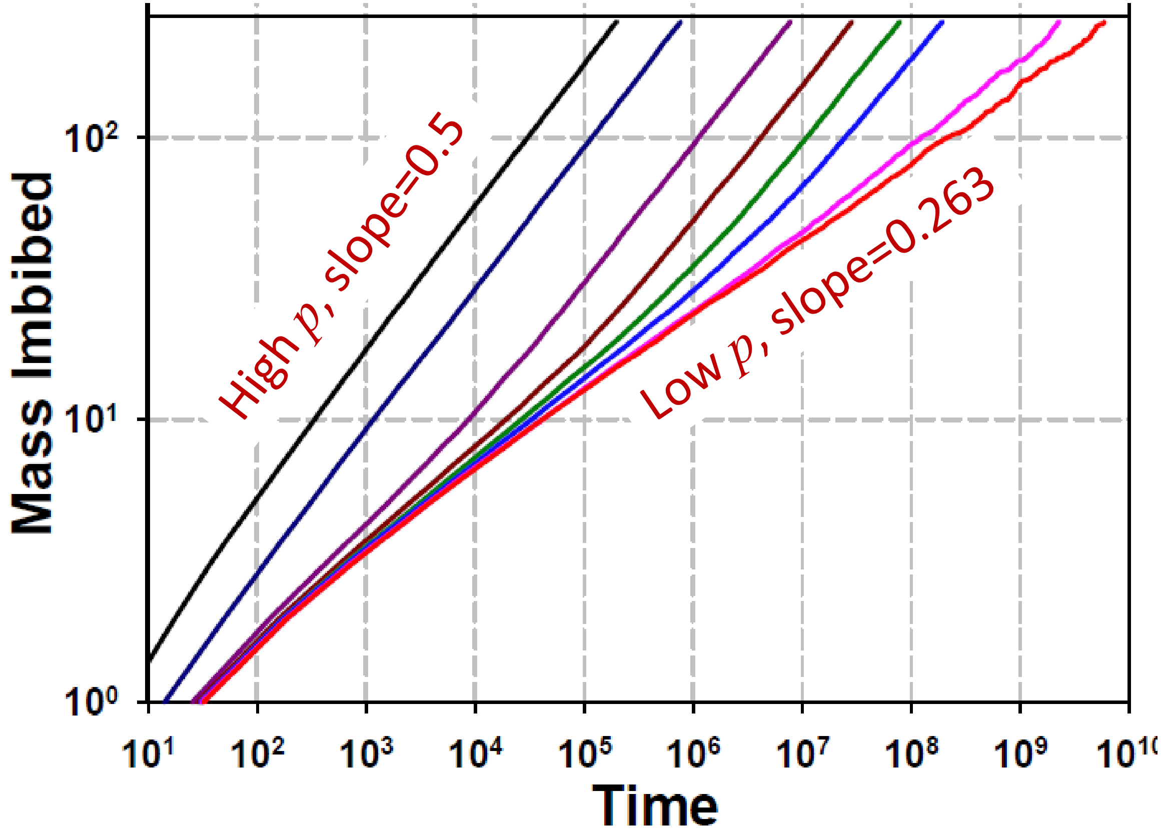

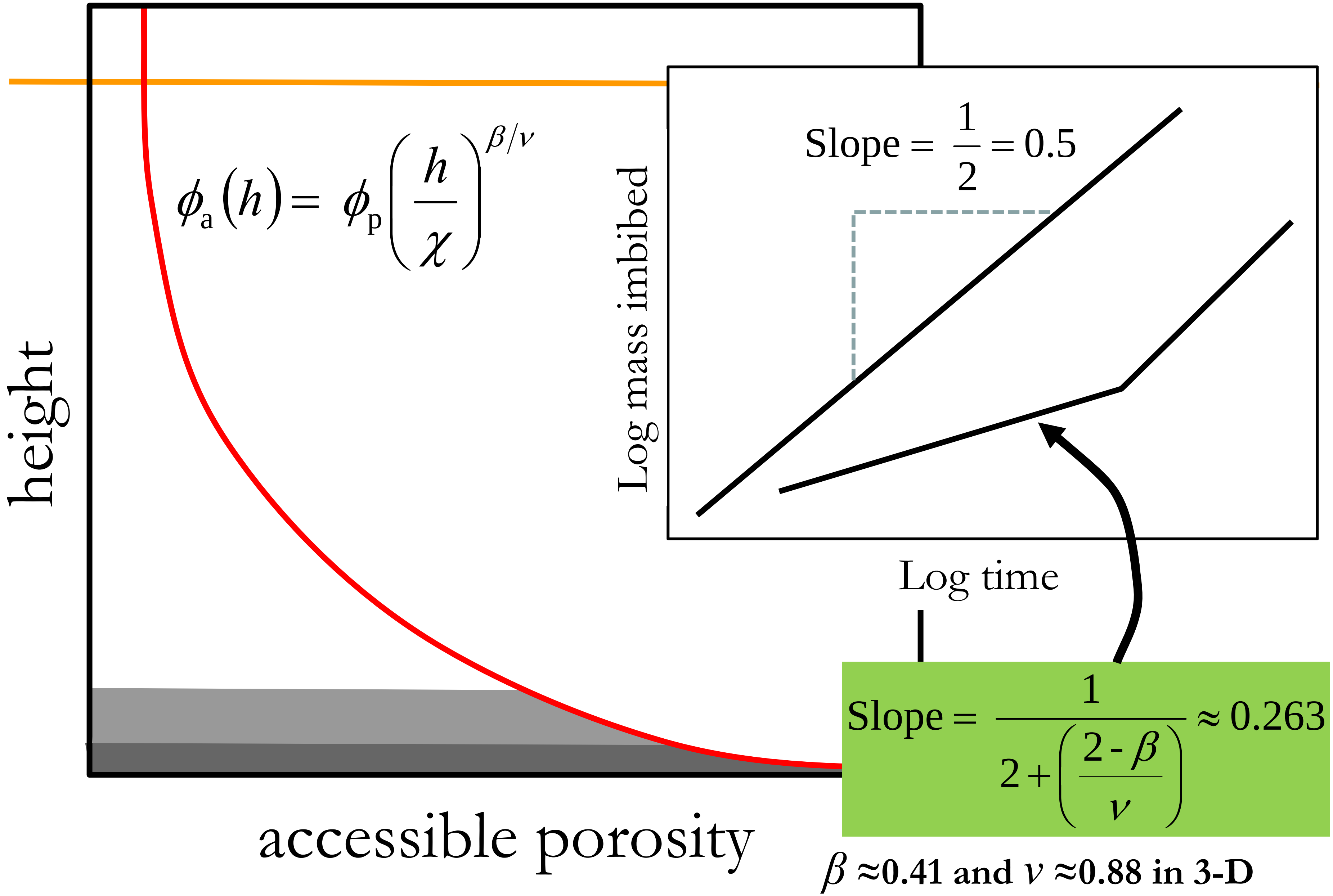

Stauffer, D., Aharony, A., 1994. *Introduction to Percolation Theory* (2nd Ed.). Taylor and Francis, London.

Tight Shales do Imbibe Liquids

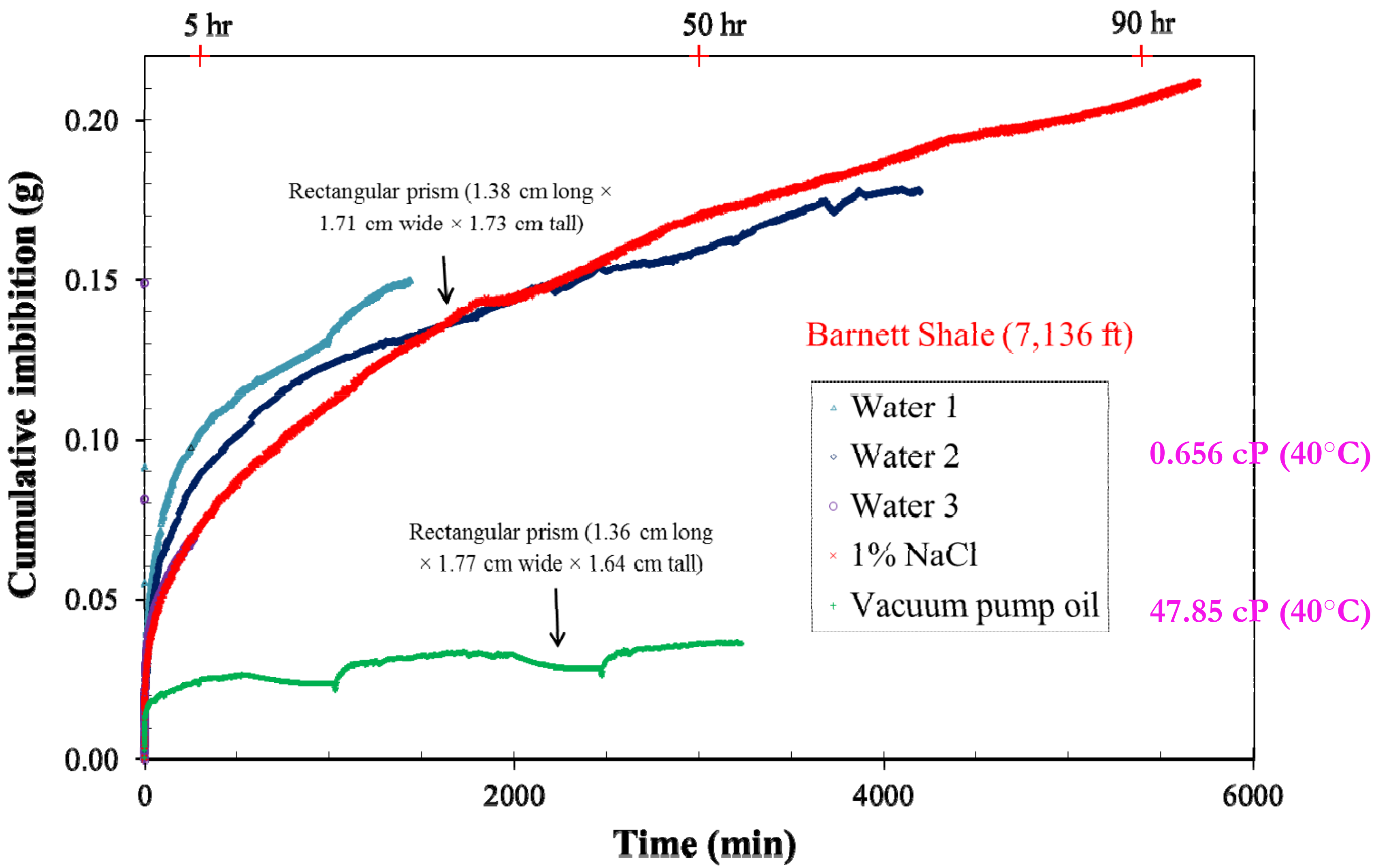

70–96% frac fluid not returned;
Imbibition of frac fluid affects gas production?

Imbibition: Work Plan

- More fluids: fracturing fluid; 1% NaCl; decane ($C_{10}H_{22}$)
- Suitable tracers in decane, and imbibition distance mapped by LA–ICP–MS

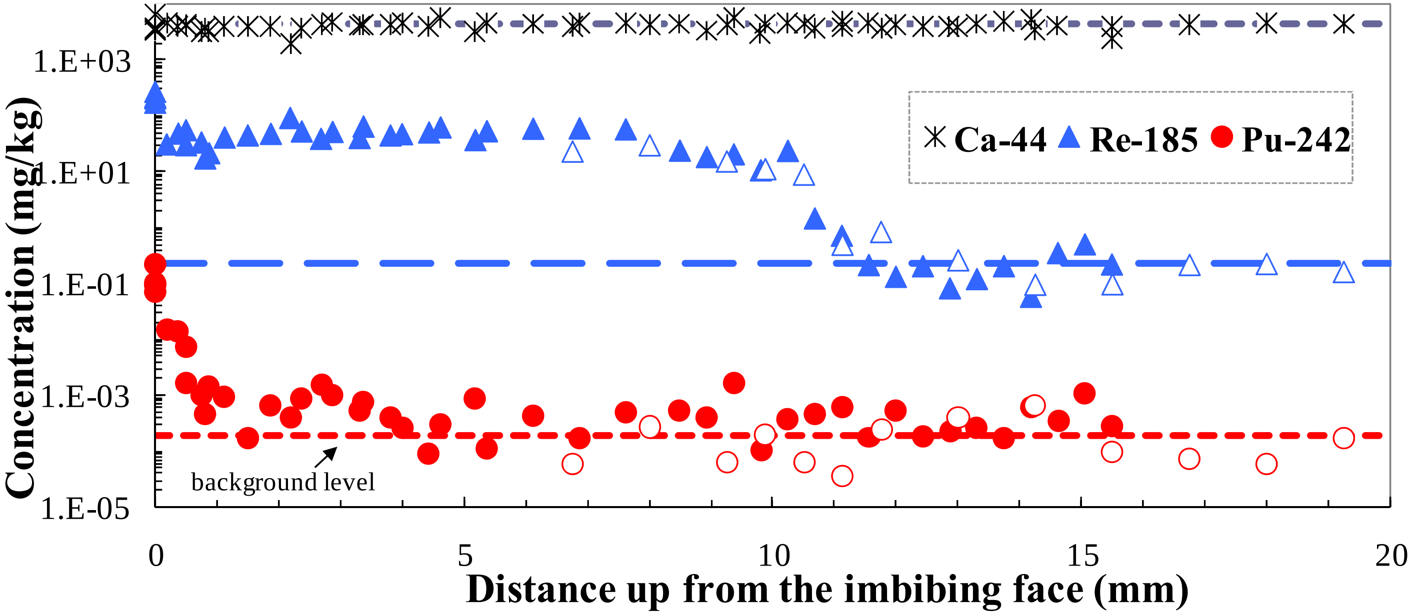

- Initially dry
- Strong capillarity
- Sharp front
- Advection dominant

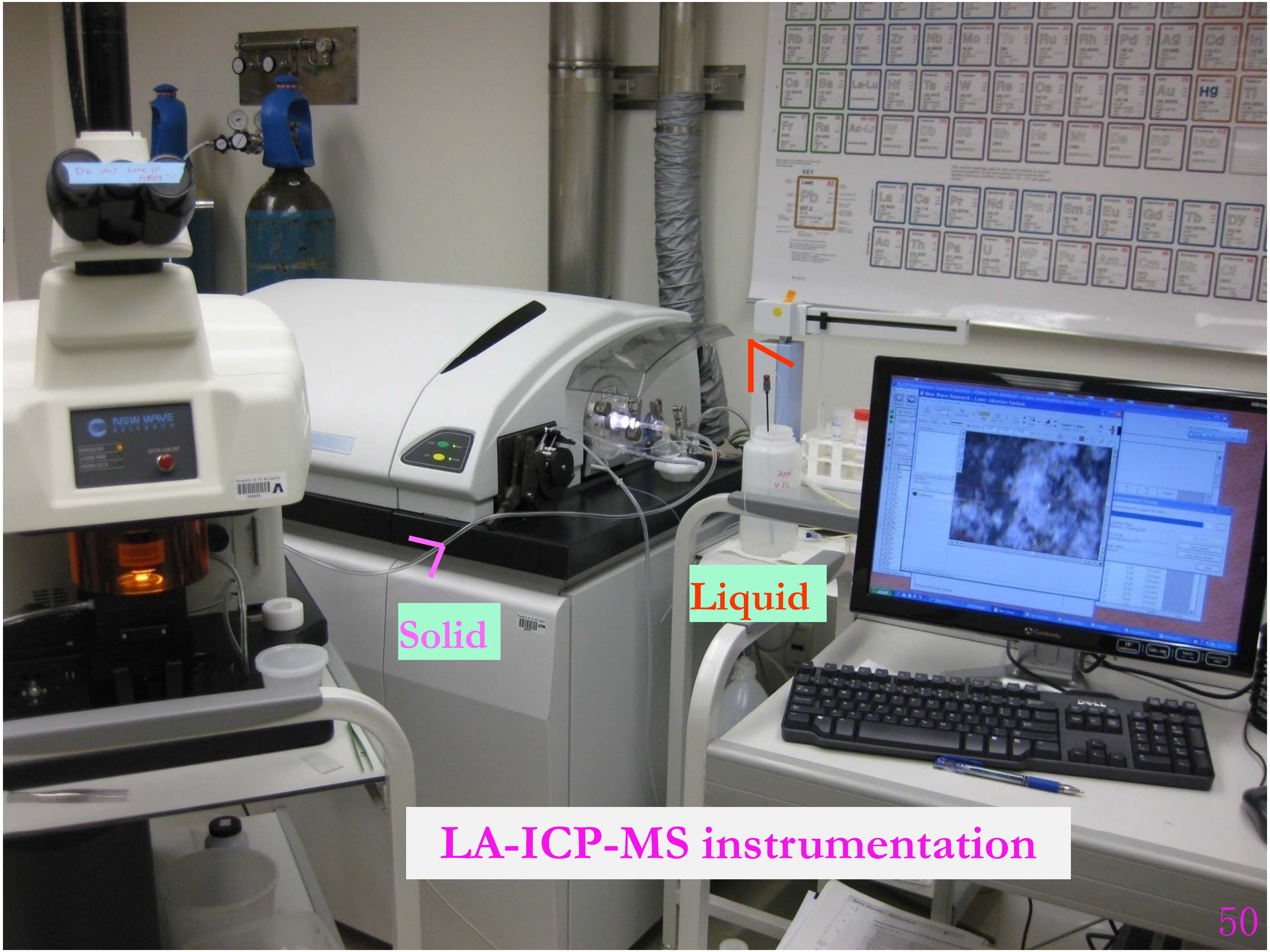

LA-ICP-MS instrumentation

3D Elemental Mapping: Edge-Accessible Porosity

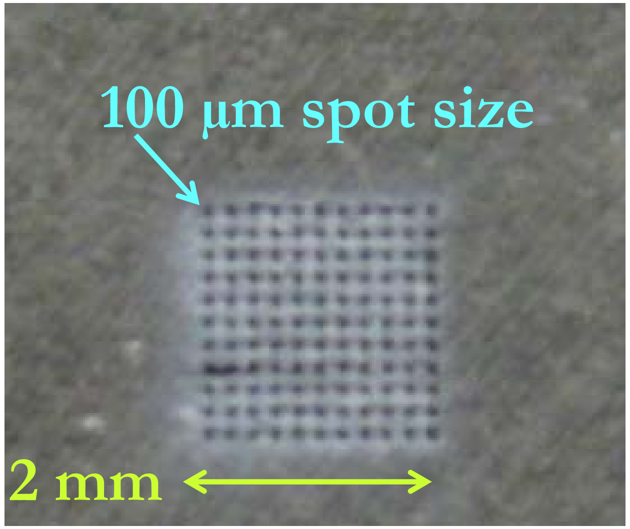

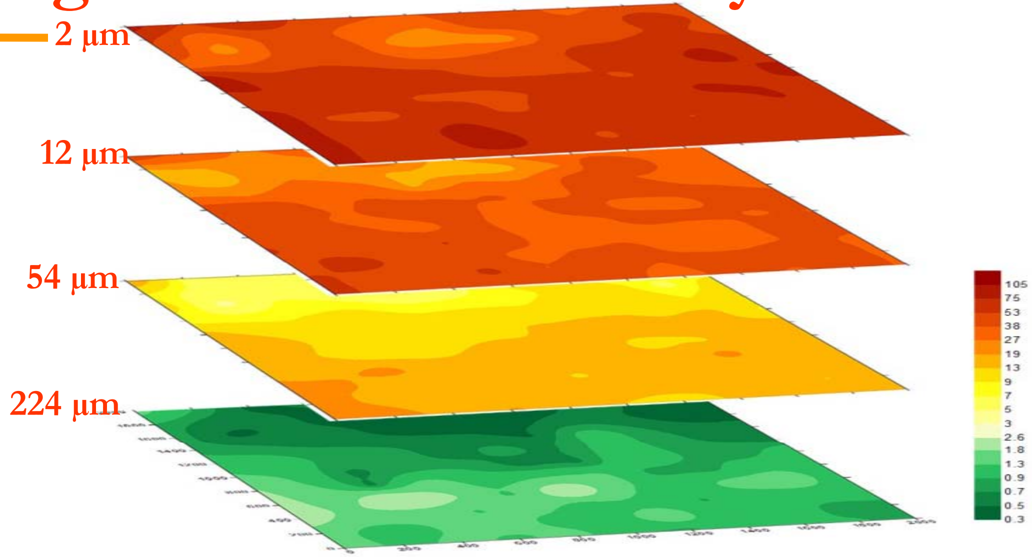

ReO_4^- (non-sorbing)

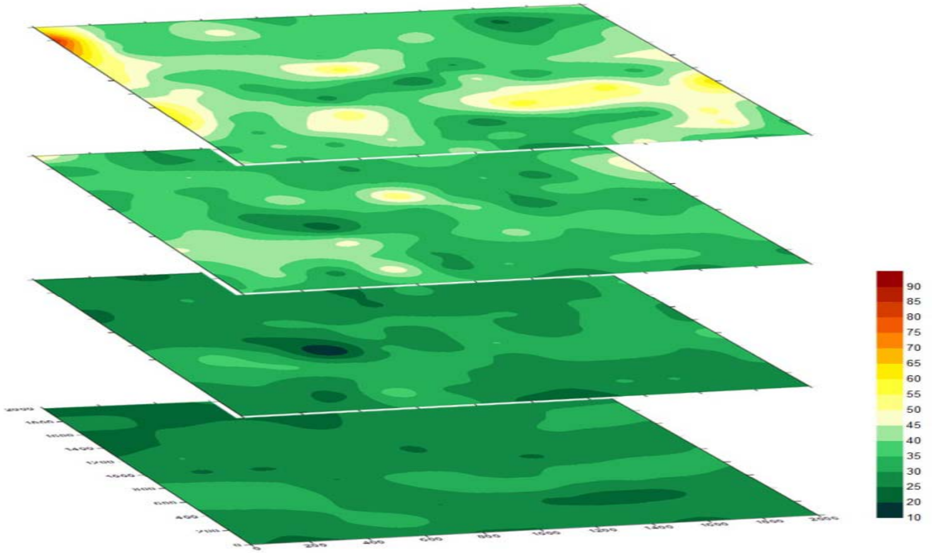

Rb (intrinsic)

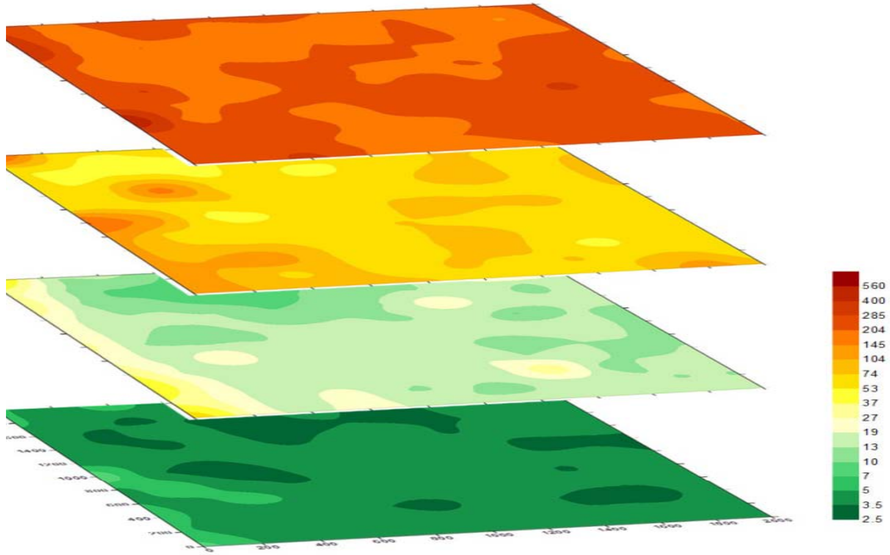

Co^{2+} (sorbing)

Averaged Concentration (N=121) vs. Depth

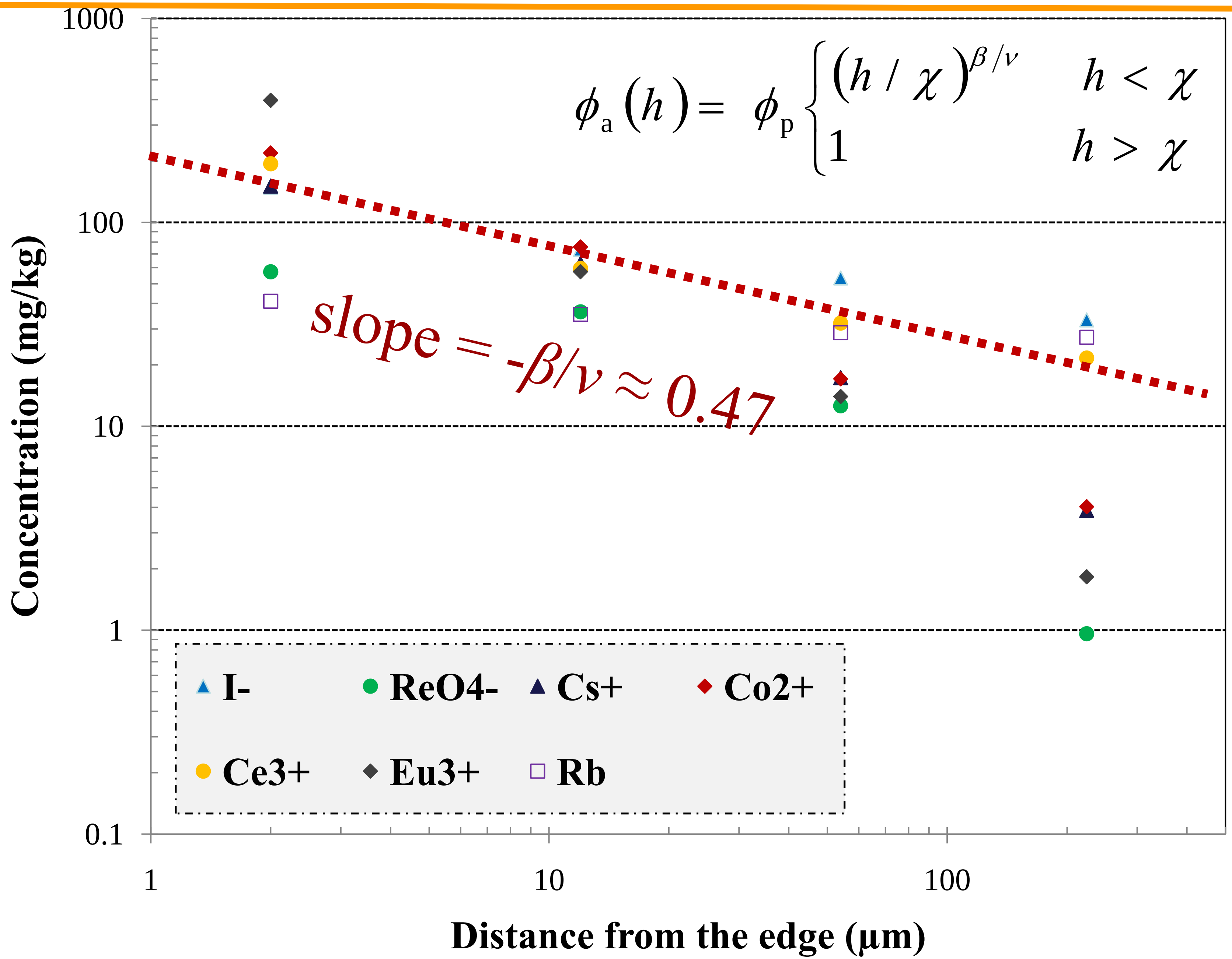

Liquid Tracer Diffusion in Saturated Samples

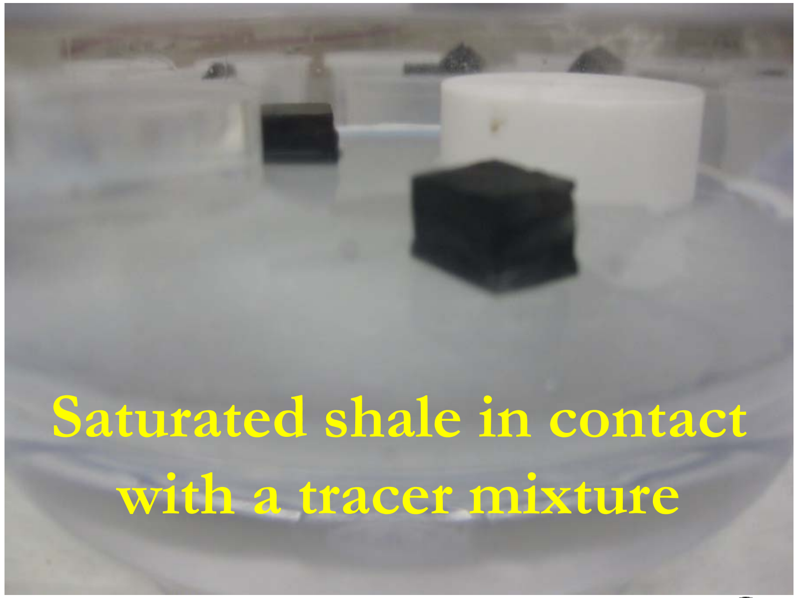

$$\frac{C}{C_0} = \frac{1}{2} erfc \frac{x}{2\sqrt{D_e t}}$$

$$\tau = \frac{D_0}{De}$$

Fitted tortuosity τ

✓ **100 (exterior); 10,000 (interior)**

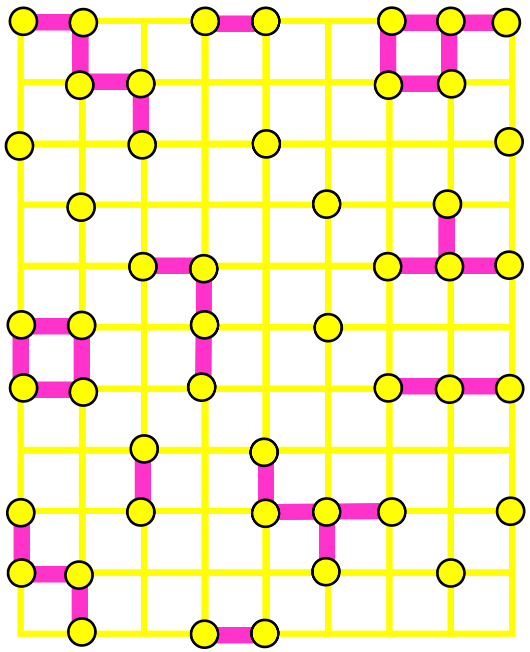

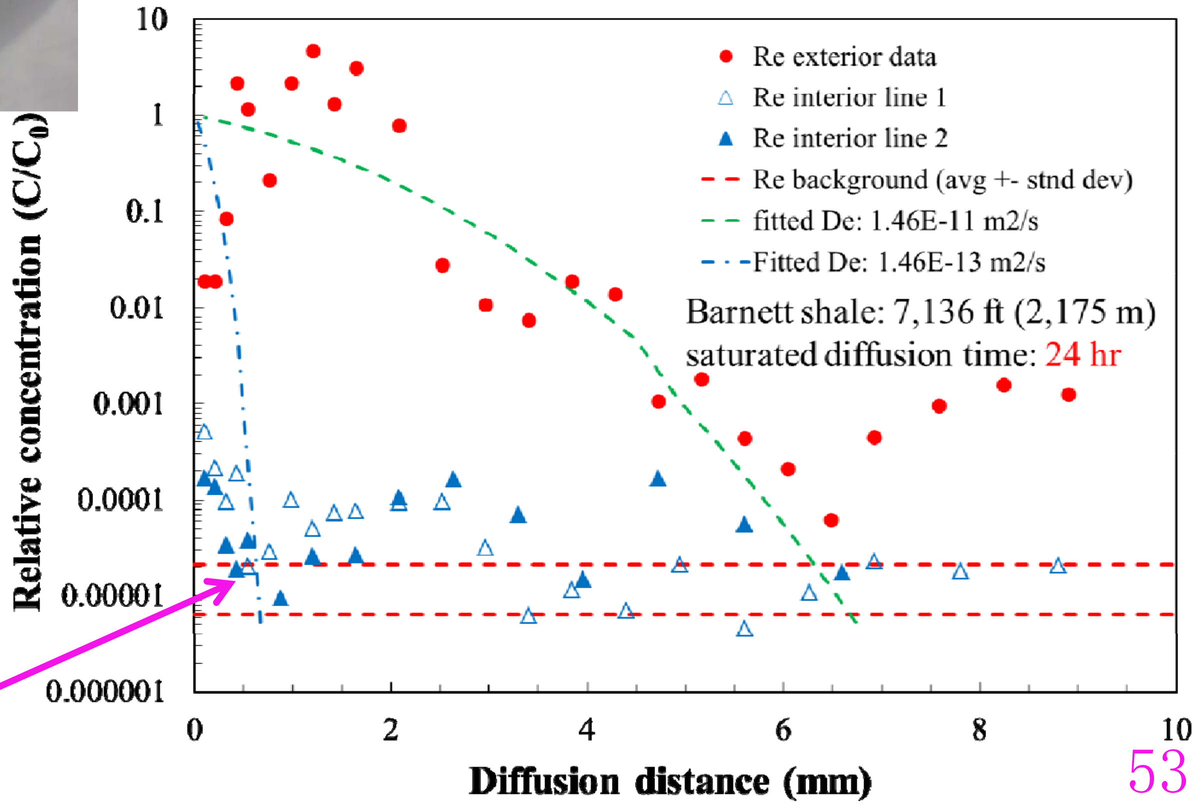

Three Data Points ⟵ anecdotal

- Gas molecule movement in shale on the order of 10 feet in the lifetime of a well - Dr. Mohan Kelcar, University of Tulsa.
- Gas molecule movement of about a meter/year modeled by Nexen's Unconventional Team, presented at Global Gas Shales Summit, Warsaw, Poland.
- Gas molecule movement of a few feet/year modeled by Dr. Chunlou Li, Shale Gas Technology Group.

$$\boxed{\frac{C(x,t)}{C_0} = erfc\left(\frac{x}{2(D_e t)^{0.5}}\right)}$$

$$\boxed{D_e = \frac{\delta D_0}{\tau}}$$

For C/C_0=0.5 @ 1 m/y, τ=613

For C/C_0=0.01 @ 1 m/y, τ=9,800

LaFollette, R. 2010. Key Considerations for Hydraulic Fracturing of Gas Shales. Manager, Shale Gas Technology, BJ Services Company, September 9, 2010.
www.pttc.org/aapg/lafollette.pdf


BJ Services (Baker Hughes) in Tomball, TX
BAKER HUGHES
Sep. 2012

Gas Diffusion in Partially–Saturated Shale Powder

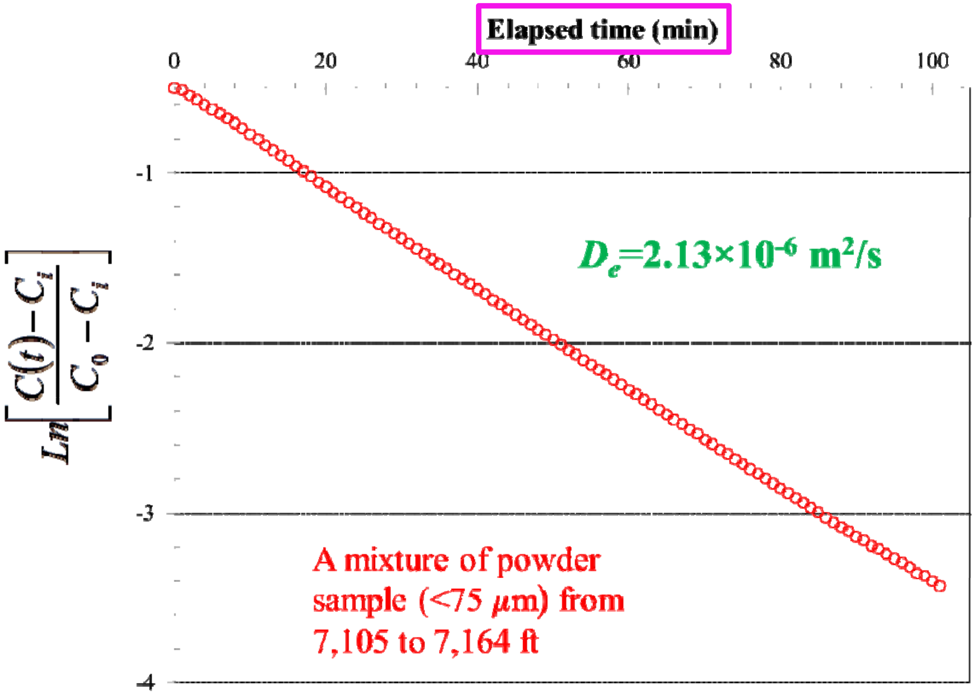

Water saturation	Air porosity (%)	D_e (m²/s)	Tortuosity
Air-dry	39.2	2.13×10^{-6}	9.59
10%	33.9	1.56×10^{-6}	13.1
20%	20.0	5.11×10^{-7}	39.8

- Powdered shales (with pore networks effects minimized) still exhibit tortuous pathways
- Tortuosity related to water saturation

Multiple Approaches to Studying Pore Structure

- Imbibition with samples of different shapes (UTA)
- Edge–accessible porosity (UTA)
- Liquid and gas diffusion (UTA)
- **Mercury injection porosimetry (UTA)**
- **N_2 adsorption isotherm (Saitama Univ.; Quantachrome)**
- **Water vapor adsorption isotherm (UTA)**
- **Nuclear Magnetic Resonance Cryoporometry (Lab-Tools, Ltd., UK)**
- SEM imaging after Wood's metal impregnation (Univ. Hannover; Swiss EPMA)
- Microtomography (high–resolution, synchrotron) (PNNL–EMSL; Swiss Light Source; Univ. Hannover; Saitama Univ.)
- Focused Ion Beam/SEM imaging (PNNL–EMSL)
- *Small–Angle Neutron Scattering (SANS) (LANL, NIST)*
- Pore–scale network modeling (ISU)

http://www.beg.utexas.edu/abs/abstract.php?d=2012-09-14

MIP Intrusion Results: Pore–Throat Size Distribution

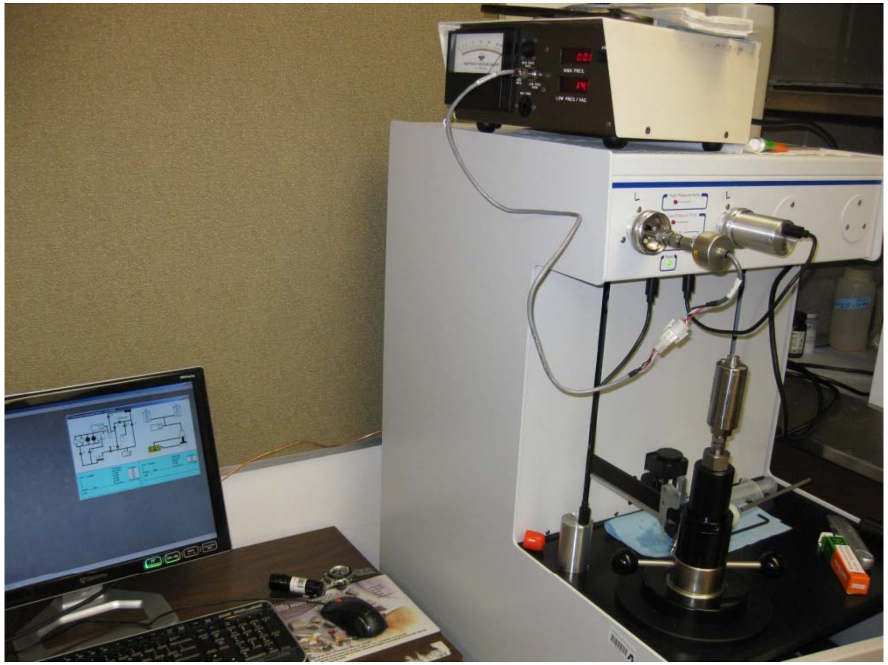

Barnett Shale sample (~15 mm cube) in the penetrometer

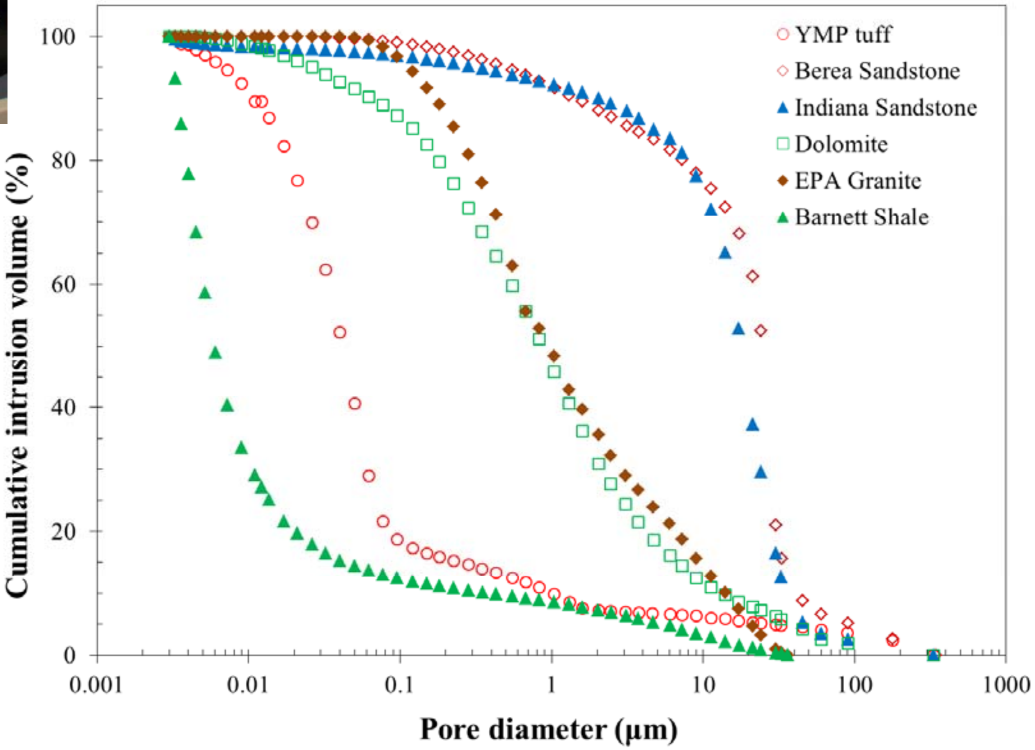

- Mercury Injection Porosimetry (MIP)
- Measurable pore diameter range: 3 nm to 360 µm

MIP Results: 6 Representative Rocks

Depth	Porosity (%)	Median pore-throat diameter (nm)	Permeability (µdarcy)	Tortuosity
Berea Sandstone	22.9±1.72	23,776±876	$(595\pm21.2)\times10^{3}$	3.31±0.33
Indiana Sandstone	16.4±0.4	19,963±2,932	$(221\pm40.8)\times10^{3}$	4.68±1.68
Welded Tuff	10.0±0.5	47±7.1	0.83±0.14	1,745±66
Dolomite	9.15	873	409	38.3
Barnett Shale (7,199')	5.97±1.43	6.1±0.3	$(4.96\pm1.42)\times10^{-3}$	12,867±16,224
NC Granite	1.05	970	12.4	38.2

Permeability: Katz and Thompson (1986; 1987)
Tortuosity: Hager (1998)

N_2 Sorption Isotherm

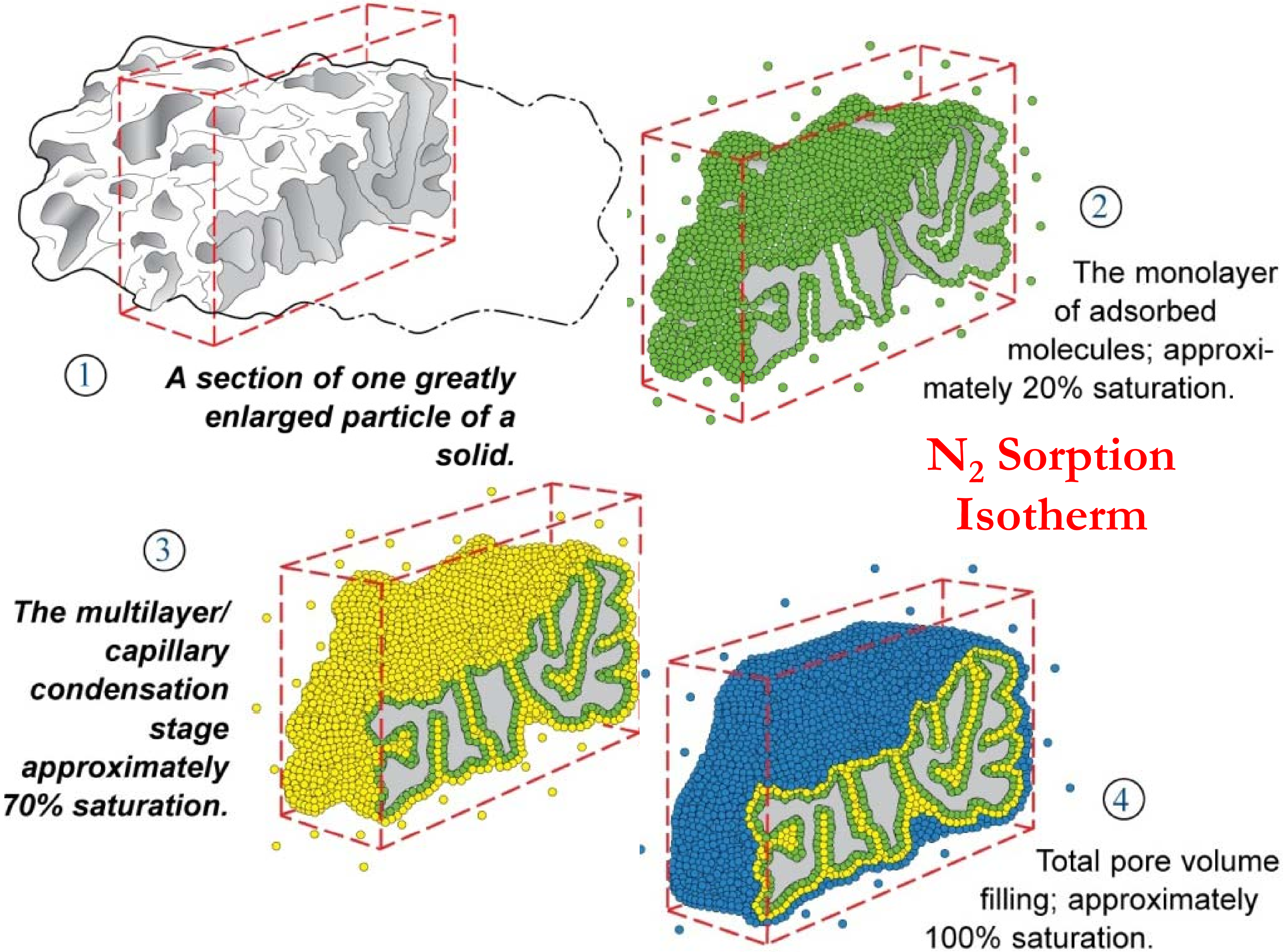

N_2 Sorption Isotherm

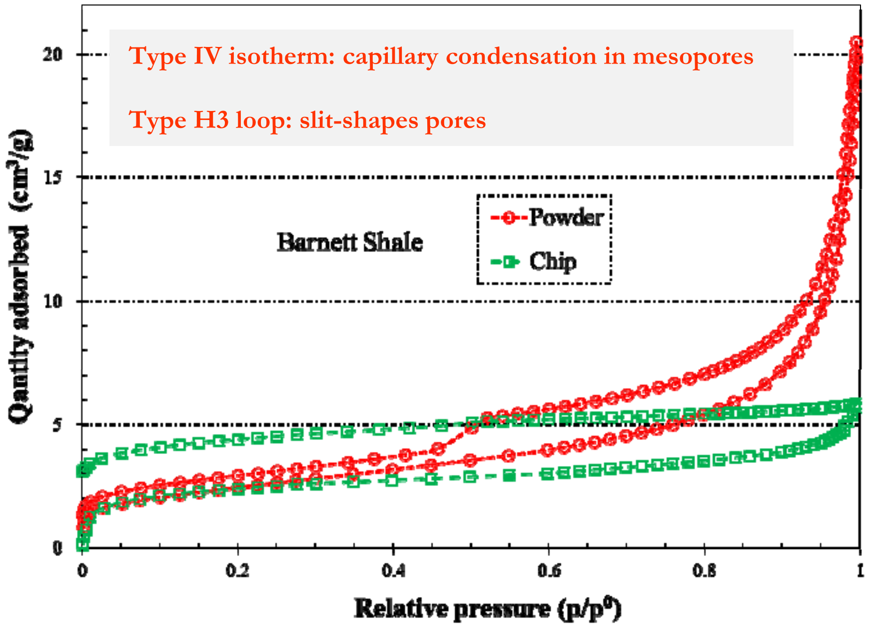

- Autosorb-IQ-MP by Quantachrome
- Pore size range: 0.35–500 nm

Shoichiro Hamamoto (Saitama University)

- Physical adsorption of N_2 at cryogenic temperatures (77K, -196°C)
- Molecular sorption by van der Waals forces; monolayer coverage; multilayer formation; capillary condensation; total pore volume filling
- Various theory to estimate pore–size distribution

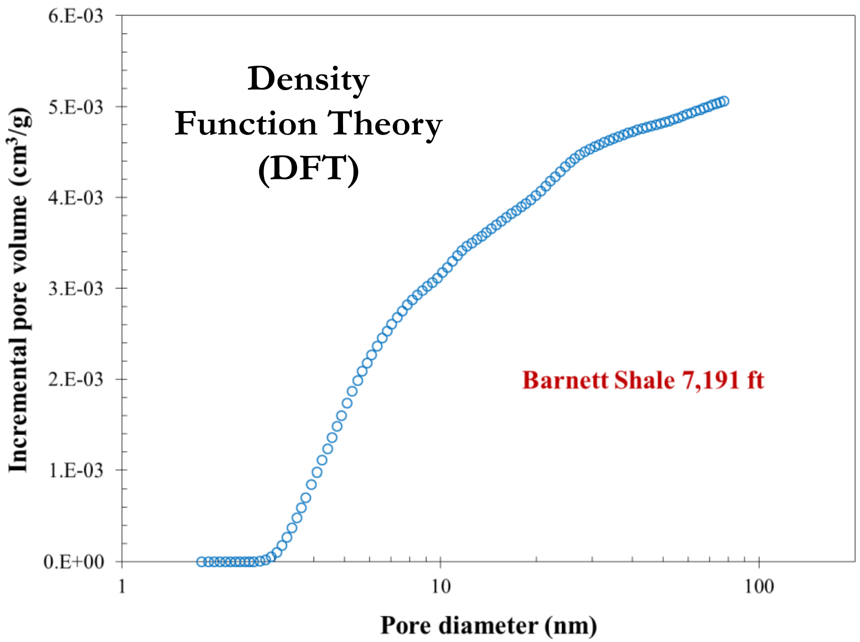

State Key Lab of Oil and Gas Reservoir Geology and Exploitation
Chengdu University of Technology

N_2 Sorption Isotherm: Hysteresis Loop

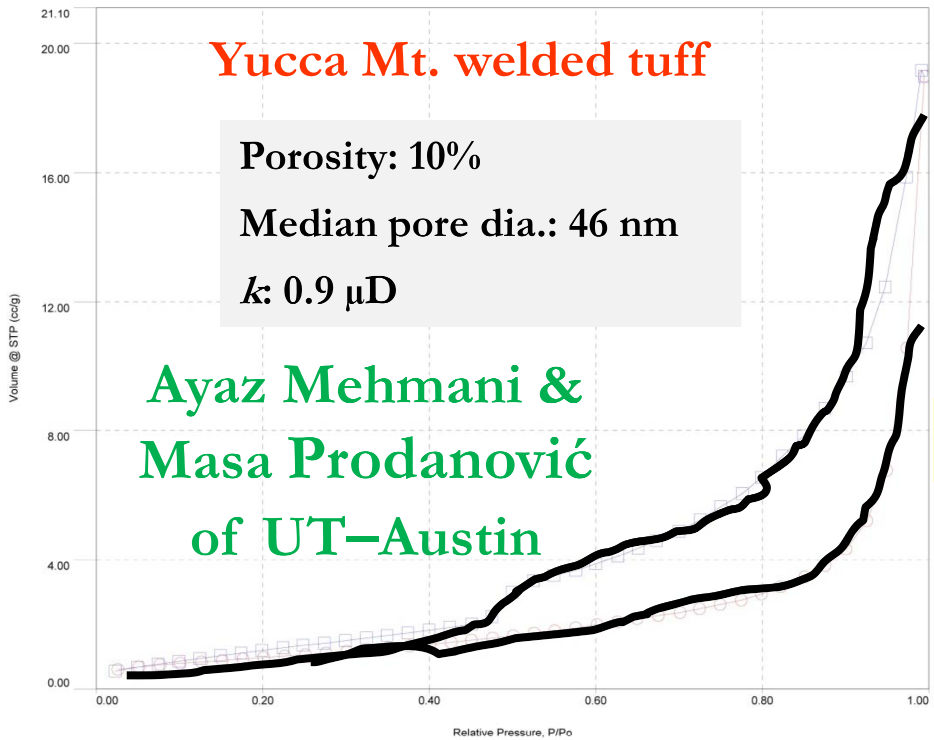

Only pore B is open to the surface

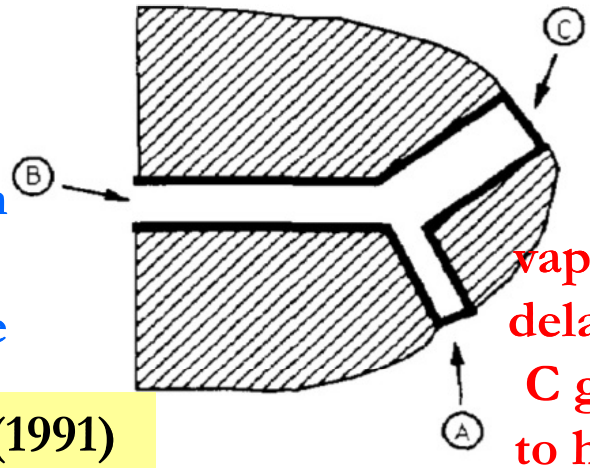

Seaton (1991)

N_2 vaporization delay in pore C gives rise to hysteresis

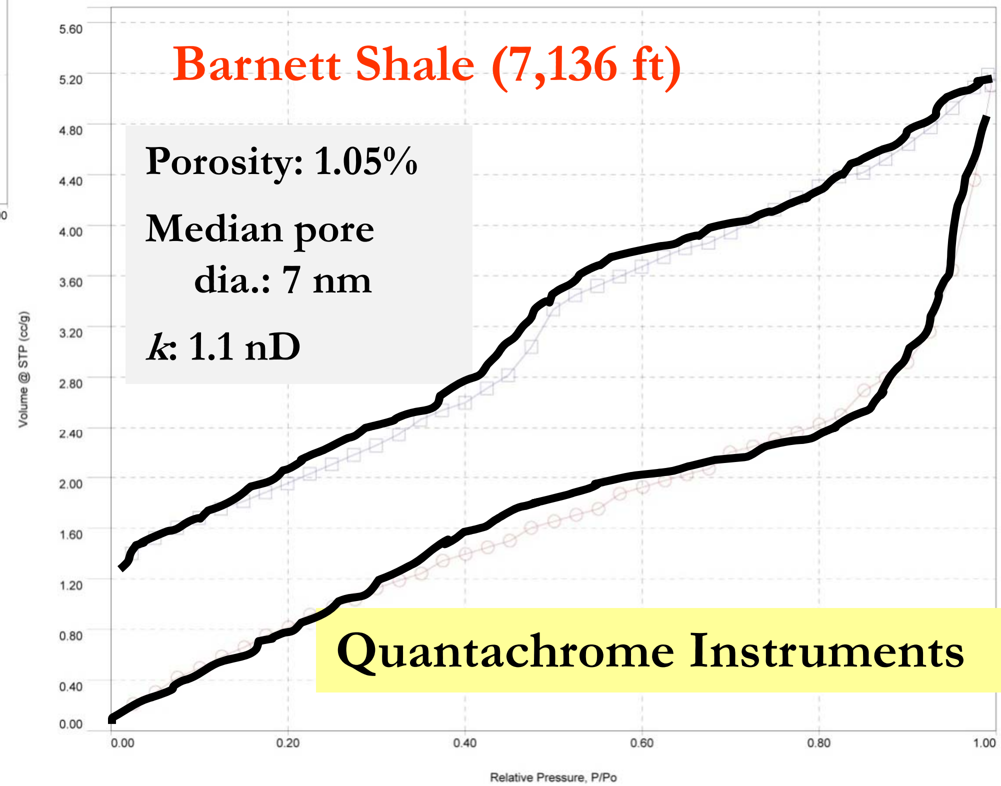

- Isotherm does not close for the Barnett Shale from extremely complex pore network effects
- CO_2 adsorption at 273.15K for micropore (0–2 nm) analysis indicates the presence of some volume of pores at ~0.35–0.7 nm

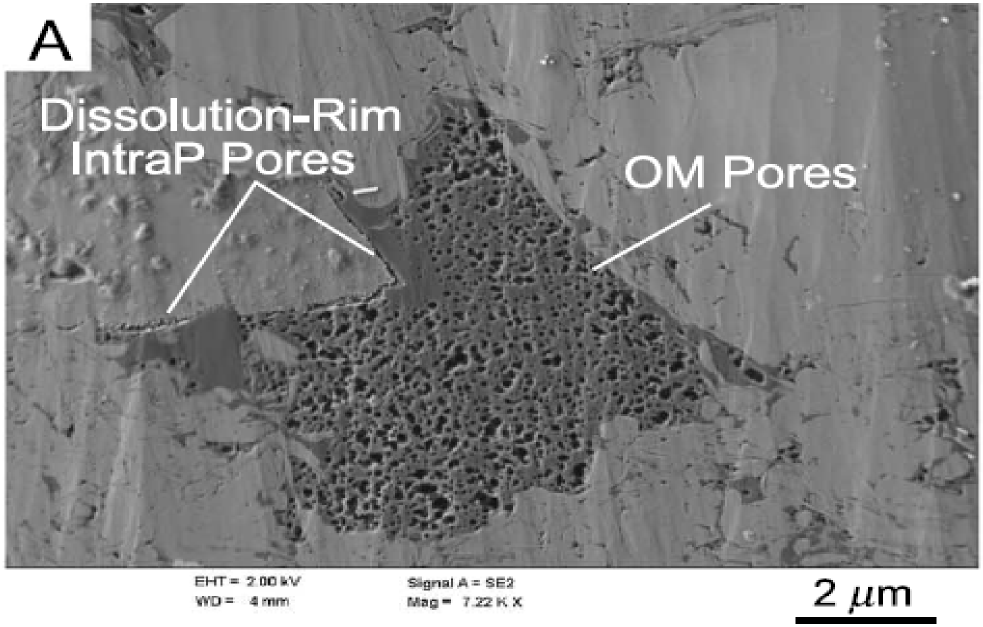

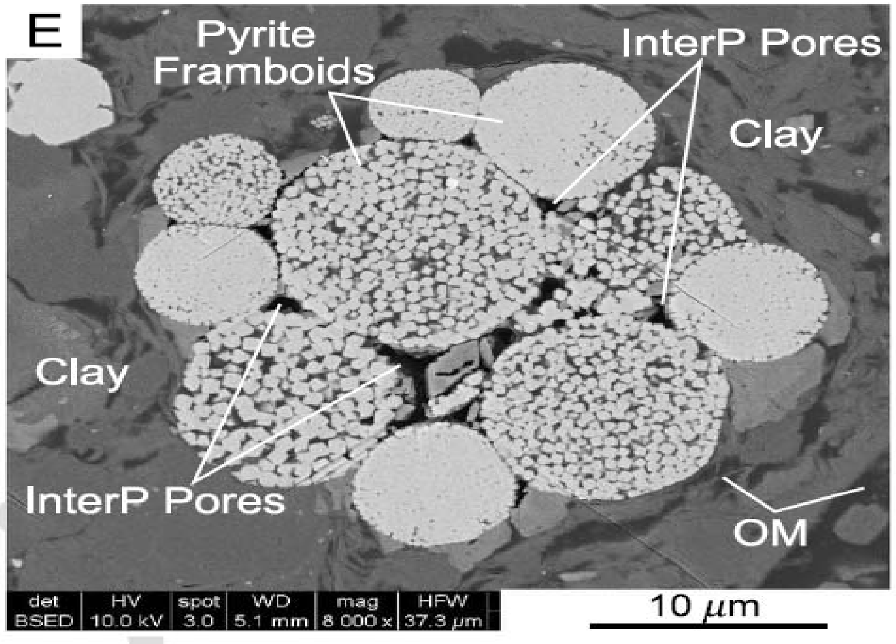

Example SEM images (Loucks et al., 2012) motivating two-scale pore network construction

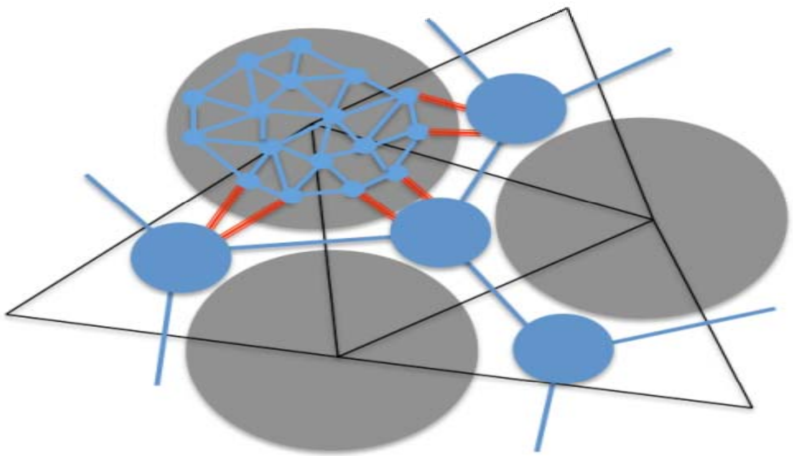

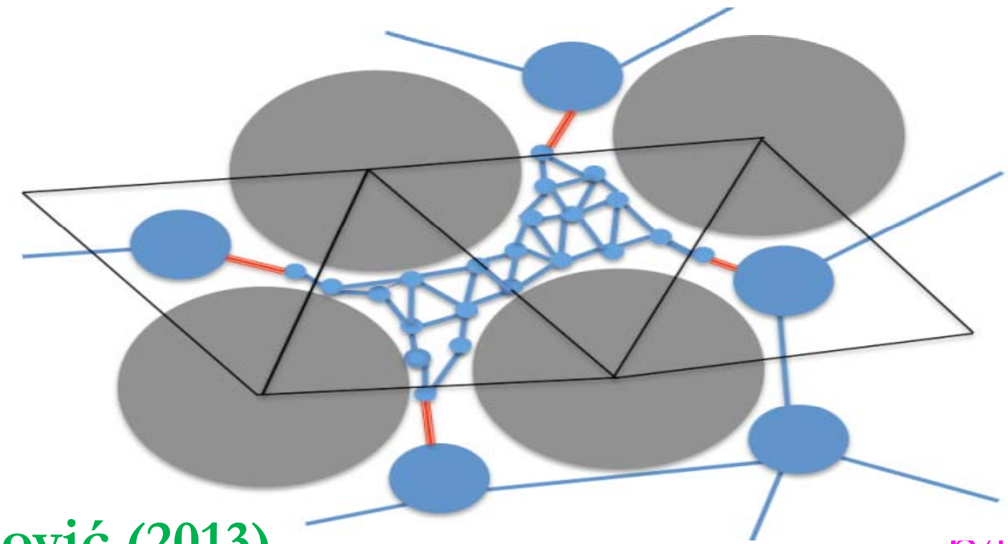

Mehmani and Prodanović (2013)

Water Vapor Absorption with RH Chambers

Drying ←									
	NaOH	CH_3COOK	K_2CO_3	$NaNO_2$	NaCl	KCl	Na_2SO_4	$CaSO_4$	H_2O
Wetting →									
RH (%)	6.96	22.9	43.2	66	75.4	84.8	93	98	99
P_c (MPa)	363	202	114	56.5	38.5	22.6	9.88	3.52	1.37
Dia. of meniscus curvature (nm)	0.80	1.45	2.54	5.13	7.55	12.9	29.4	106	212

Capillary Pressure Curve: Hysteresis Loop

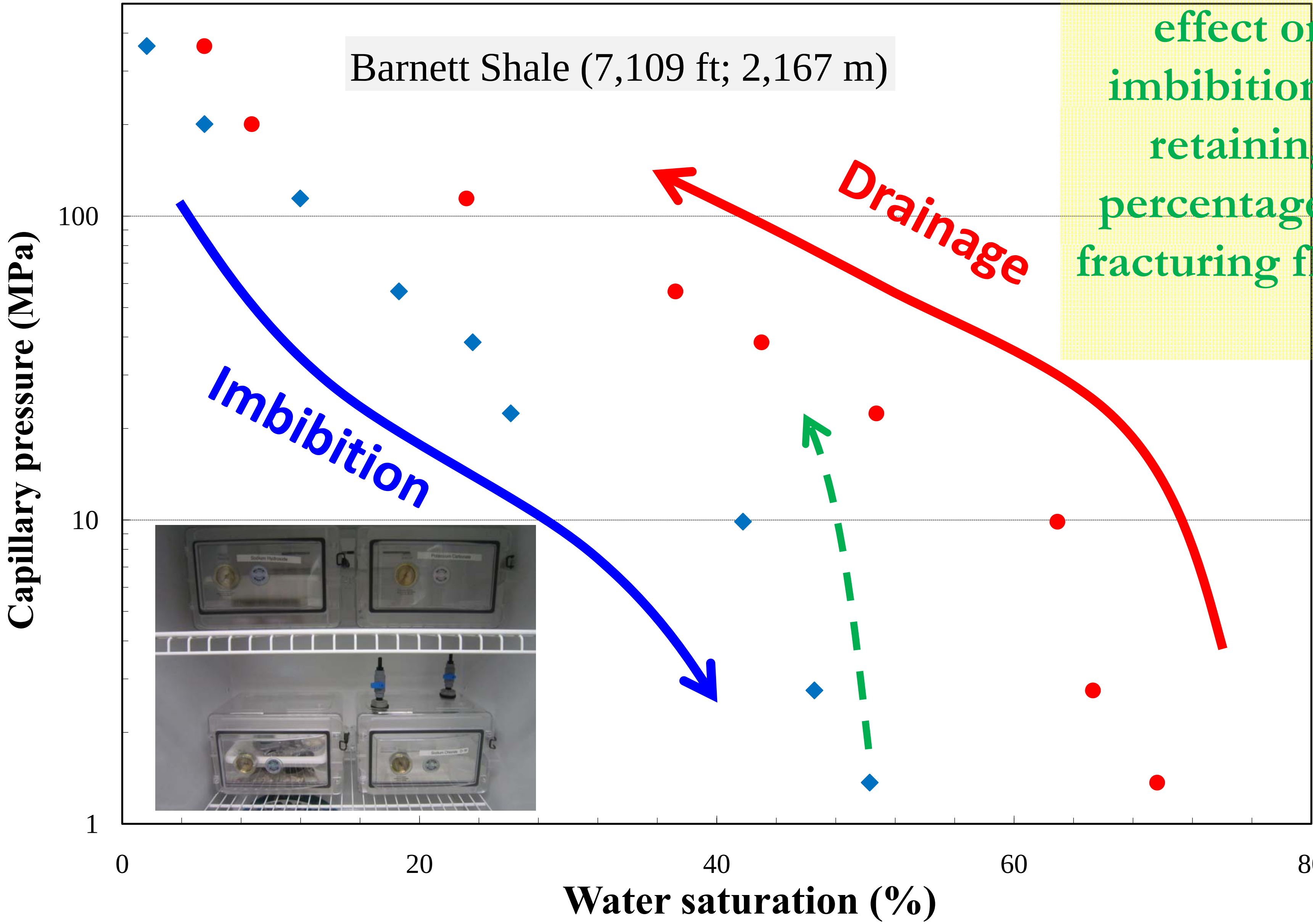

Hysteresis effect on imbibition & retaining percentage of fracturing fluid?

NMR Cyroporometry (NMRC)

- Use melting curve to calculate the pore size distribution by Gibbs–Thomson equation
- Measureable pore diameter range: ~1 nm to 10 µm
- Sample size: NMR probe/tube 2.5 mm dia. × 12 mm (30 to 300 mg)
- Measurement time: a few hrs to >24 hrs

Pore Size Distribution: Method Comparison

(NMRC data from Beau Webber, University of Kent

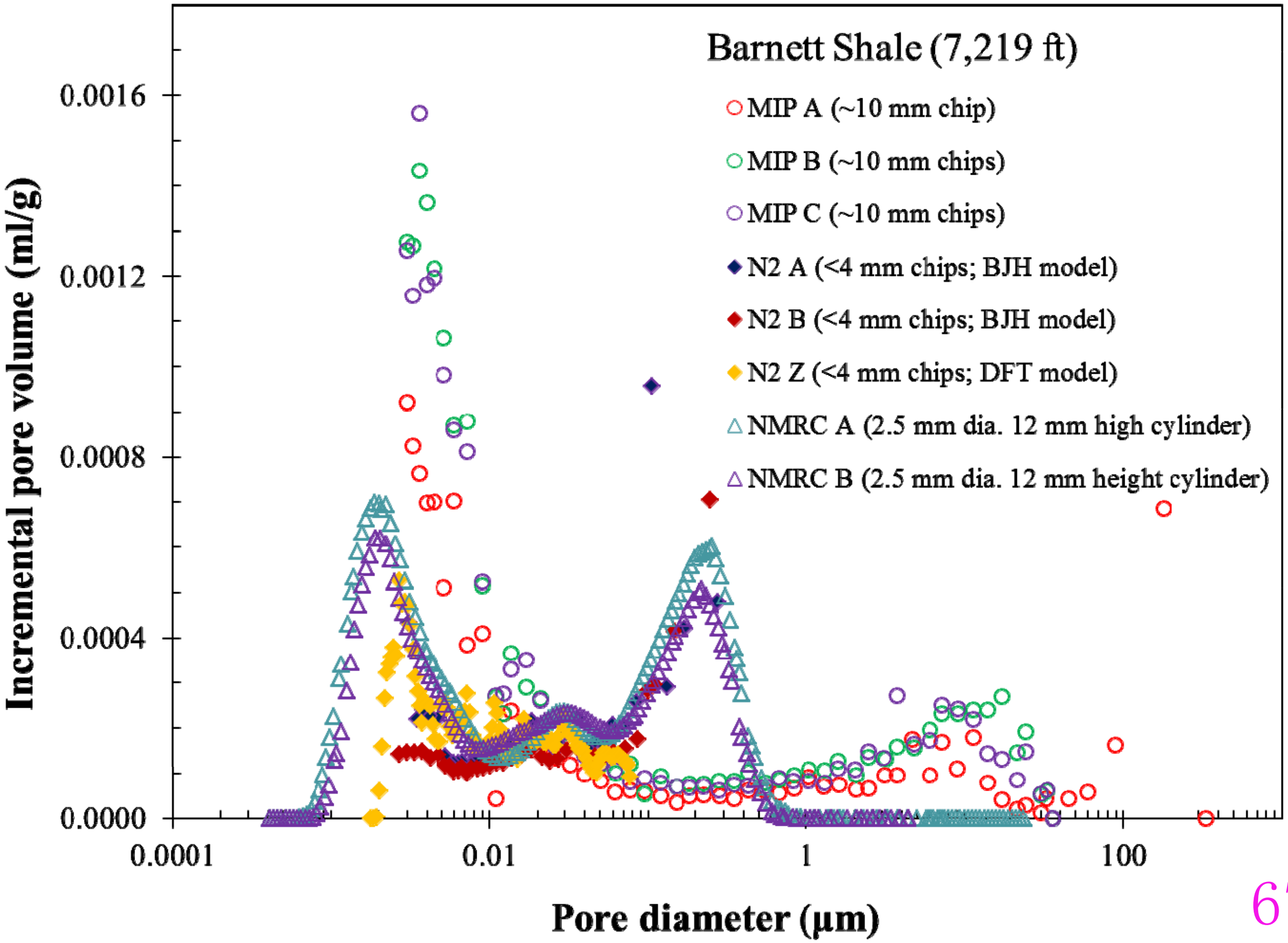

Multiple Approaches to Studying Pore Structure

- Imbibition with samples of different shapes (UTA)
- Edge–accessible porosity (UTA)
- Liquid and gas diffusion (UTA)
- Mercury injection porosimetry (UTA)
- N_2 adsorption isotherm (Saitama Univ.; Quantachrome)
- Water vapor adsorption isotherm (UTA)
- Nuclear Magnetic Resonance Cryoporometry (Lab-Tools, Ltd., UK)
- **SEM imaging after Wood's metal impregnation (Univ. Hannover; Swiss EPMA)**
- **Microtomography (high–resolution, synchrotron) (PNNL–EMSL; Swiss Light Source; Univ. Hannover; Saitama Univ.)**
- **Focused Ion Beam/SEM imaging (PNNL–EMSL)**
- ***Small–Angle Neutron Scattering (SANS) (LANL, NIST)***
- Pore–scale network modeling (ISU)

http://www.beg.utexas.edu/abs/abstract.php?d=2012-09-14

Wood's Metal Intrusion and Imaging

- Wood's metal (50% Bi, 25% Pb, 12.5% Zn, and 12.5% Cd) solidifies below 78°C without shrinking
- Heat the metal slowly (about 1 hr) above the melting point (120–150°C)

Dultz at al. (2006)

- Inject molten metal into the connected pore spaces under high pressure; sample size (up to 5 mm dia. and 15 mm long)
- Image metal distribution in polished sections 150 μm thick

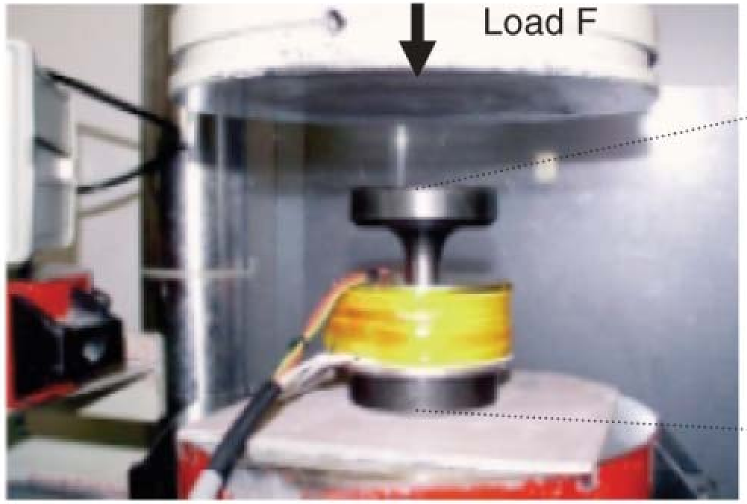

Kaufmann (2010)

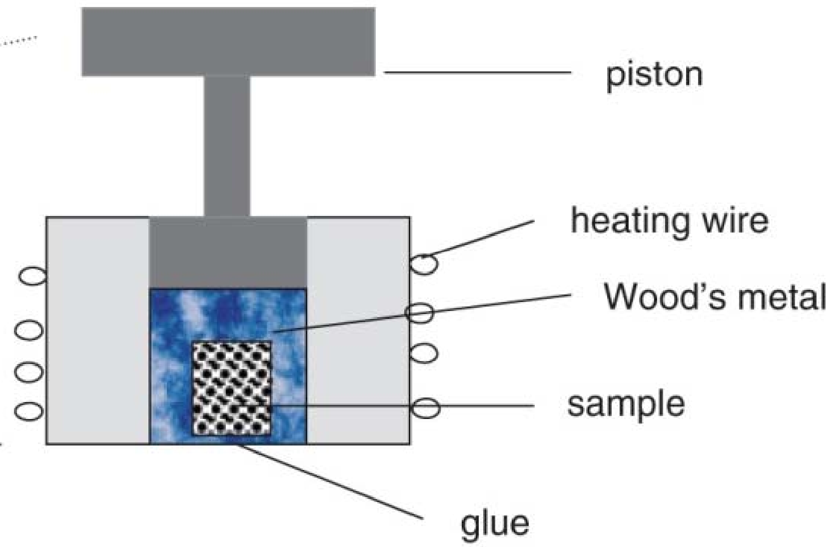

Fig. 1. Apparatus Wood's metal intrusion.

600 bars used (invade 20 nm)

Wood's metal injection

Stefan Dultz (University of Hannover)

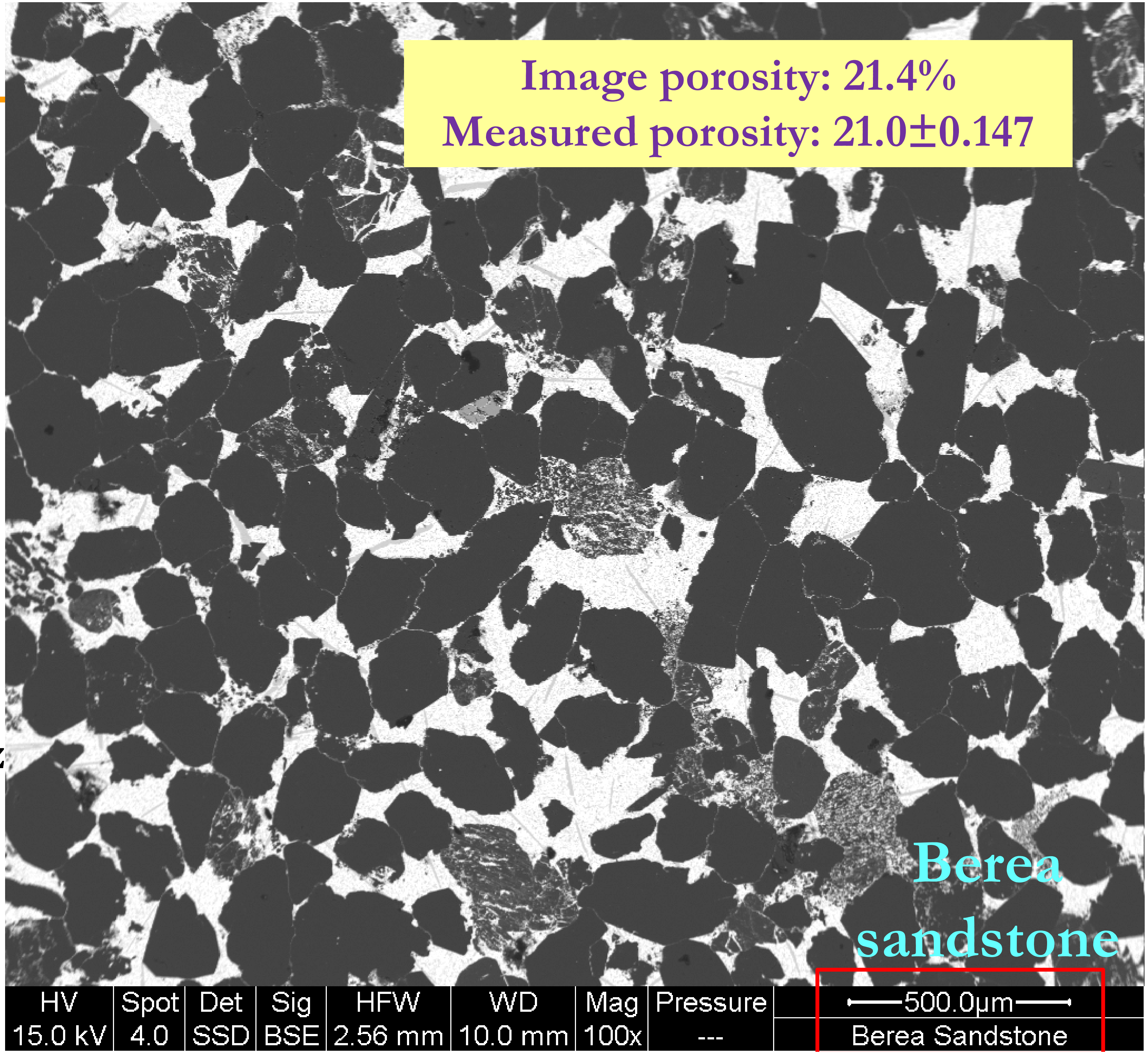

600 bars used (invade 20 nm)

Wood's metal injection

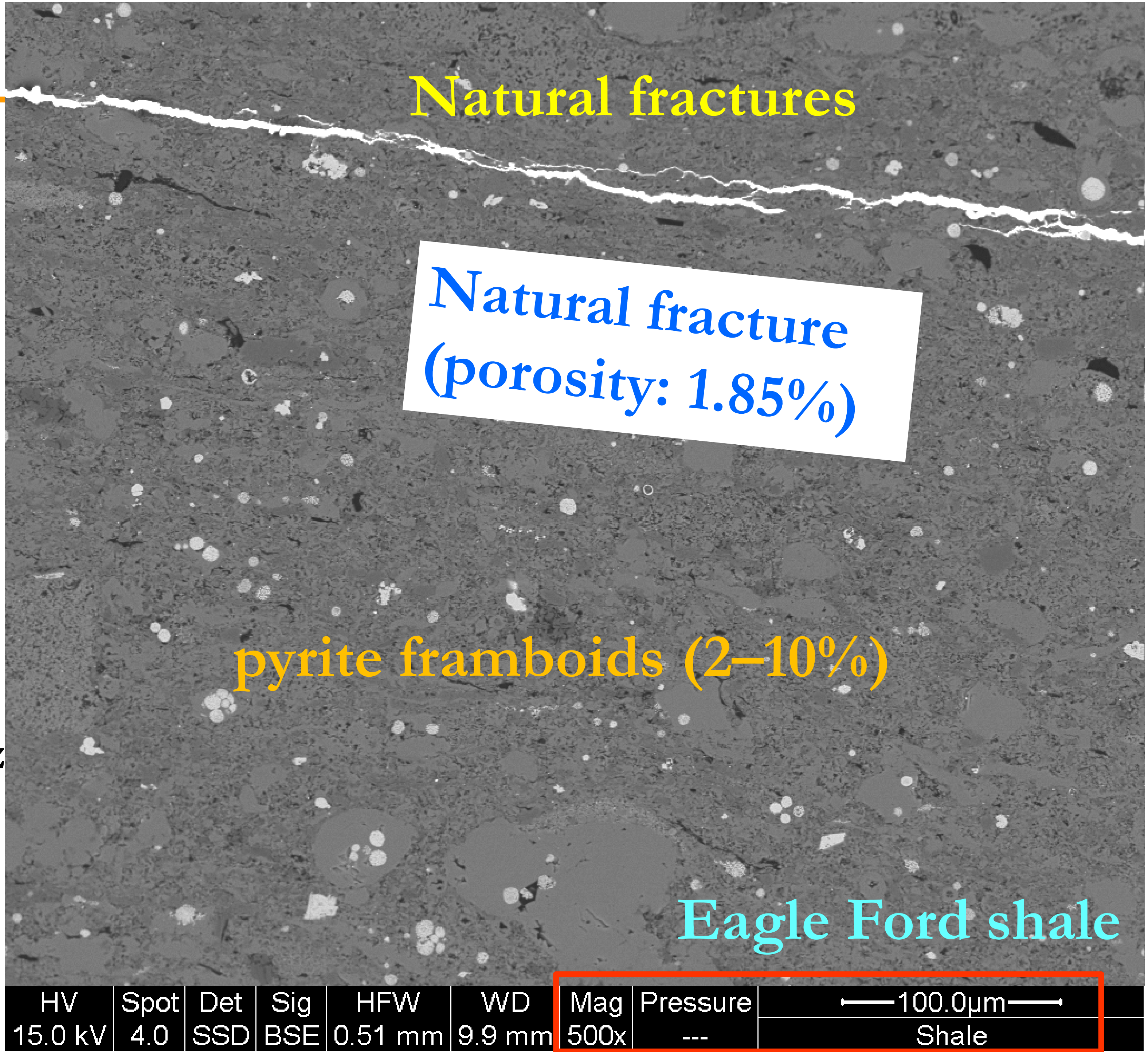

Stefan Dultz (University of Hannover)

1,542 bars used (invade 9 nm in pore dia.) by Josef Kaufmann of EPMA

Wood's metal injection

SEM-BSE by Stefan Dultz (University of Hannover)

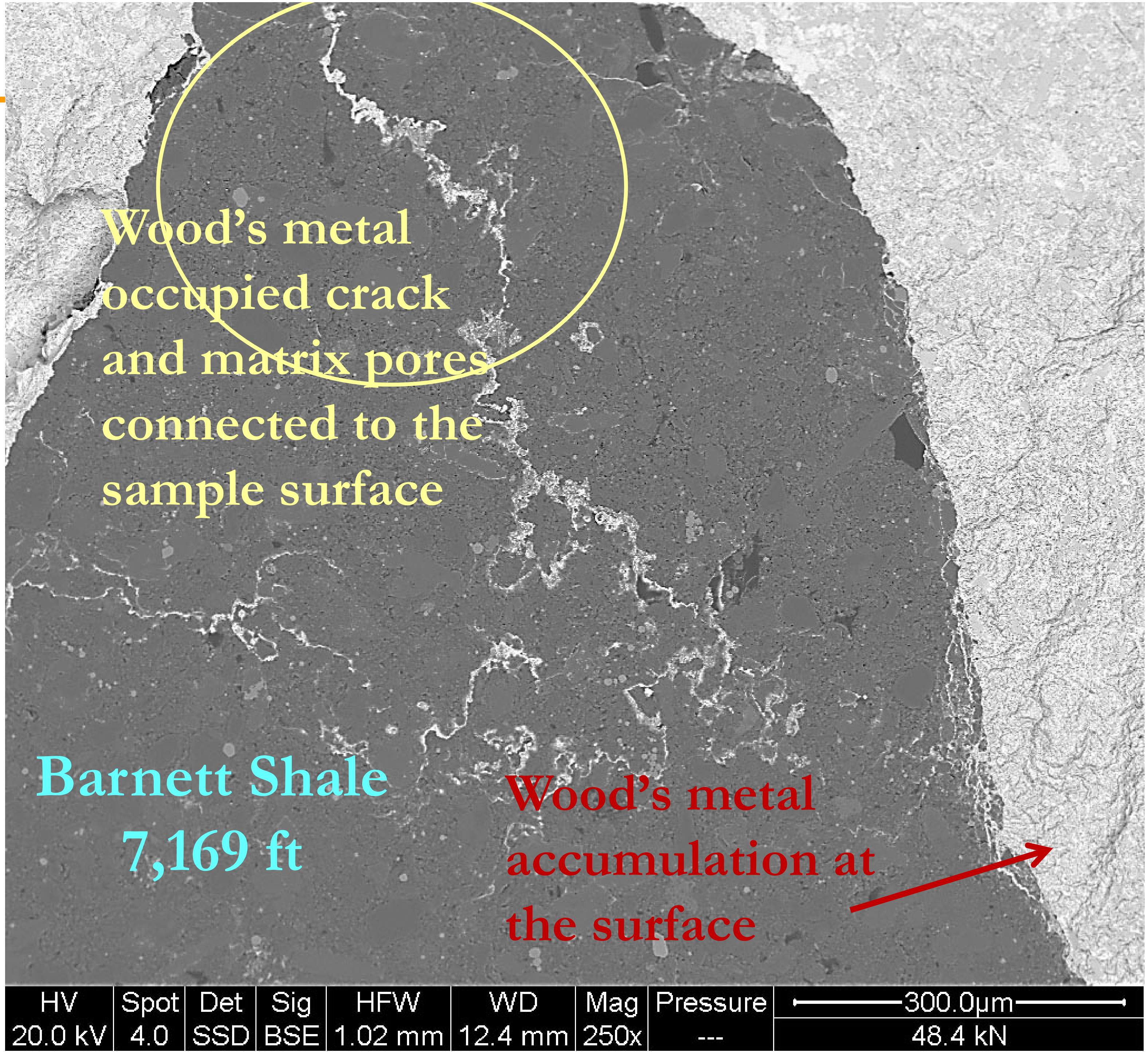

EMSL: Environmental Molecular Sciences Laboratory

CT Scanning Results: Indiana Sandstone

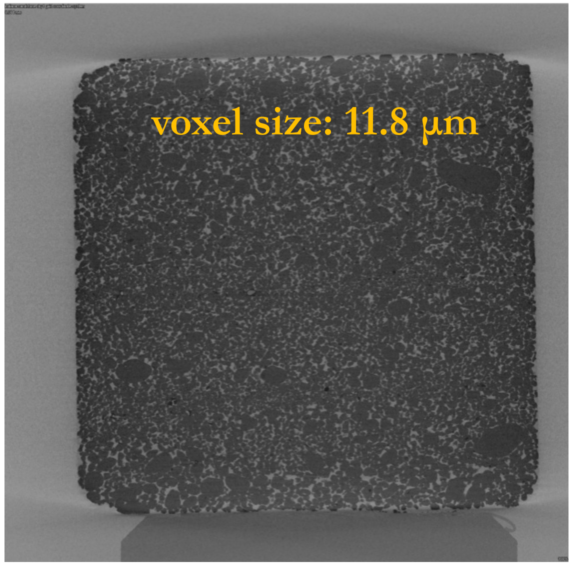

ExFact software (3DMA Rock)

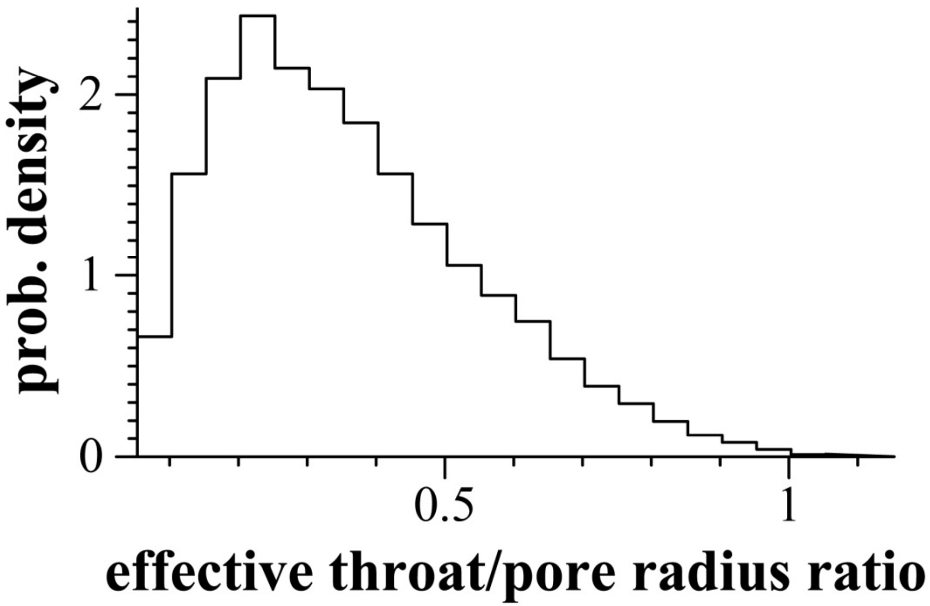

- Avg. pore diameter: 50 μm (20 μm pore–throat by MIP)
- Tortuosity: X–X 3.24; Y–Y 3.42; Z–Z 3.17 (3.22 from MIP)

CT Scanning Results: Metagraywacke

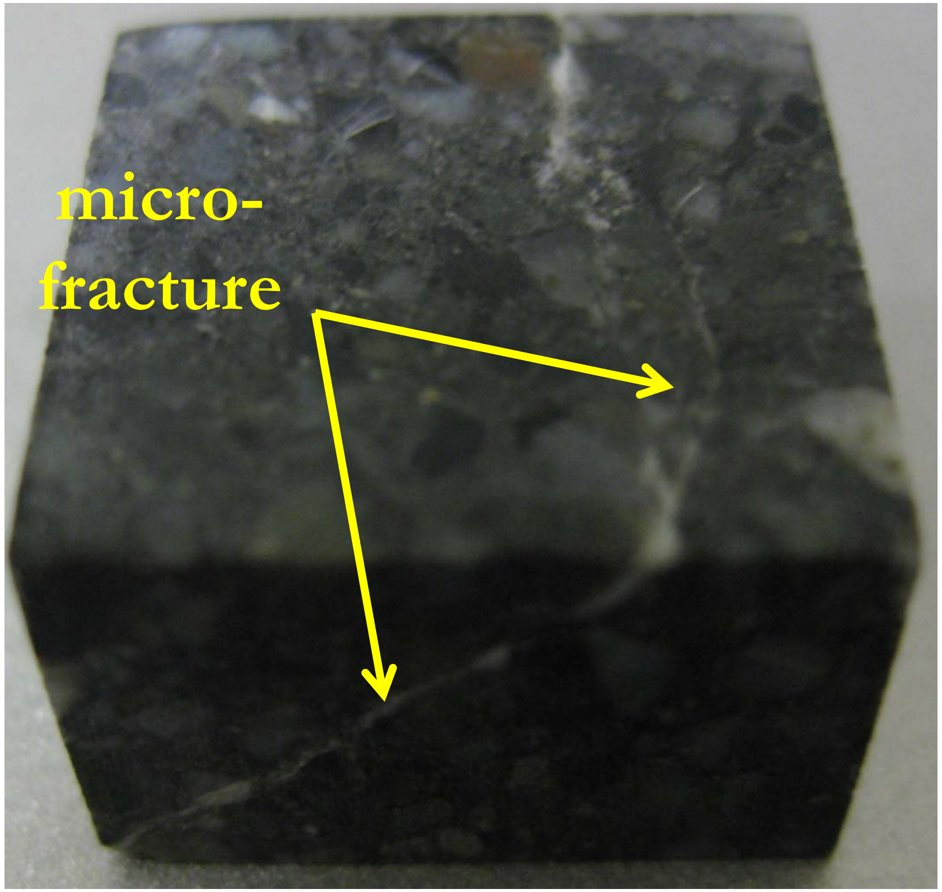

Fracture volume of 1.09%, calculated from reconstructed 3D volume of CT images

Sample dimension: 1.50 cm × 1.50 cm × 1.05 cm

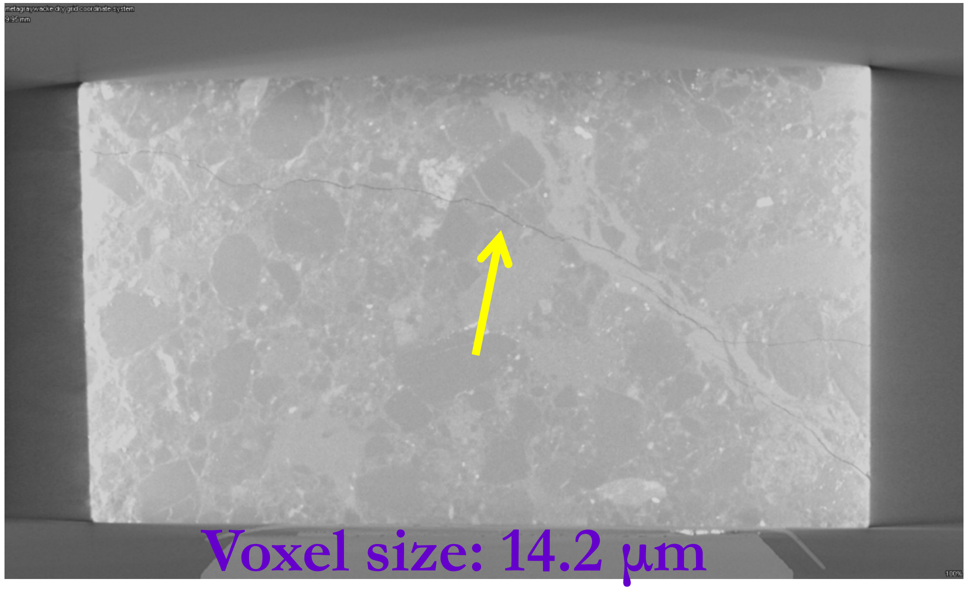

Voxel size: 14.2 µm

Nano–Scale FIB–SEM Imaging

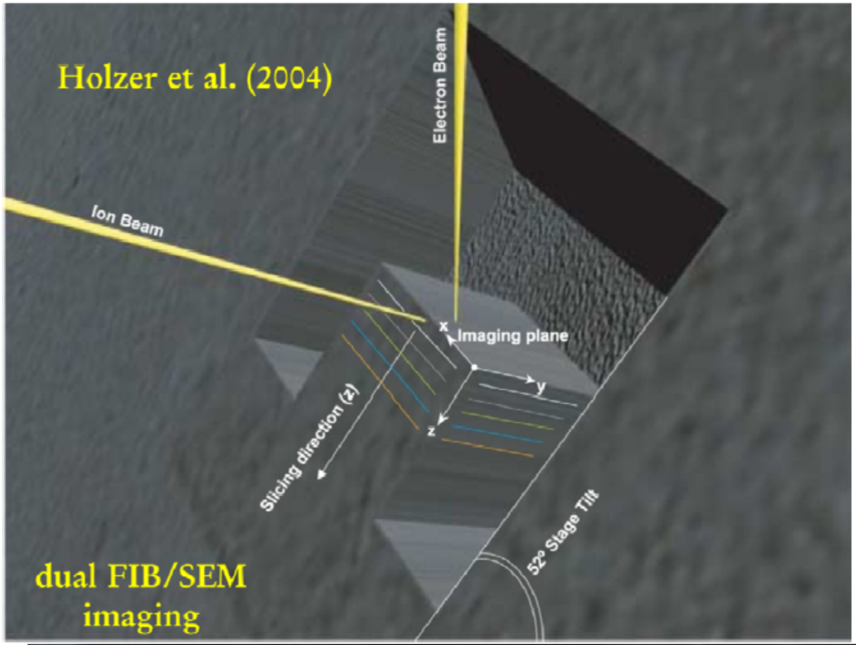

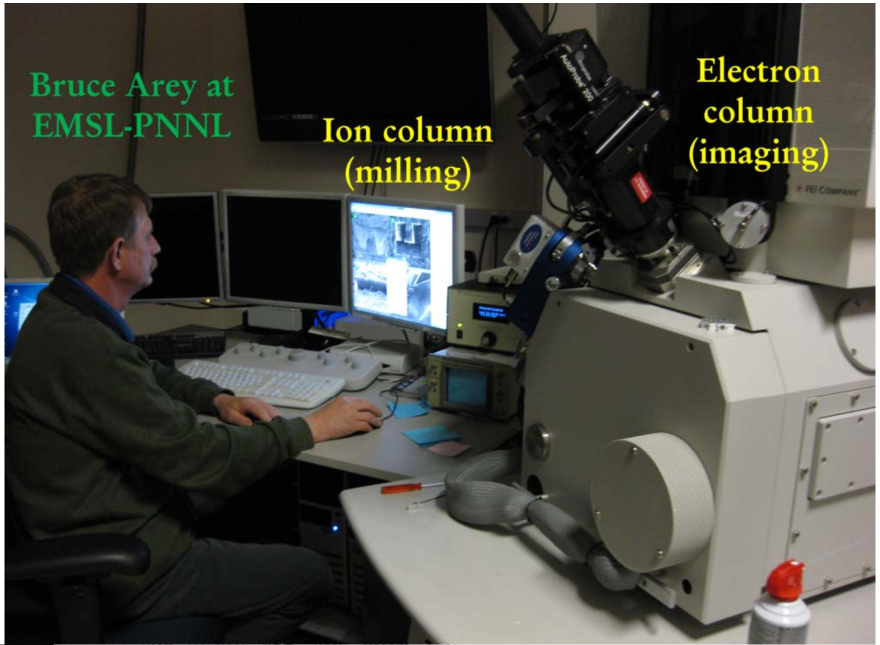

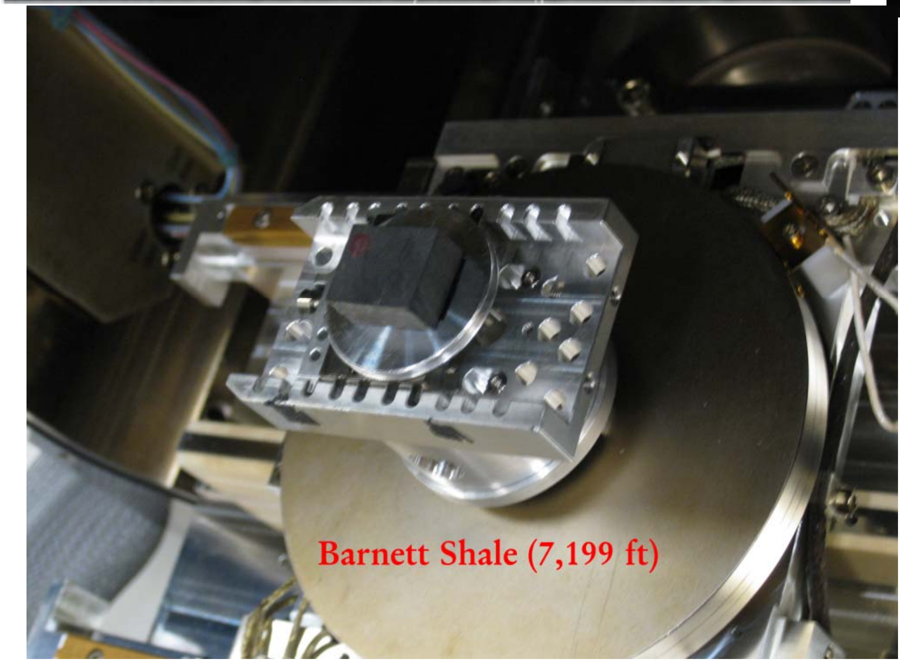

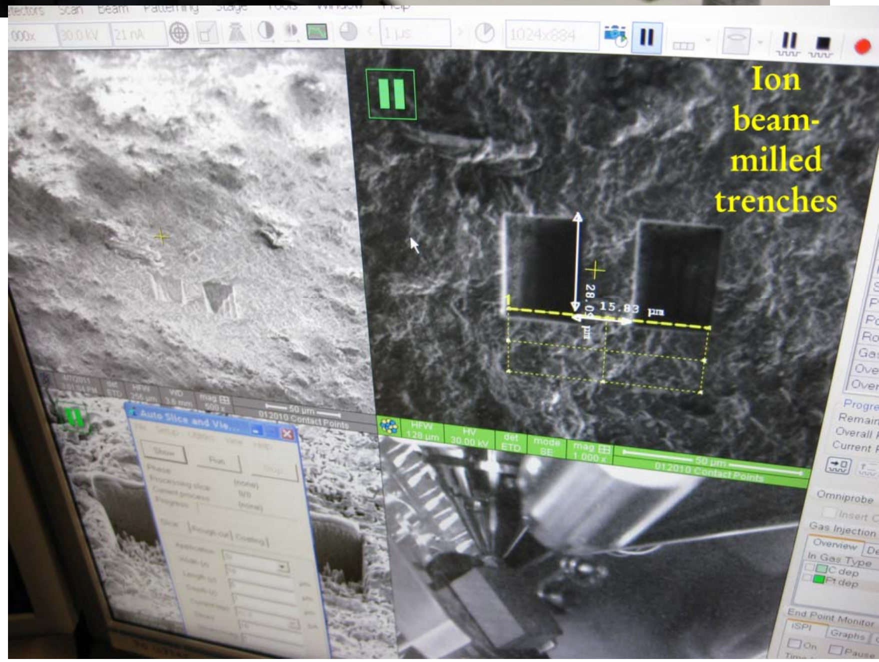

Nano–Scale FIB–SEM Imaging

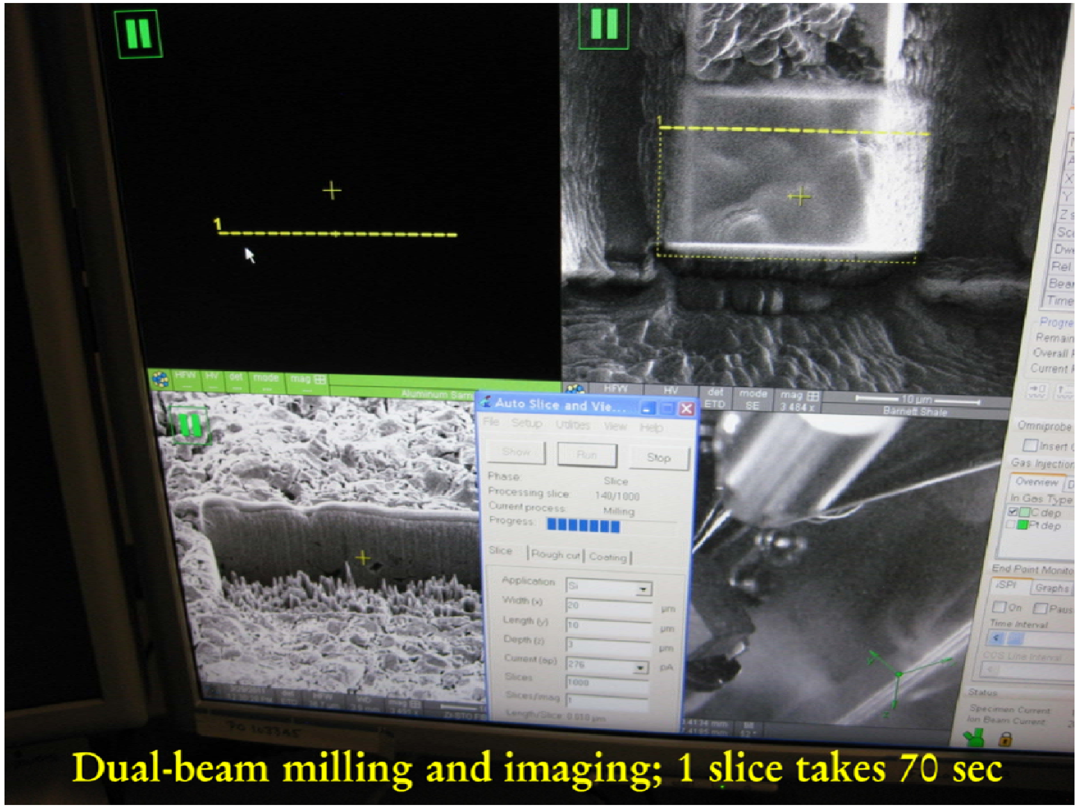

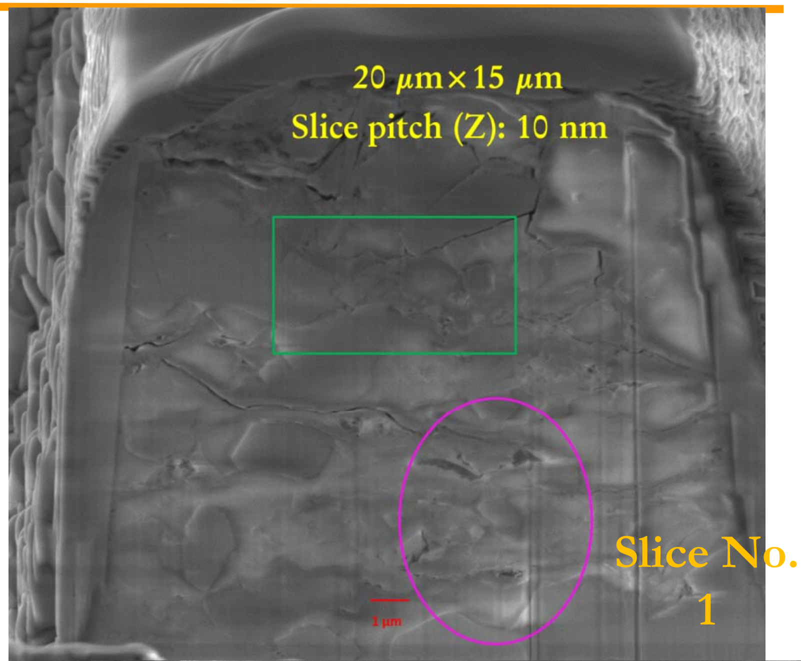

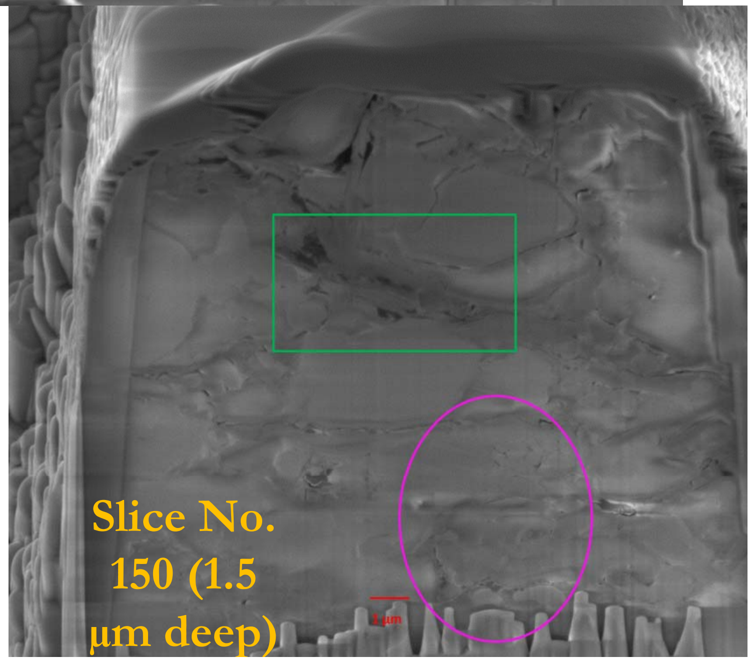

- μm scale observation scales
- Need 3–D reconstruction imaging software (e.g., Avizo Fire)
- Working with Hongkyo Yoon of Sandia Lab about pore structure processing

Small–Angle Neutron Scattering (SANS)

- Developed and refined over the past 2 decades for structural characterization of various natural and engineered porous materials
- Non–destructive
- Record the scattering from all pores (connected and closed); closed pores are inaccessible to fluids and, therefore, immeasurable by other techniques
- Have the ability to investigate ***pore structure at realistic (reservoir) P–T conditions*** and changes in pore structure at variable P–T conditions
- BT–5 perfect crystal USANS at NIST Center for Neutron Research (NCNR); General–Purpose SANS instrument at Oak Ridge National Lab (ORNL); The Lujan Neutron Scattering Center at Los Alamos National Lab
- Measurable pore diameter range: 0.5 to 200 nm (for SANS) and ~10 µm (for ultra SANS or USANS)
- Measurement time: ~ 60 min for SANS and 7 hrs for USANS

Melnichenko, Y. B. and G. D. Wignall. 2007. Small-angle neutron scattering in materials science: Recent practical applications. *J. Appl. Phy.* 102(2), 021101.

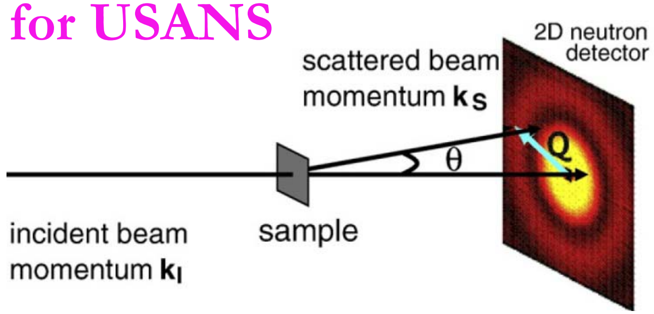

Lujan Neutron Scattering Center

- **A national user facility funded by Basic Energy Sciences of the Department of Energy**
- **Neutron scattering instruments are available to qualified scientists worldwide with time allocated based on a proposal system**
- **There are two proposal deadlines each year (Summer of 2013)**
- **LQD (Low-Q Diffractometer): uses an intense source of long-wavelength ("cold") neutrons over a range of 1 to 16 Å, making it the brightest TOF low-Q instrument in the world**

http://lansce.lanl.gov/lujan/index.shtml

NIST SANS Instruments

There are three Small-Angle Neutron Scattering (SANS) Instruments and one Bonze-Hart perfect crystal (USANS)

NG3 SANS

- NG3 SANS 30m Instrument
- NG3 Current Schedule
- NG3 Past Schedules
- NG3 Operating Status
- *NG3 Live Webcam

NG7 SANS

- NG7 SANS 30m Instrument
- NG7 Current Schedule
- NG7 Past Schedules
- NG7 Operating Status
- *NG7 Live Webcam

BT5 USANS

- BT5 USANS Instrument
- BT5 Current Schedule
- BT5 Past Schedules

User proposals submitted in May 2013 for analyzing 20 samples during Oct.-Dec., 2013

http://www.ncnr.nist.gov/programs/sans/sans_inst.html

ORNL Neutron Sciences

http://neutrons.ornl.gov/about/

the High Flux Isotope Reactor (HFIR): uses a reactor to generate neutrons in a steady beam (CG-2: general-purpose SANS diffractomer)

the Spallation Neutron Source (SNS): uses an accelerator to generate pulsed beams (1a: time-of-flight ultra-small-scale neutron scattering; 6: extended Q-range SANS)

Low gas recovery in Barnett Shale

Question

Hypothesis

Pore geometry and topology

Complementary measurements

Theory

Modeling

Analysis and evaluation

Ongoing work: CH_4 retention and transport in crushed and intact Barnett Shale

NATURAL GAS:

Geology is behind rapid decline in dry gas wells, researchers say

Environment and Energy Publishing

Gayathri Vaidyanathan, E&E reporter

Published: Tuesday, November 6, 2012

CHARLOTTE, N.C. -- A major decline in production from shale gas wells in their first year could be a reason why companies are moving their operations out of "dry" gas plays containing only natural gas.

Production data suggests that wells decline by more than 60 percent in the first year. So a well producing about 5 million cubic feet of gas at the beginning would produce only 2 million cubic feet by the end of the year. That's true in geologies across the United States, though researchers at the University of Texas, Arlington, focused on the Barnett Shale in Texas.

The implication is that companies would need to keep drilling new wells to maintain their production level. The new wells would compensate for the rapid loss of production from older ones.

Behind the rapid decline in "dry" shale plays is geology and the pore connectivity in the shale rock, said Zhiye Gao, a doctoral student.

To extract shale gas, companies use hydraulic fracturing, a process where they blast pressurized water, chemicals and sand at shale rock to creates fractures in shale. Gas contained in the rock migrates to the newly created channels and then up into the well bore, where the companies trap it for consumption.

But not all gas migrates out. Some plays, such as the Barnett, contain pores smaller than the tip of a needle, of about 7 nanometers. Some of the methane contained within these pores is floating freely, but a majority of the gas is in loose association with the rock.

The free methane flows out easily, but the methane associated with the rocks does not, since it may be subject to different physical laws of flow.

Another major reason is the pores are poorly connected to each other, hindering flow.

This means that when a well is drilled, the free methane flows out first, leading to a high production rate. Once much of the free gas escapes, the production rate declines rapidly.

The researchers do not yet know if companies have only tapped free gas so far in the plays across the United States, the implication of which would be that a steep decline in production is on the horizon.

Some commenters on the investors website Seeking Alpha have suggested as much after examining production data from gas companies. For example, an **examination** of Southwestern Energy's results from the second quarter this year found that the company increased overall gas production by 5 billion cubic feet even though it had brought 131 new wells into production in the same quarter. The new wells had only compensated for the decline from older wells.

Outline

- Porosity and permeability
- Multiple pore structure characterization approaches
- **Methane sorption/desorption**
- Production decline analyses
- Summary

Hydrogeological Properties of the Barnett Shale

	Curtis (2002)	Bowker (2007)	Gale et al. (2007)	Grieser et al (2006)	Hill et al. (2007)	Sigal and Qin (2008)	Zhao et al. (2007)
Porosity (%)	4.4	6	5.52±0.28		6	4–8	3.8–6.0
Permeability (μd)				0.07–5	20	0.01–0.6	0.15–2.5
TOC by weight (%)	4.5			4.5			3.5–4.5
Free gas (%)					55		
Sorbed gas (%)					45		
Water saturation (%)	43	25	28.9±7.2				

Gas Production Rate in a Fractured Shale System

Silin and Kneafsey (2012). **Shale Gas: Nanometer-Scale Observations and Well Modelling.** ***Journal of Canadian Petroleum Technology,*** **51(6): 464-475.**

Early-time recovery rate

$$\boxed{Q(t) = 2A\frac{c_g}{\rho_0}\sqrt{\left(\phi + \frac{\rho_0 \rho_k S_k c_f}{c_g}\right)\frac{k}{\mu p_R}}\,\frac{p_R^2 - p_w^2}{\alpha\sqrt{t}}}$$

$$t^* = \left(1 + \frac{\rho_0 \rho_k S_k c_f}{c_g \phi}\right)\frac{\mu \phi D^2}{k p_R}\frac{1}{\alpha^2}$$

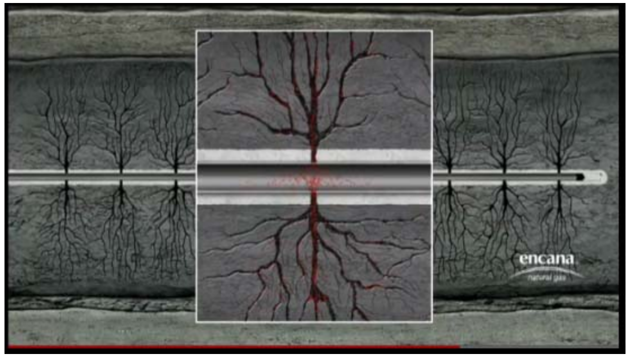

$$\boxed{Q(t) = 2A\frac{c_g}{\rho_0}\frac{k}{\mu D}\left(p_R^2 - p_w^2\right)\exp\left[-3\frac{p_w}{p_R}\frac{1}{\left(\phi + \frac{\rho_0 \rho_k S_k c_f}{c_g}\right)}\frac{k p_R}{\mu D^2}t - \frac{1}{\alpha^2}\right]}$$

Late-time recovery rate

c_f: gas desorption rate [m^3/(kg Pa)]

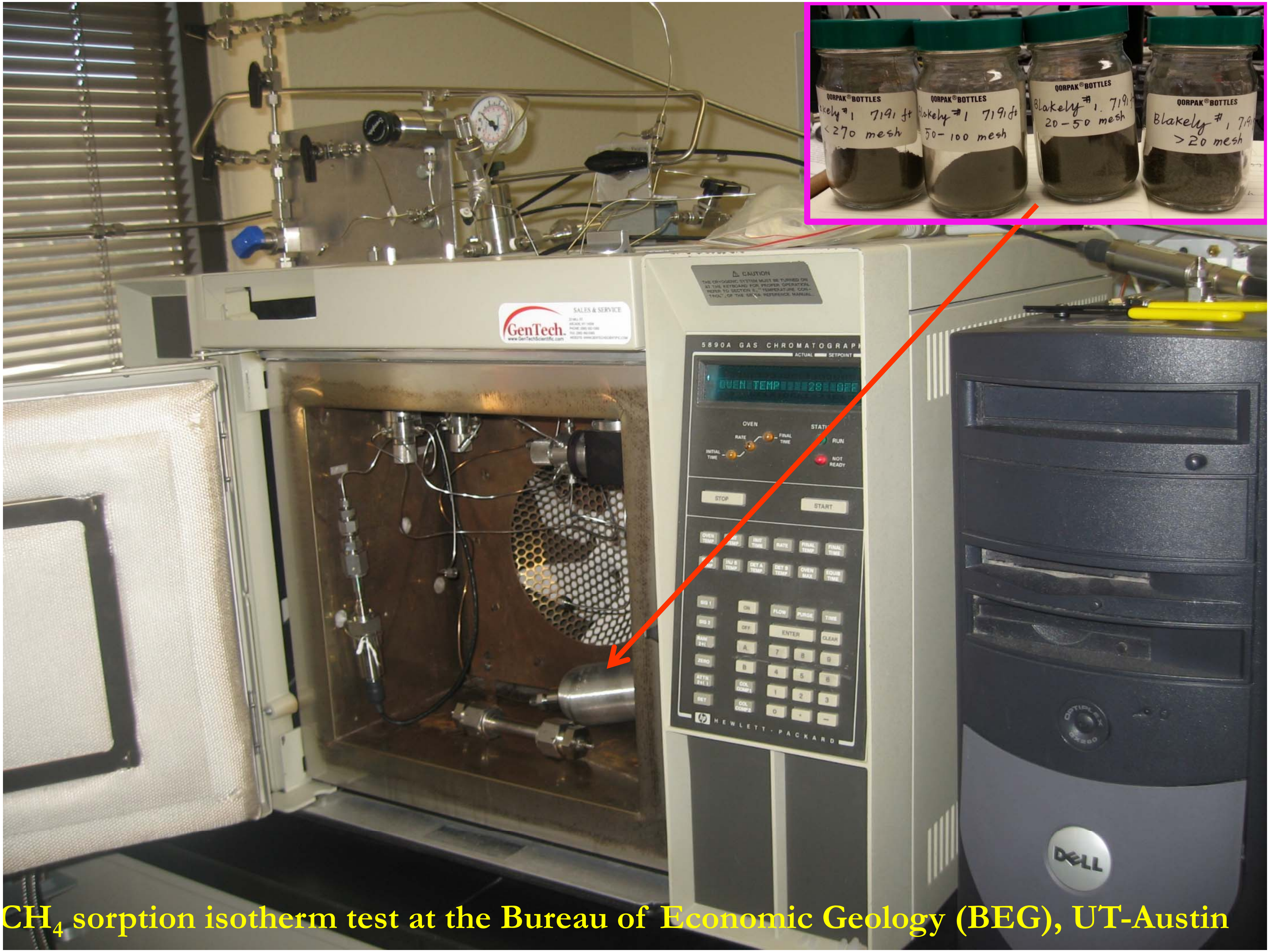

CH_4 sorption isotherm test at the Bureau of Economic Geology (BEG), UT-Austin

Methane Sorption onto Barnett Shale

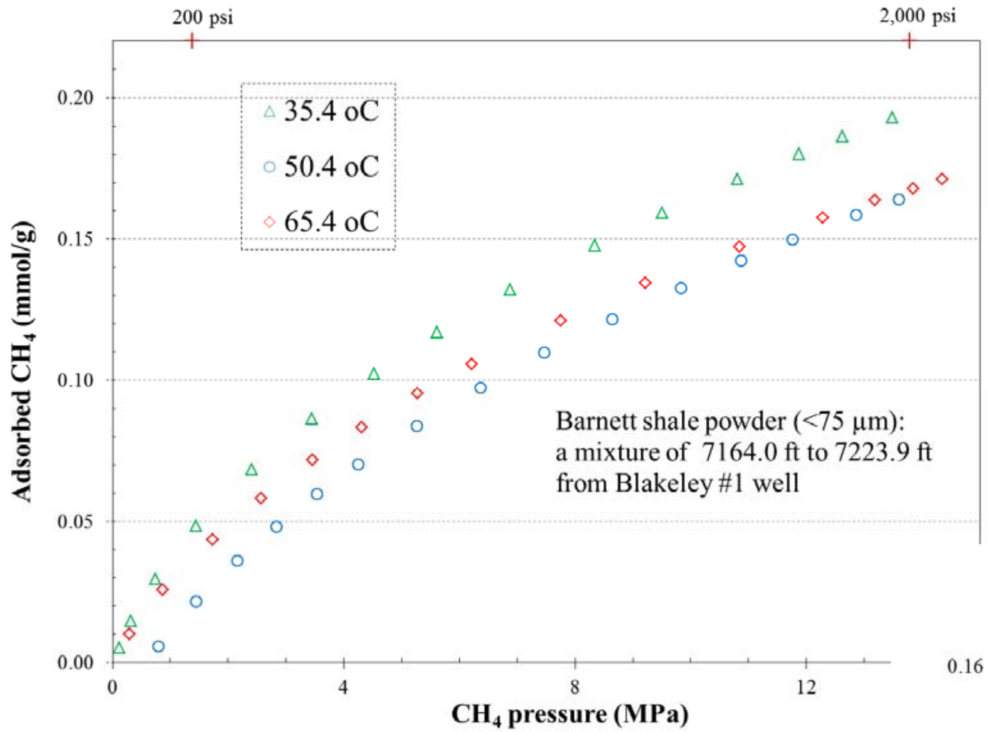

- Reservoir conditions: 3,500 psi and 77 °C
- CH_4 sorption strongly pressure–dependent

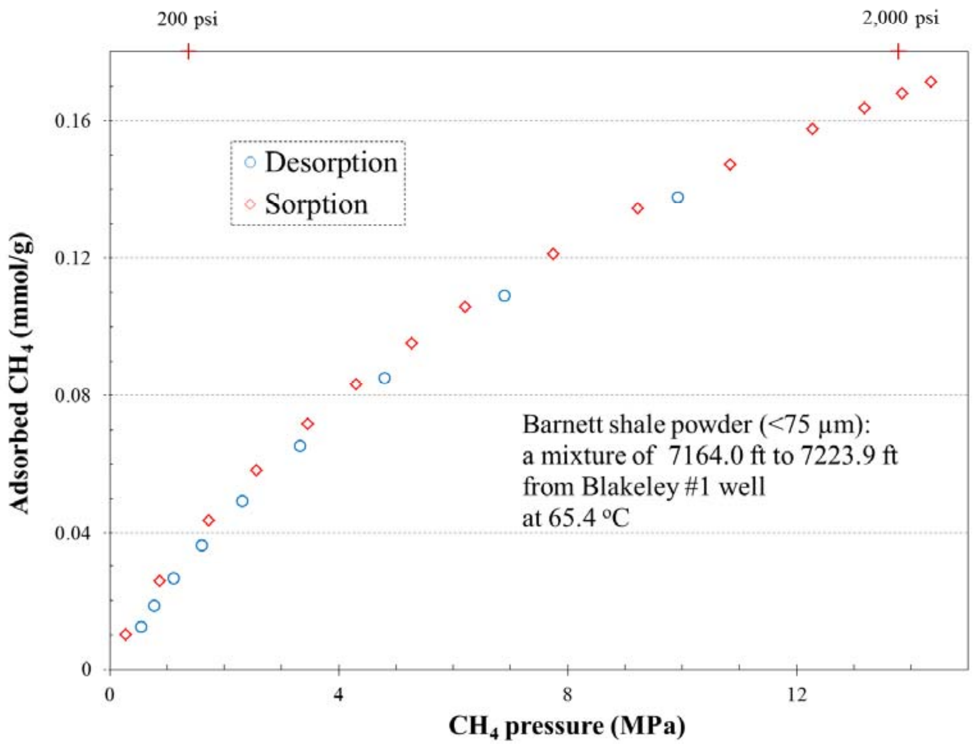

- Reversible CH_4 sorption–desorption isotherm
- Sorption parameters to be used for production decline analysis

Methane Transport: Ongoing Work

Barnett shale powder sample

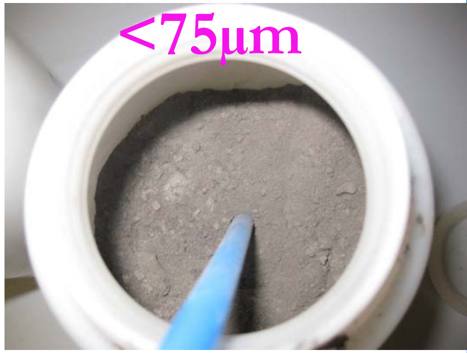

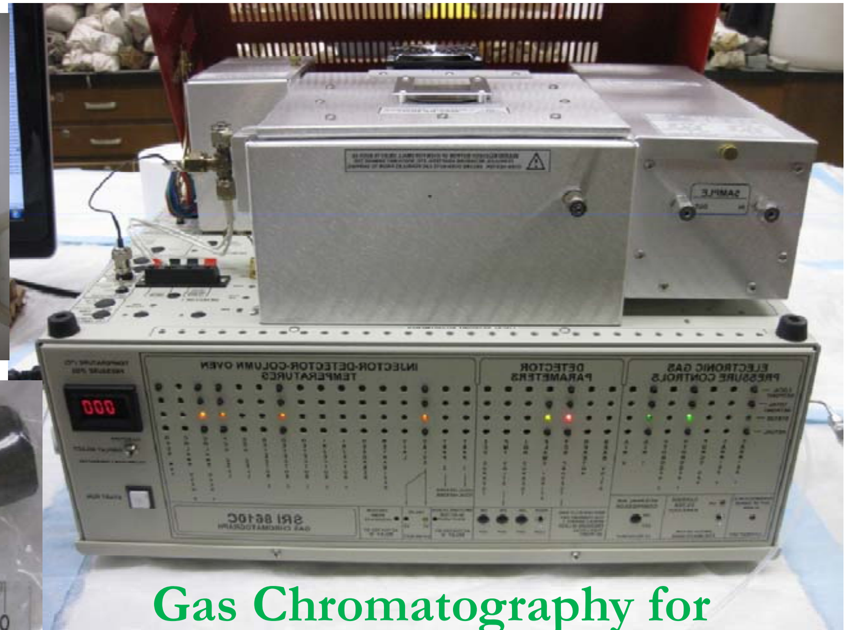

Gas Chromatography for in-line methane detection

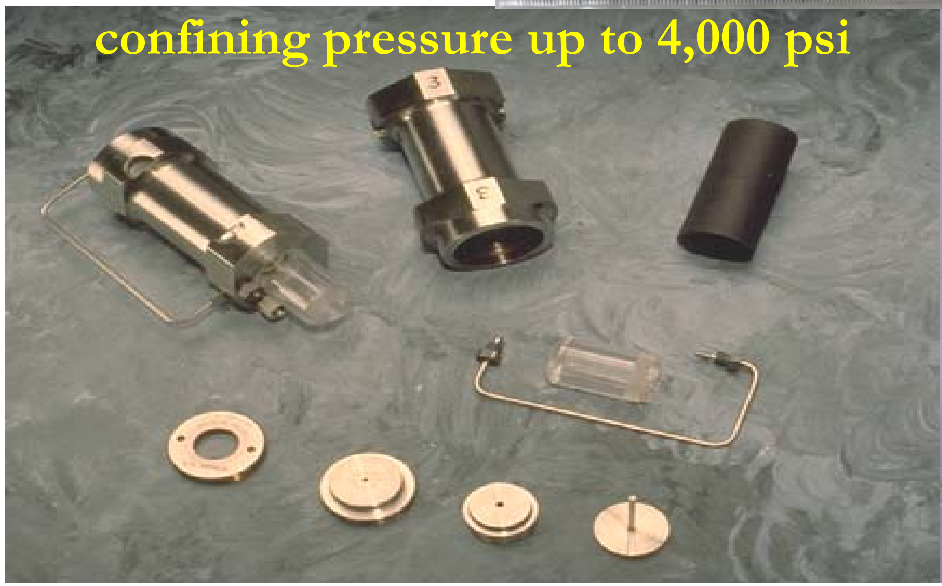

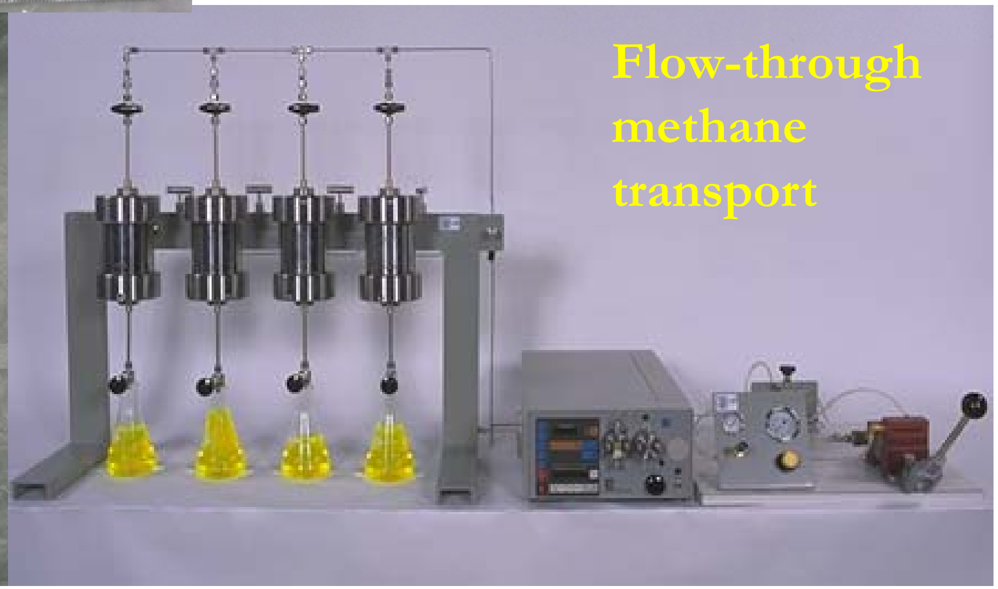

State Key Lab of Oil and Gas Reservoir Geology and Exploitation
Chengdu University of Technology

ISOSORP-GAS Sc high-pressure gas sorption (Rubotherm)
70 Mpa@150°C

Outline

- Porosity and permeability
- Multiple pore structure characterization approaches
- Methane sorption/desorption
- **Production decline analyses**
- Summary

Shale Gas Flow: Matrix "diffusion" vs. "Darcy" flow

drive
your car
out of
neighbor
hood
blind-
folded

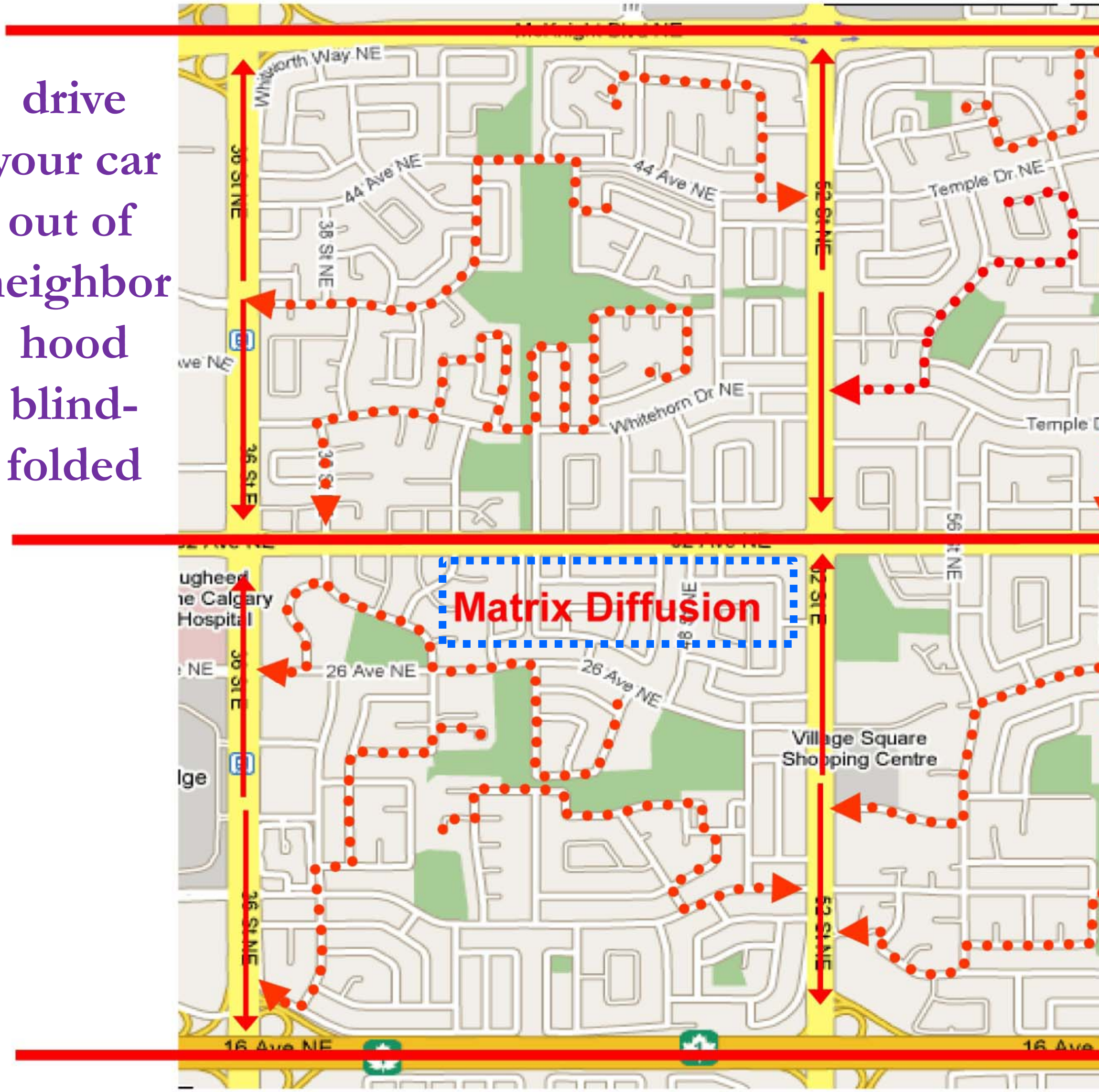

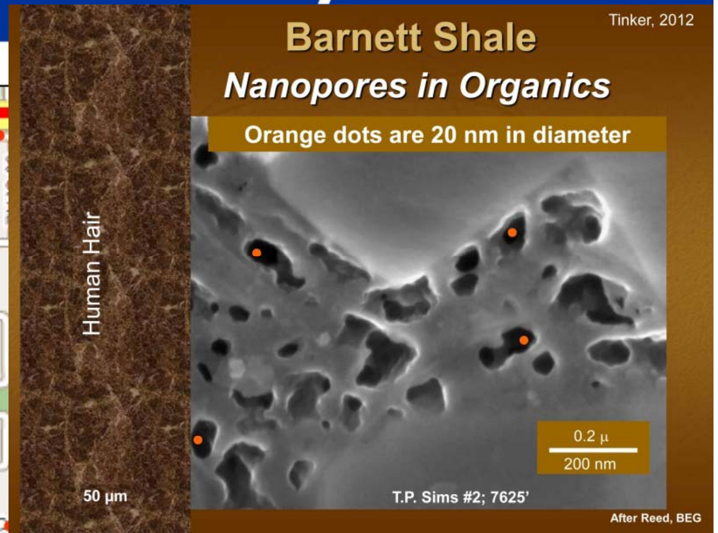

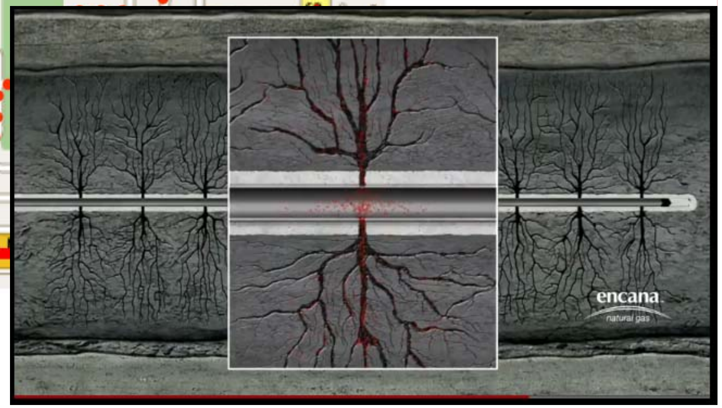

http://www.transcanada.com/customerexpress/docs/presentations_general/2009_North_American_Shale_Gas_Overview_NECA.pdf

Haynesville Shale Performance Possibilities

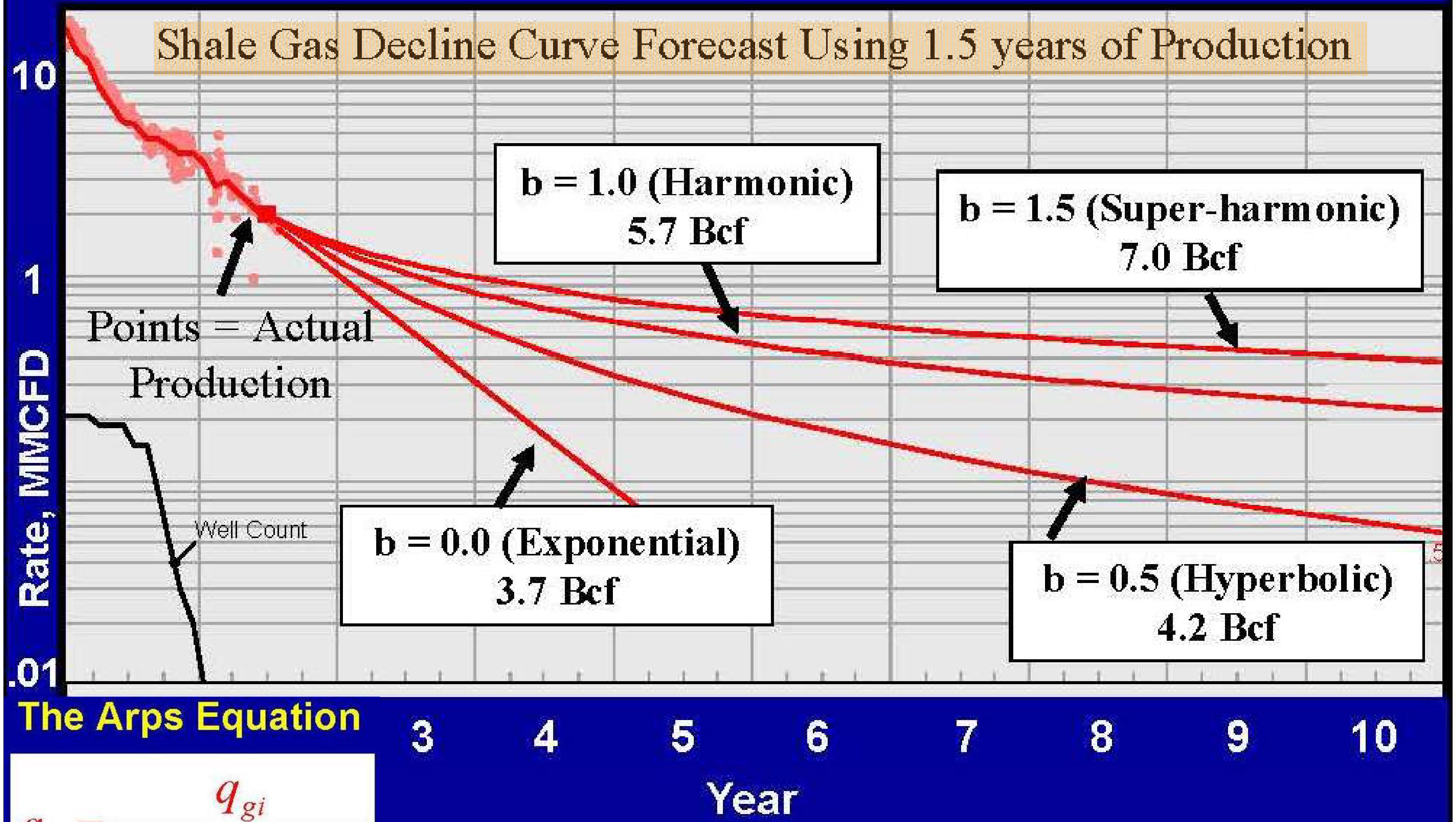

The Arps Equation

$$q_g = \frac{q_{gi}}{(1+bD_i t)^{(1/b)}}$$

Jenkins and Ilk (2010)

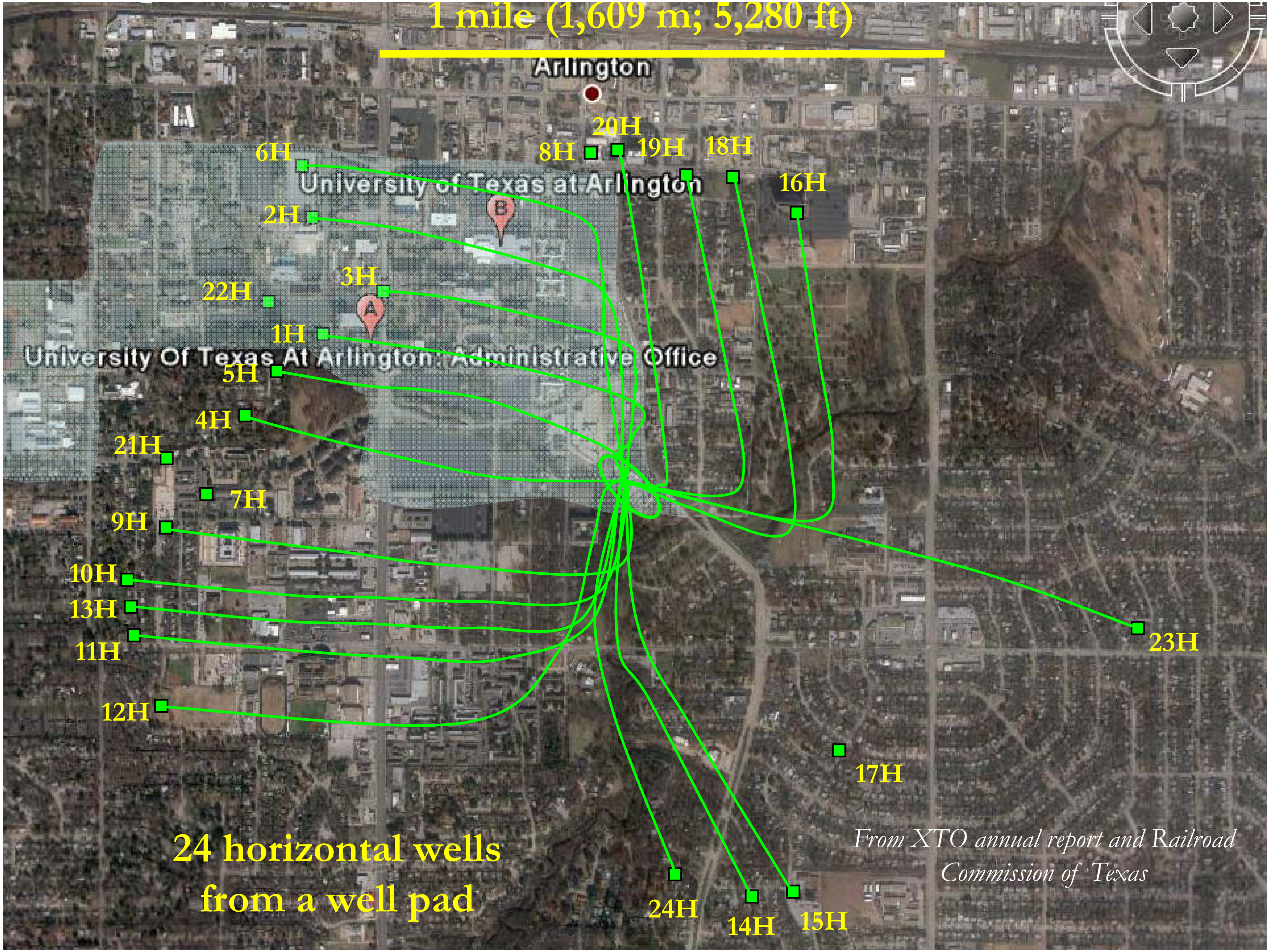
1 mile (1,609 m; 5,280 ft)
Arlington
University of Texas at Arlington
University Of Texas At Arlington: Administrative Office
20H
8H
19H
18H
6H
16H
2H
3H
22H
1H
5H
4H
21H
7H
9H
10H
13H
11H
12H
23H
17H
24H
14H
15H
24 horizontal wells
from a well pad
From XTO annual report and Railroad Commission of Texas

Drillinginfo

http://info.drillinginfo.com/

- The most complete source of North American and offshore waters oil and gas information, data and tools providing a comprehensive and integrated database of land, well and production information

- Subscription: Drillinginfo Pro ($51,000/yr): the most comprehensive package available for North American and Canadian data

EnergyStrategyPartners | Barnett wells histogram & bubbled by GOR – past 2 years

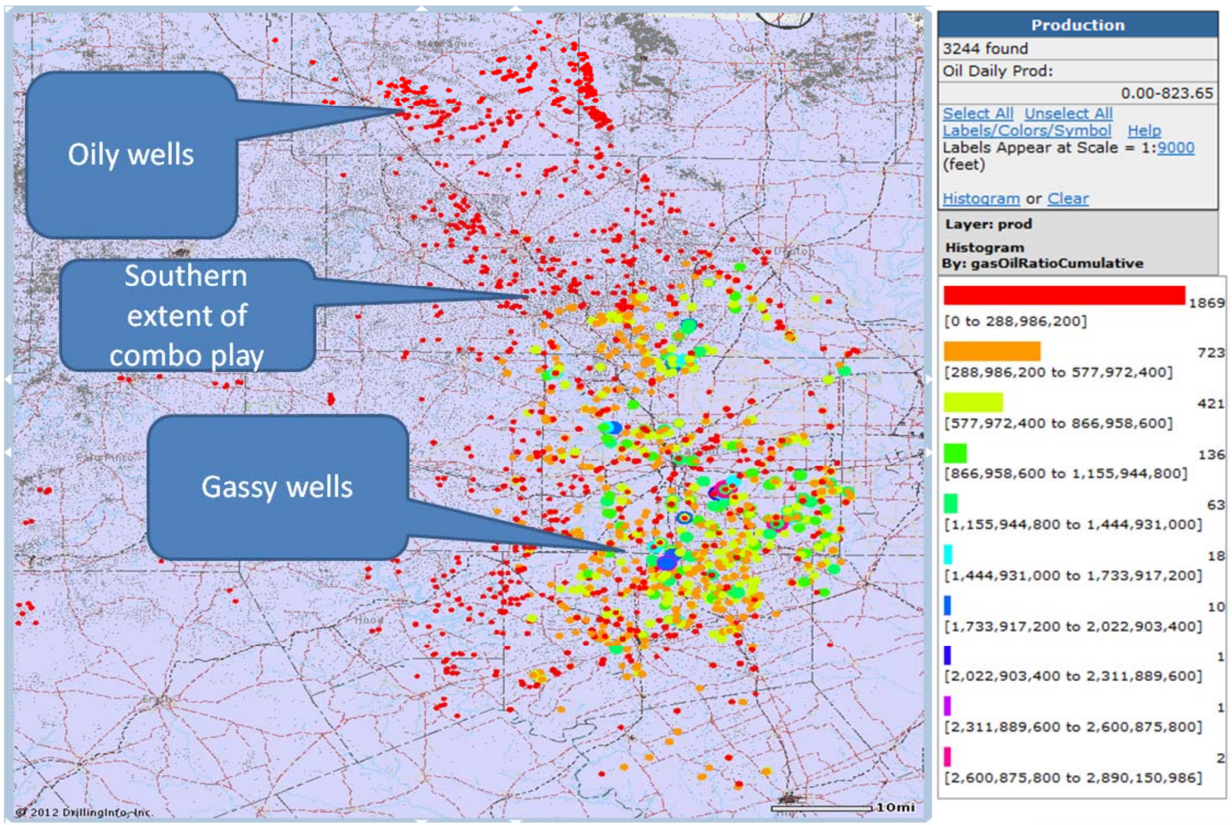

All 22 Producing UTA Horizontal Wells

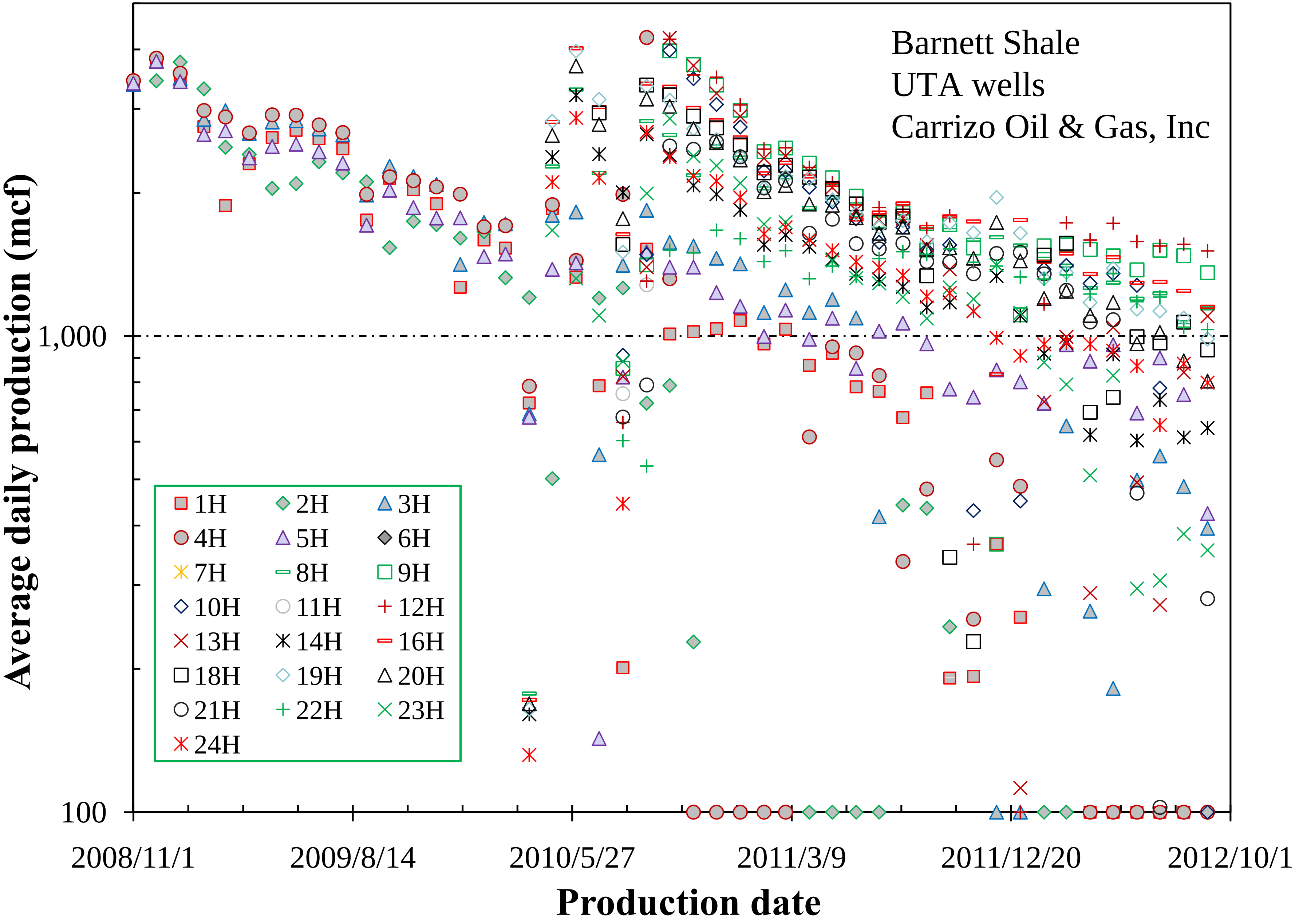

Decline Slope of 2/3 for 11 UTA Wells (50% of All) in Tarrant County

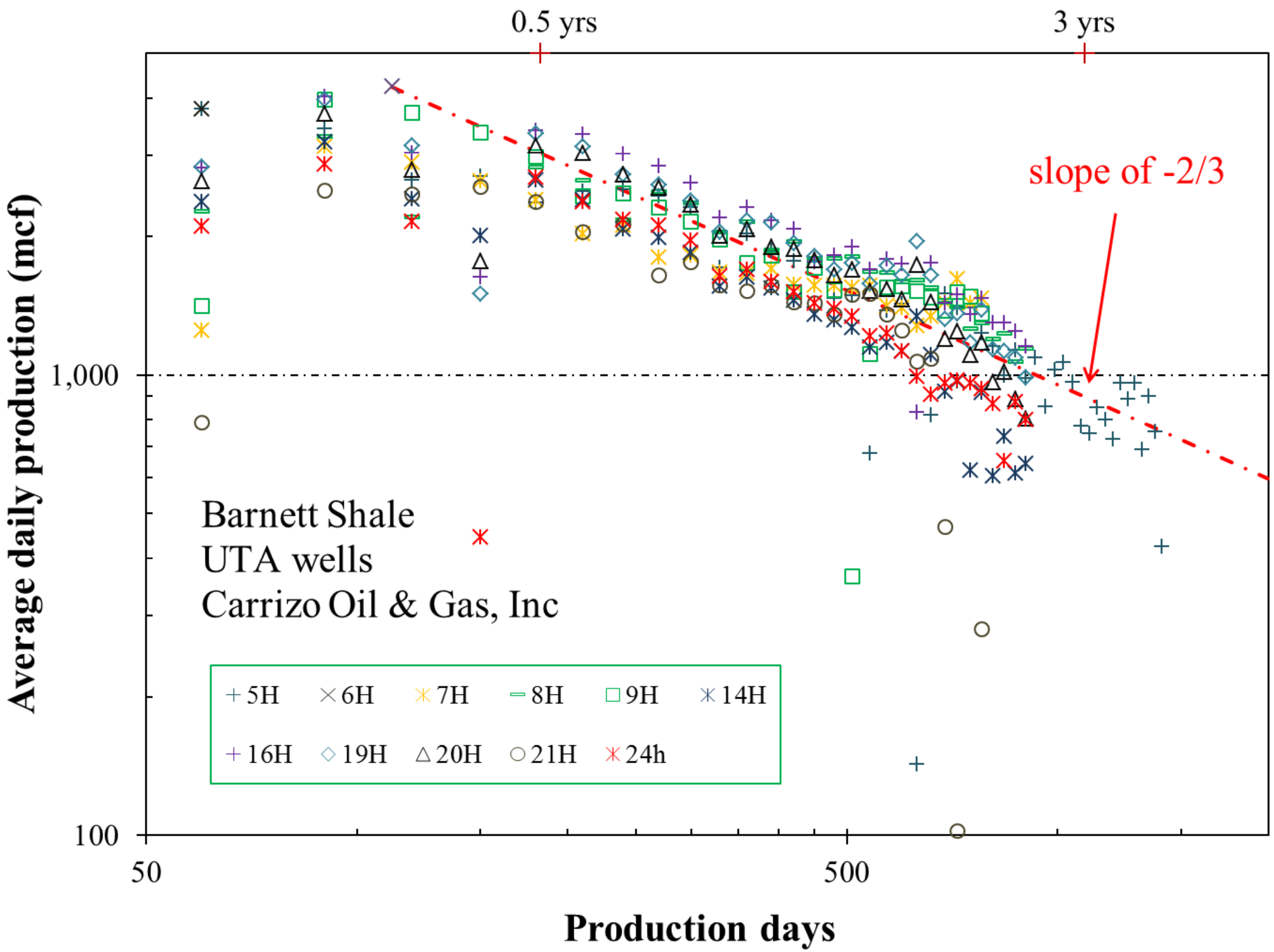

ECLIPSE 2012: solving reservoir engineering challenges

- Chemical EOR
- CO_2 storage and EOR
- Coal and shale gas
- Heavy oil recovery
- Complex wells
- CO_2 storage and EOR
- Flexible reservoir control
- Streamline–based screening and pattern flood management
- Faster runtimes with parallel processing
- Reservoir geomechanics
- History matching
- Uncertainty and sensitivity analysis
- Design optimization

http://www.slb.com/services/software/reseng/eclipse.aspx


ConocoPhillips
600
“Characterization of Shale Samples for
Improved Hydrocarbon Recovery”
March 2013

Summary

- Steep 1st year decline and low overall hydrocarbon production observed in stimulated shales
- Shales show low pore connectivity, which reduces gas diffusion from matrix to stimulated fractured network
- Several complementary approaches are used to investigate pore structure in natural rock
  - ✓ Imbibition and diffusion: macroscopic method
  - ✓ Porosimetry and vapor condensation: indirect method
  - ✓ Imaging (Wood's metal, FIB/SEM, SANS): nano–scale tool
- Pore structure and gas desorption mechanism are linked to field–scale hydrocarbon recovery

Shale Gas Flow: Matrix "diffusion" vs. "Darcy" flow

drive your car out of neighborhood blind-folded

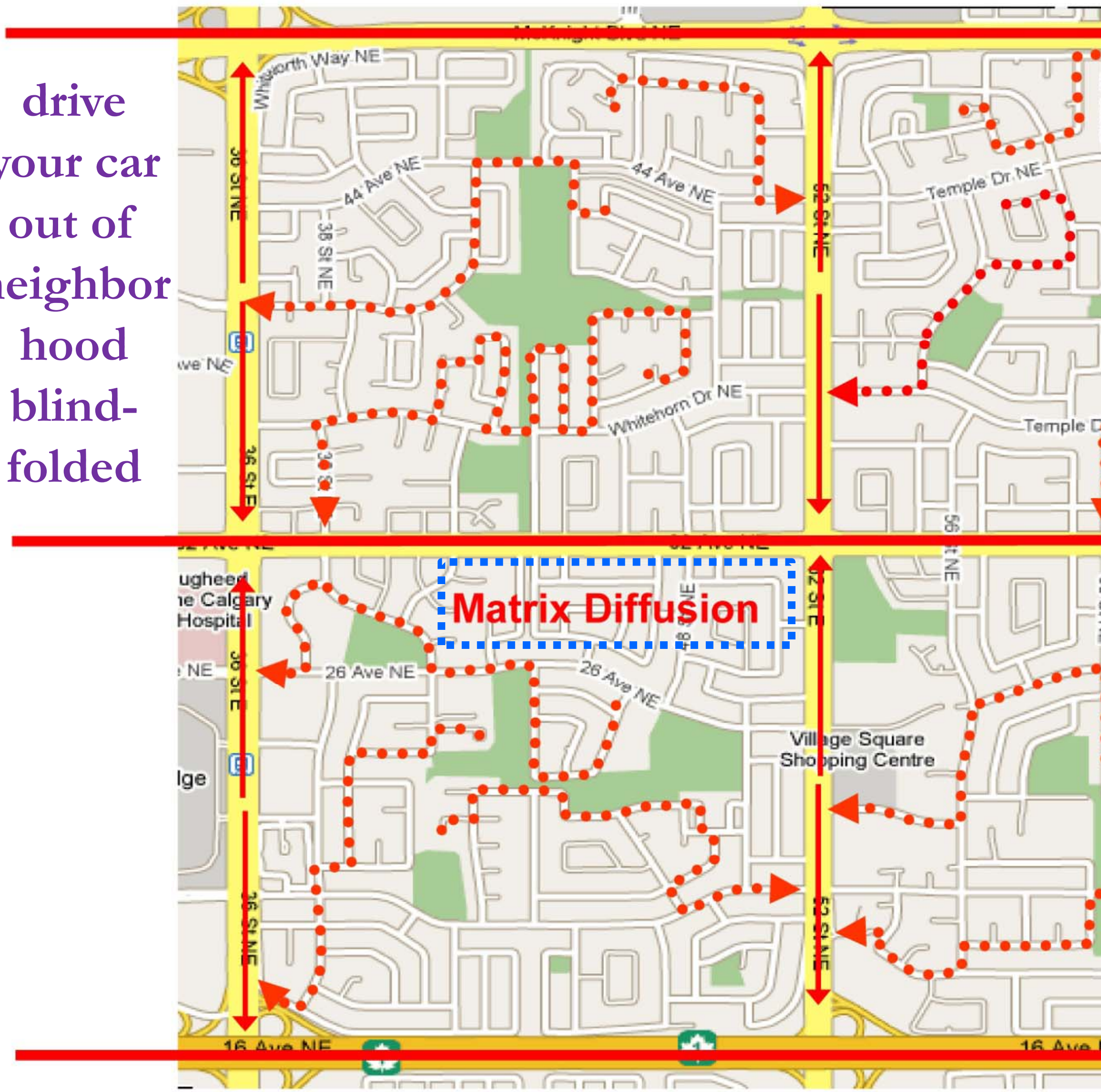

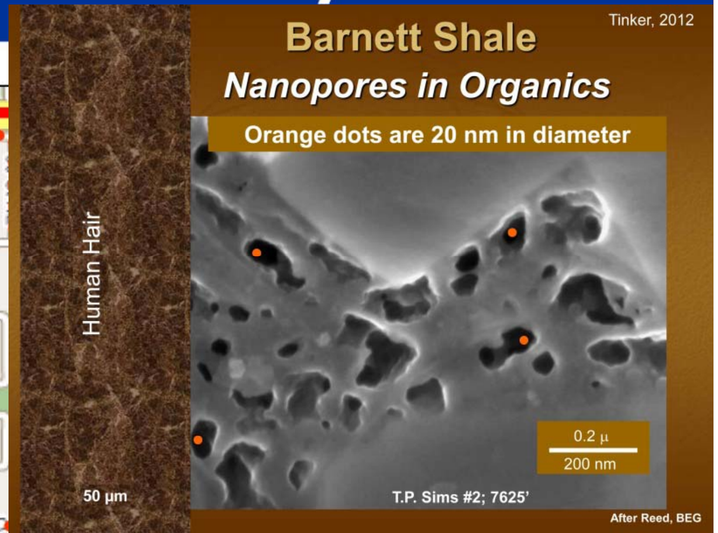

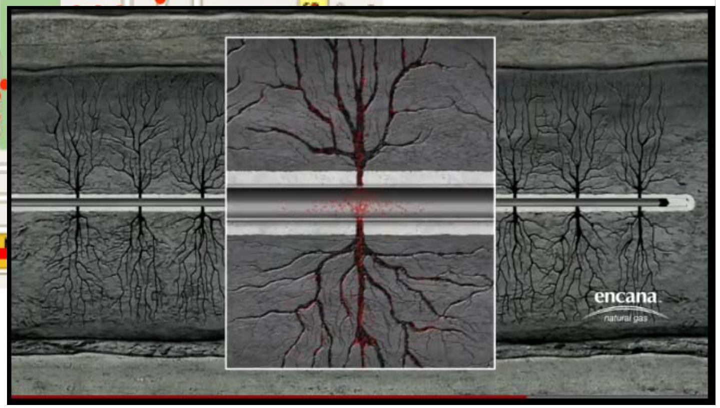

http://www.transcanada.com/customerexpress/docs/presentations_general/2009_North_American_Shale_Gas_Overview_NECA.pdf